UNIVERSIDAD DE CHILE

FACULTAD DE CIENCIAS QUÍMICAS Y FARMACÉUTICAS

THE PROGRESSIVE BRAIN DAMAGE OBSERVED FOLLOWING PERINATAL ASPHYXIA IS SUSTAINED BY A LONG-TERM IMPAIRMENT OF REDOX HOMEOSTASIS: EFFECT OF NICOTINAMIDE

Tesis presentada a la Universidad de Chile para optar al grado de Doctor en Farmacología

CAROLYNE ANDREA LESPAY REBOLLEDO

Director de Tesis: Prof. Mario Herrera-Marschitz, MD, Sci. PhD

Santiago-CHILE

2019

UNIVERSIDAD DE CHILE
FACULTAD DE CIENCIAS QUÍMICAS Y FARMACÉUTICAS

INFORME DE APROBACIÓN DE TESIS DE DOCTORADO

Se informa a la Dirección de la Escuela de Graduados de la Facultad de Ciencias Químicas y Farmacéuticas que la Tesis de Doctorado presentada por el candidato

CAROLYNE ANDREA LESPAY REBOLLEDO

Ha sido aprobada por la Comisión de Evaluadora de Tesis como requisito para optar al grado de Doctor en Farmacología, en el examen público rendido el día

_____

Director de Tesis:
Dr. Mario Herrera-Marschitz _____

Comisión Evaluadora de Tesis:

Dr. Pablo Caviedes _____

Dr. Luis Segura Aguilar _____

Dr. German Ebensperger _____

Dr. Jaime Eugenin _____

UNIVERSITY OF CHILE

FACULTY OF CHEMICAL AND PHARMACEUTICAL SCIENCES

THE PROGRESSIVE BRAIN DAMAGE OBSERVED FOLLOWING PERINATAL ASPHYXIA IS SUSTAINED BY A LONG-TERM IMPAIRMENT OF REDOX HOMEOSTASIS: EFFECT OF NICOTINAMIDE

A thesis submitted to University of Chile for the degree of Doctor of Philosophy in Pharmacology

CAROLYNE ANDREA LESPAY REBOLLEDO

Director of Thesis: Prof. Mario Herrera-Marschitz, MD, Sci. PhD

Santiago-CHILE

2019

Abstract.

Perinatal asphyxia (PA) is a clinical condition characterized by oxygen deprivation, following PA brain damage progresses, leading to behavioural cognitive disabilities affecting surviving neonates. There is still lack of consensus on suitable therapeutic approaches and protocols preventing the progression of neuronal damage. Reduction of oxidative stress is one of the identified molecular targets, based on the fact that the immature brain is highly susceptible to free radicals, showing scarcely developed antioxidant defences.

In the present thesis it was proposed the hypothesis that progression of brain damage during a delayed cell death period in vulnerable brain areas of animals exposed to perinatal asphyxia is associated with sustained oxidative stress along development, impairing redox homeostasis. Nicotinamide enhances the response of glutathione-dependent enzymes by a pentose phosphate dependent pathway, preventing asphyxia-dependent brain damage. The hypothesis was evaluated using a rat model of severe perinatal asphyxia.

The first part of the present Thesis evaluated the effect of global perinatal asphyxia on several parameters of oxidative stress and cell death in rat brain tissue sampled at an extended neonatal period of 14 days. Brain samples (mesencephalon, telencephalon and hippocampus) were assayed for glutathione (reduced and oxidized levels; spectrophotometry), tissue reducing capacity (potassium ferricyanide reducing assay, FRAP), catalase (the key enzyme protecting against oxidative stress and reactive oxygen species, Western blots and ELISA) and cleaved caspase-3 (the key executioner of apoptosis, Western blots) levels. It was found that global PA produced a regionally specific and sustained increase in GSSG/GSH ratio, a regionally specific decrease in tissue reducing capacity and a regionally and time specific decrease of catalase activity and increase of cleaved caspase-3 levels, indicating a long-term impairment in redox homeostasis. Multivariate analysis demonstrated that progression of brain damage along postnatal days is importantly influenced by changes on glutathione ratio, cleaved caspase-3 levels and catalase activity.

In the second part of the Thesis, the experimental approach focused on the damage induced in hippocampus at P1 and P14. Glutathione, glutathione reductase (GR), glutathione peroxydase (GPx) (all by spectrophotometry), catalase (Western blots and ELISA), TIGAR

(Western blots), calpain (fluorescence), and XRCC1 (Western blots) were assayed for characterizing the glutathione-dependent redox pathway and for determining the effect of nicotinamide; a precursor of NAD^+ and $NADP^+$, on death cell mechanisms in hippocampus.

It was found that global PA produced (i) a sustained increase of GSSG levels and GSSG/GSH ratio at P1 and P14; (ii) a decrease of GR, GPx, and catalase activity at P1 and P14; (iii) a decrease at P1, followed by an increase at P14 of TIGAR levels; (iv) an increase of calpain activity at P14; and (v) an increase of XRCC1 levels, but only at P1. (vi) Nicotinamide prevented the effect of PA on GSSG levels and GSSG/GSH ratio, and on GR, GPx, and catalase activity, also on the enhancement of TIGAR levels and calpain activity observed at P14.

The present thesis demonstrates that PA induces a sustained oxidative stress along development in mesencephalon and hippocampus, both vulnerable brain areas of animals exposed to PA, whereas telencephalon, a resistant brain area, displayed an increasing of antioxidant response mediated by glutathione and FRAP. The progression of brain damage during a delayed cell death period is associated mainly with glutathione ratio, cleaved caspase-3 levels and catalase activity. Nicotinamide enhanced the response of glutathione-dependent enzymes by a pentose phosphate dependent pathway, preventing asphyxia-dependent brain damage by a reduction of death cell mechanisms mediated by calpain.

In conclusion the present thesis demonstrates that changes in redox environment induced by PA are sustained along the time, contributing to progression of brain damage, but also resistance to further damage during the delayed death cell period. The changes in redox environment can be modulated, controlling the cell metabolism induced by pentose phosphate dependent pathways.

PREFACE

DATA FROM THIS THESIS HAVE BEEN PUBLISHED AS:

Lespay-Rebolledo C, Pérez-Lobos R, Tapia-Bustos A, Vio V, Morales P, Herrera-Marschitz M (2018). Regionally Impaired Redox Homeostasis in the Brain of Rats Subjected to Global Perinatal Asphyxia: Sustained Effect up to 14 Postnatal Days. Neurotoxicity Research. 34(3):660-676.

Lespay-Rebolledo C, Tapia-Bustos A, Bustamante D, Morales P, Herrera-Marschitz M (2019). The long-term impairment in redox homeostasis observed in the hippocampus of rats subjected to global PA implies changes in glutathione-dependent antioxidant enzymes, and TIGAR-dependent shift towards the pentose phosphate pathways: Effect of nicotinamide. Neurotoxicity Research. doi: 10.1007/s12640-019-00064-4.

DATA FROM THIS THESIS HAVE BEEN PRESENTED AT THE NEXT CONGRESSES:

Redox homeostasis in brain of rats subjected to global perinatal asphyxia. 12th Annual Canadian Neuroscience Meeting 2018 13 May 2018 - 16 May 2018. Vancouver, Canada. Poster presentation.

Effects of oxidative stress induced by perinatal asphyxia on catalase activity in hippocampus of neonatal rats. European Congress of Neuropsycopharmacology ECNP 17-20 September 2016. Vienna, Austria. Poster presentation.

Asphyxia perinatal induces changes in the expression and activity of catalase in an experimental rat model of perinatal asphyxia. International Congress of Brain Research IBRO 7-11 July 2015. Rio of Janeiro, Brazil. Poster presentation.

OTHER PUBLICATIONS NOT INCLUDED IN THE THESIS.

Flores-Balter G, Cordova-Jadue H, Chiti-Morales A, **Lespay C**, Espina-Marchant P, Falcon R, Grinspun N, Sanchez J, Bustamante D, Morales P, Herrera-Marschitz M, Valdés JL (2016). Effect of perinatal asphyxia on tuberomammillary nucleus neuronal density and object recognition memory: A possible role for histamine? Behavioral Brain Research, Vol 313, 226-232. doi:10.1016/j.bbr.2016.07.026.

Tapia-Bustos A, Pérez-Lobos R, Vío V, **Lespay-Rebolledo C**, Palacios E, Chiti-Morales A, Bustamante D, Herrera-Marschitz M, Morales P (2016). Modulation of Postnatal Neurogenesis by Perinatal Asphyxia: Effect of D1 and D2 Dopamine Receptor Agonists. Neurotoxicity Research, Vol 31(1): 109-121. doi: 10.1007/s12640-016-9669-6.

Fernando Ezquer, María Elena Quintanilla, Paola Morales , Marcelo Ezquer , **Carolyne Lespay-Rebolledo**, Mario Herrera-Marschitz & Yedy Israel (2017). Activated mesenchymal stem cell administration inhibits chronic alcohol drinking and suppresses relapse like drinking in high-alcohol drinker rats. Addiction Biology. Vol 24(1): 17-27. doi:10.1111/adb.12572, 1-11.

Mario Herrera-Marschitz, Ronald Perez-Lobos, **Carolyne Lespay-Rebolledo**, Andrea Tapia-Bustos, Emmanuel Casanova-Ortiz, Paola Morales, Jose-Luis Valdes, Diego Bustamante, Bruce K. Cassels. (2018). Targeting Sentinel Proteins and Extrasynaptic Glutamate Receptors: a Therapeutic Strategy for Preventing the Effects Elicited by Perinatal Asphyxia? Neurotoxicity Research. Vol 33(2):461–473. doi 10.1007/s12640-017-9795-9.

Fernando Ezquer, Paola Morales, María Elena Quintanilla, Daniela Santapau, **Carolyne Lespay-Rebolledo**, Marcelo Ezquer, Mario Herrera-Marschitz & Yedy Israel. (2018). Intravenous administration of anti-inflammatory mesenchymal stem cell spheroids reduces chronic alcohol intake and abolishes binge-drinking. Scientific reports 8(1):4325. doi 10.1038/s41598-018-22750-7.

Vio V, Riveros AL, Tapia-Bustos A, **Lespay-Rebolledo C**, Perez-Lobos R, Muñoz L, Pismante P, Morales P, Araya E, Hassan N, Herrera-Marschitz M, Kogan MJ. (2018). Gold nanorods/siRNA complex administration for knockdown of PARP-1: a potential treatment for perinatal asphyxia. International Journal of Nanomedicine. Vol 2018: 13, 6839-6854. doi: 10.2147/IJN.S175076.

THE RESEARCH OF THIS THESIS WAS FINANCIAL SUPPORTED BY:

CONICYT-Chile, Fellowship Nº 21140281.

FONDECYT-Chile Nº 1120079/1190562/1180042.

THIS THESIS WAS DEVELOPMENT IN:

Programme of Molecular and Clinical Pharmacology, ICBM, Laboratory of Dr. Mario Herrera-Marschitz, Medical Faculty, University of Chile.

SCHOLARCHIPS AWARDED TO STUDENT DURING THE DOCTORAL PROGRAM:

Doctoral Scholarship, Faculty of Chemical and Pharmaceutical Sciences, University of Chile, 2013.

Doctoral National Scholarship CONICYT-Chile 2014 (21140281).

Scholarship for 4th ISN Latin American School of Advanced Neurochemistry. Brain Pathologies and Natural Products. 2017. Institute of Biological Research Clemente Estable, Montevideo, Uruguay.

Scholarship for IBRO-USCRC School of Neuroscience: Neural Circuits and Plasticity in Health and Disease. 2018. Montreal, QC and Vancouver, BC. Canada.

Acknowledgements

I would like to acknowledge to two big persons that made possible my PhD studies:

To my mother for helping to remember the importance for pursuing my doctoral studies, supported me during the most difficult moments in my studies and listen all my scientific problems.

To my supervisor Dr. Mario Herrera-Marschitz for his important support and mentorship throughout my PhD studies. Many thanks, for contributing to my scientific career.

Also, I want to thank my sister, father, little cat Chii and especially to my brother Hernán. Many thanks for their support and motivation.

I need to thank my uncle Javier for receiving me in his home during begin of my PhD studies and María Inés for her delicious food and help with my adaptation to Santiago city.

To members of Herrera-Marschitz Lab; Andrea Tapia-Bustos, Ronald Perez, Valentina Muñoz, Paola Morales, Diego Bustamante, Carmen Almeyda and Esteban Palacios. Many thanks, for their company and constant support. I also want to grateful to Dr. María Elena Quintanilla for her compression and for all the expertise shared with me and contribution to my scientific career.

I thank all the members of my PhD committee; for all their input into this Thesis. I am grateful for all the expertise shared with me.

For last, I want to thank to a group very important people: *Daniela Jeria,* María José Velázquez, Camila Muñoz, Carolina Nuñez, Cecilia Cuevas, Natalia Collio, Angélica Morales, Aura Pérez, Vanessa Fabi, Sergio Delgado, Nelson Rozas, Tamara Sabay, María Isabel Sobarzo, Vanessa Berrios, Franco Fernández, Denisse Bravo, Miguel Ángel Zúñiga, Catalina Catalán, and Nicolás Cava. Finally, to María Cecilia Carreño, María Inés Pinilla, Carlos Fuentes, Karime Moreno and Claudia Nuñez. *Many thanks, to all you for helping me to adapt me to the diary job, increase my social skills, their presence made me a better person and I was happy during the job, which was very important to finish my experiments of doctoral thesis after the job.*

Many thanks God for all lived during my PhD studies.

Table of Contents

List of Tables

List of Figures

List of Abbreviations

Ac-LLY-AFC, Ac-Leu-Leu-Tyr-7-amino-4-trifluoromethylcoumarin

ADP/ATP ratio, Adenosine diphosphate/ Adenosine Triphosphate ratio

AFC, 7-amino-4-trifluoromethylcoumarin

AIF, apoptosis inducing factor

AS, asphyxia-exposed rats

a.u., arbitrary units

Bax, Bcl-2 associated X protein apoptosis regulator

Bcl-2, protooncogen Bcl-2 (B-cell lymphoma 2)

Bid, BH3 interacting domain death agonist

BCA, bicinchoninic acid

BSA, bovine serum albumin

β-NADPH, β-Nicotinamide adenine dinucleotide 2′-phosphate

C, cerebellum

Cdk, cyclin-dependent kinase

CNS Central Nervous System

CS, control saline rats

DTNB, 5, 5′-Dithio-bis-[2-nitrobenzoic acid]

DTT, dithiothreitol

ΔA, changes in absorbance per minute

EDTA, Ethylenediaminetetraacetic acid

EGTA, Ethylene glycol-bis (β-aminoethylether)-N, N, N′, N′-tetraacetic acid

ELISA Enzyme-linked immunosorbent assay

FRAP, ferric reducing antioxidant power

Fe^{+2} iron in oxidation state +2

GPx, glutathione peroxidase

GR, glutathione reductase

GSH, reduced glutathione

GSSG, oxidized glutathione

G22, gestation day 22

HI Hypoxic-ischemic

HIE Hypoxic-ischemia encephalopathy

HRP, Horseradish peroxidase

H_2O_2, hydrogen peroxide

H2Od, distillate water

HK2, hexokinase 2

i.p intraperitoneal injection

IgG (H+L), immunoglobulin type G (Heavy + Light chains)

L, liver

mU/mL, mill units enzymatic per millilitre

NaCl, sodium chloride

NAD^+, oxidized nicotinamide adenine dinucleotide

NADH, reduced nicotinamide adenine dinucleotide

$NADP^+$, oxidized β-Nicotinamide adenine dinucleotide 2′-phosphate

NADPH, reduced β-Nicotinamide adenine dinucleotide 2′-phosphate

NADK, NAD^+ kinase

NaF, sodium fluoride

NAMPT, nicotinamide phosphoribosyltransferase

Nico, nicotinamide

NMNAT, nicotinamide mononucleotide adenyltransferase

NMN, nicotinamide mononucleotide

O_2, oxygen

PA, perinatal asphyxia

PARP1, Poly(ADP-ribose) polymerase 1

PB, pink-blue

PBS, phosphate buffer saline

PK, pyruvate kinase

PKC, protein kinase C

PMSF, Phenylmethylsulfonyl fluoride

PFK1, phosphofructokinase 1

PPP, pentose phosphate pathway

P, postnatal day

TP53, tumour protein p53

p53, cellular tumour antigen p53

RE, reticulum endoplasmic

RIPA, radio-immune precipitation assay buffer

ROS Reactive oxygen species

R5P, ribulose-5-phosphate

SEM, standard error of the means

SOD Superoxide dismutase

SDS, Sodium dodecyl sulphate

SDS-PAGE, sodium dodecyl sulphate polyacrylamide gel

SSBR, single strand break DNA

TIGAR, TP53-induced glycolysis and apoptosis regulator

Tris-HCl, tris(hydroxymethyl)aminoethane-chloride acid buffer

TBST, Tris-buffered saline containing 0.1% Tween-20

TNF-alpha, tumour necrosis factor alpha

TUNEL, terminal deoxynucleotidyl transferase dUTP nick end labeling

U/ml, units enzymatic per millilitre

Veh, vehicle

WB, Western blots

XIAP, X-linked inhibitor of apoptosis protein

XRCC1, X-ray repair cross-complementing protein 1

Chapter 1

Introduction

1.1. Perinatal Asphyxia

Oxygen deprivation as a consequence of an impaired placental gas exchange between the mother and the foetus during the perinatal period, or as a consequence of a delay in starting or interruption of autonomous pulmonary-dependent respiration is a clinical condition known as perinatal asphyxia (Herrera-Marschitz et al. 2011; Barkhuizen et al. 2017). The interruption of optimal oxygenation can occur in utero, during labour, delivery, and/or during the first neonatal period (Golubnitschaja et al. 2011). Clinical manifestations of perinatal asphyxia are acidemia (pH < 7) in the umbilical cord, persistence of APGAR scores 0–3 for longer than 5 min, neurological deficits, such as seizures, coma, hypotonia and/or multiorgan system dysfunction (Hankins et al. 2003, Antonucci et al. 2014).

Among the risks for perinatal asphyxia can be pointed out maternal and foetal factors, such as hypertensive disease during pregnancy or preeclampsia, intrauterine growth restriction, placental abruption, foetal anaemia (e.g. rhesus incompatibility), delayed physiological labour (e.g. requiring induction), and/or mal-presentation, including vasa praevia (Nelson et al. 1981; Thornberg et al. 1995). Also, for the Apgar score (Nelson et al. 1981) the presence of meconium stained amniotic fluid, hypoxia-ischemia encephalopathy grading, indicators of maternal infection, presentation and method of delivery and multiorgan system dysfunction are considered (Nelson et al. 1981).

The incidence of perinatal asphyxia is 2-10 per 1000 newborns among on term delivery (Aslam et al. 2014). Perinatal asphyxia is responsible for 38% of death among children under 5 years of age (Bryce et al. 2005), and it is estimated that perinatal asphyxia causes 56 millions of deaths every year (Golubnitschaja et al. 2011). In high-income countries, approximately a 12% of neonatal deaths are related to asphyxia (Ariff et al. 2016, Almeida et al. 2017). In contrast, in low-and middle-income countries, most of neonatal deaths occurring yearly (740.000-1.480.000) are associated with intrapartum asphyxia (Lawn et al. 2005).

Oxygen deprivation following perinatal asphyxia may result in foetal demise, neonatal death or neurological long-term consequences in the neonate's survivors. The neurological damage induced by perinatal asphyxia is known as hypoxic-ischemic encephalopathy (HIE) and is the most serious consequence of perinatal asphyxia, being the major cause of mortality and morbidity in infants affected by perinatal asphyxia. The incidence of HIE has

been estimated to be 1.5 per 1,000 live births (Barkhuizen et al. 2017, Aliyu et al. 2018), shown by 45% of newborn with low Apgar score (Finer et al. 1981).

1.2 The brain injury induced by perinatal asphyxia

The hypoxic-ischemic encephalopathy induced by perinatal asphyxia causes a reduced cerebral blood flow (ischemia) and reduced blood oxygenation (hypoxemia), therefore most of affected neonates manifest hypoxemia and brain hypoxia. If hypoxemia persists for a long time, reduced cardiac output and brain ischemia will result in death or severe damage affecting the neonate (Huang et al. 2008). The outcome implying only hypoxia is less likely to cause brain injury, unless the hypoxia persists for a prolonged time (Huang et al. 2008, Johnston et al. 2001).

The brain of both neonatal and adult subjects is selectively vulnerable to hypoxic-ischemic insults, since not all brain areas are affected in the same degree, or are vulnerable at the same time (Huang et al. 2008). Factors related to maturation, blood irrigation, energy demands, severity and nature of the hypoxia-ischemia, as well as weight of the newborn determine the outcome and the pattern of brain injury, implying neurodevelopmental disabilities in the neonates affected by perinatal asphyxia (Herrera-Marschitz et al. 2011; Golubnitschaja et al. 2011; Barkhuizen et al. 2017). Infants suffering of mild asphyxia might not show any evidence of neurological injury. Nevertheless, cases of moderate asphyxia may present cognitive and behavioural deficits, such as hyperactivity, autism, and attention deficits, or even decreased intelligence scores, but with an onset long after the initial perinatal period. Perinatal asphyxia has been associated with psychosis and schizophrenia, which are syndromes debuting first at post pubertal periods. Severe asphyxia has also been associated with cerebral palsy, mental retardation, neurodegenerative diseases and epilepsy (see Herrera-Marschitz et al. 2011, Golubnitschaja et al. 2011).

Several neuroanatomical patterns of injury (**Figure 1**) have been observed in infants suffering perinatal asphyxia (Huang et al. 2008, Swarte et al. 2009), including:

- **Deep grey matter injury** (Pattern 1, 2 and 3), involving thalamus, putamen, subthalamic nucleus, cortex, striatum, globus pallidus, hippocampus, central gyri, paracentral lobule, white matter, substantia nigra, brainstem, cerebellum and spinal cord. Neonates with extensive deep grey matter injury die a few days after birth or

develop spastic/dyskinesia and/or quadriplegia.

- **Isolated watershed injury** (Pattern 4), involving posterior parietal and subcortical areas. The neonates develop deficits without apparent motor dysfunction, although childhood seizures can occur.
- **Primary leukomalacia** (Pattern 5): It affects white matter and neocortex. The neonates show motor impairment affecting legs, as well as visual functions.
- **Isolated cortical necrosis** (Pattern 6), affecting hippocampus mainly, subiculum and H1. The internal cerebellar granular layer can also be affected.

1.3 Molecular mechanism for progression of brain injury induced by perinatal asphyxia and/or hypoxia-ischemia

The pathogenesis of hypoxic-ischemic encephalopathy is characterized by progressive activation of several molecular and cell events, explaining the extension of brain damage, from weeks to months as well as delayed neurological disabilities. The biochemical changes in the immature brain lead to neuronal death, and alteration of brain development and maturation. Neuronal death occurs at two periods following perinatal asphyxia (Stone et al. 2008). The first period implies primary cell death, occurring during the hypoxia-ischemia event. The second period implies delayed cell death, occurring hours after the hypoxia-ischemia event, continuing even for several weeks. The energy failure triggers cell death during both periods (Vannucci et al. 2004, Alonso-Spilsbury et al. 2005). A third period of neuronal death has been described, occurring months and/or years after the insult (Hassell et al. 2015).

Primary cell death period

During a hypoxia-ischemia event, low oxygen and glucose supplementation modifies the energetic metabolism of the immature brain, from aerobic to anaerobic metabolism. Glucose is metabolized by anaerobic glycolysis under the hypoxia period and its turnover is increased to maintain ATP levels. Therefore, glucose uptake and glycolysis increase (Alonso-Spilsbury et al. 2005). However, glycolysis is not enough to maintain ATP levels, because glucose availability is decreased as a consequence of a decreased cerebral perfusion. Furthermore, lactate and protons accumulate as the result of anaerobic

glycolysis, decreasing the perfusion pressure, impairing further the cerebral blood flow (Lai et al. 2011). Thereby, during an extent hypoxia-ischemia event, ATP levels fall further, worsening the primary energy failure, decreasing Na^+/K^+-pump and Ca^{2+} ATPase activity, but also producing lactic acid accumulation and acidosis, importing Na^+ from the extracellular compartment, via the Na^+/H^+ exchanger (NHE) of the plasmatic membrane. This increased cytosolic Na^+ is exported through the Na^+/Ca^{2+} exchanger causing an increase in cytosolic calcium, promoted also by the failure of Ca^{2+} ATPase. However, although NHE exports Na^+ to the extracellular space, it also accumulates at high concentration in the cytosol, delaying the recovering of homeostasis due to reduced activity of Na^+/K^+-pump (Brookes et al. 2004). Thereby, a failure in the Na^+/K^+-pump and Ca^{2+} ATPase leads to membrane depolarization and presynaptic release of glutamate, an excitatory neurotransmitter, which also binds to available extrasynaptic glutamate receptors. The activation of these receptors contributes to increase calcium conductance, leading to overload of cytosolic calcium (Johnston 2005), resulting in:(i) activation of lipases, proteases and endonucleases, which in turn destroy intracellular structures; (ii) activation of neuronal nitric oxide synthase (nNOS), which increases nitric oxide (NO) levels, and (iii) Ca^{2+} mitochondrial overload, causing mitochondrial dysfunction, triggering further calcium-dependent events (Brookes et al. 2004; Blomgren et al. 2006), i.e. activation of mitochondrial nitric oxide synthase (mNOS), generating NO, inhibiting complex I and IV of the electron transport chain, increasing superoxide anion levels; dissociation of cytochrome c from the inner mitochondrial membrane; cardiolipin (1,3-bis(sn-3'-phosphatidyl)-sn-glycerol) oxidation by mitochondrial ROS, promoting the release of cytochrome c to cytosol, opening of transition pore to calcium and superoxide anions, leading to mitochondrial depolarization, and apoptosis activation.

Secondary or delayed cell death

After a hypoxia-ischemia event, perfusion and oxygenation have to be restored for recovering ATP levels and cellular homeostasis (Lorek et al. 1994). However, in the following 24h there is a secondary ATP decreasing period, which is more pronounced at 48 hours, an event known as secondary energy failure, beginning 8-16 hours during the reperfusion-oxygenation (RO) period, ATP reaching the lowest point at 24-48h, depending

upon the nature of the insult (Thoresen et al. 1995, Vannucci et al. 2004). The neuronal death occurring during the RO period is called delayed cell death and results in the activation of several mechanisms, during and after the RO period (Dirnagl et al. 1999, Jin et al. 2010). Under the first minutes during the RO period, up to the first hours, neuronal death occurs by excitotoxicity-mediated mechanisms, involving glutamate, leading to mitochondrial dysfunction, free radicals and apoptosis (Dirnagl et al. 1999). After the RO period the neuronal damage continues for days and weeks because of the activation of inflammatory responses (Benjelloun et al. 1999; Hudome et al., 1997). Inflammation is triggered by activation of microglia, resulting in infiltration of inflammatory cells, including neutrophils, macrophages, and T cells into the damaged brain region (Ryan et al. 2012; Liu et al. 2013). The activated microglia release NO by activation of iNOS, and pro-inflammatory cytokines, such as TNF-α, IL1β, IL6, MCP1, MIP1α; inducing ICAM1, P-selectin, E-selectin and integrin expression in local vasculature, promoting adhesion and transmigration of leukocytes and platelets into the injured brain area (Ryan et al. 2012). The accumulation of leukocytes into the injured brain area is crucial to the extent of inflammation and secondary brain damage. Leukocytes release pro-inflammatory cytokines, proteases, prostaglandins, complement factors, free oxygen and nitrogen species (Jin et al. 2010). These neurotoxic factors damage neuronal populations and brain microvasculature, including contractile pericytes on capillary walls (Nortley et al. 2019) contributing to disruption of blood brain barrier and formation of vasogenic oedema (Nguyen et al. 2007).

The secondary damage promoted by the inflammatory response can last days or months (Benjelloun et al. 1999; Winerdal et al. 2012). Therefore, the RO period is considered as an opportunity for treatment, due to its wide therapeutic window. The severity of a secondary energy failure in neonates determines death or survival, and it correlates with the severity of the neurological outcome (Polin et al. 2007).

Tertiary cell death period

The pathological process of brain damage induced by a hypoxia-ischemia insult can continue for months and years, for which this period or phase is known as tertiary brain

injury (Hassell et al. 2015, Fleiss et al. 2012). The infants show persisting cerebral lactic acidosis over the first year after birth and adverse neurodevelopmental outcomes (Robertson et al. 1999). The mechanisms of persisting brain damage involve gliosis, inflammatory receptor activation and epigenetic changes (Fleiss et al. 2012, Hagberg et al. 2015).

1.4 Therapeutic strategies for brain injury induced by perinatal asphyxia

Several specific neuroprotective pathways are available as targets for minimizing the extent of neuronal damage. Some therapeutic strategies imply N-acetylcysteine, allopurinol, magnesium sulphate, glutamate receptors blockers, erythropoietin and hypothermia (Hobson et al. 2013; Cerio et al. 2013). However, at present, these strategies have not proven to be safe and/or effective against the neurological sequels observed in neonates, mainly due to insufficient knowledge about the timing and extend of a therapeutic window viable for human newborns (Cerio et al. 2013).

Mild hypothermia is the only treatment approved for perinatal asphyxia (Shah 2010, Eicher et al. 2005), together with intensive neonatal care (Arnaez et al. 2018, Antonucci et al. 2014). Hypothermia can be applied to the head or to the whole body of the neonate, cooled for 48 to 72 hours, decreasing the infant's body temperature to 33°-36.5°C (Gunn et al. 1998). Its effectivity and safety has been proved by several clinical trials, demonstrating a reduced rate of cerebral palsy, death and improving mental and psychomotor outcomes (Edwards et al. 2010, Jacobs et al. 2013). However, there is still a 45% of infants dying or not showing any real improvement of disabilities (Robertson et al. 2012). Furthermore, neuroprotection by hypothermia is limited by a narrow therapeutic window, needed to be applied within a 6-hour window to be effective (Azzopardi et al. 2016). There are other clinical conditions affecting the neonates surviving perinatal asphyxia, such as inflammation (Osredkar et al. 2014, Wintermark et al. 2010), and immune response induced by hypothermia that may contribute to a poor recovery (An et al. 2014).

Experimental treatments with EPO (Zhu et al. 2009, Elmahdy et al. 2010), DHA (Berman et al. 2009, Suganuma et al. 2010), Xenon (Dingley et al. 2006, Thoresen et al. 2009) have been attempted in trials with HIE infants, but similar to hypothermia a recovery has only

been seen among infants following moderate HIE, but not following severe HIE, with a therapeutic window limited to 4 hours (Elmahdy et al. 2010) after PA.

1.5 The role of oxidative stress in neonatal brain injury following hypoxia-ischemia conditions

The oxidative stress generated by perinatal asphyxia is an important target for reducing brain damage, since free radicals are biomolecules involved in apoptosis, also because of the enhanced susceptibility of the immature brain to oxidative stress (Vasiljević et al. 2012).

The role of oxidative stress in neuronal damage has been evidenced by administration of antioxidant molecules. The administration of alpha-tocopherol before hypoxia-ischemia or immediately after reperfusion-oxygenation in human neonates exposed to asphyxia perinatal showed a reduction of oxidative stress, increasing glutathione (GSH) levels (Karim et al. 2005). In a similar way, the administration of amentoflavone to neonatal 7 day old rats, before a postnatal hypoxia-ischemia event, decreased neuronal damage, preventing the activation of caspase-3 (Shin et al. 2006). These results support the role of oxidative stress in the neurological damage induced by hypoxia-ischemia and therefore, the potential therapeutic impact of antioxidant strategies.

The main mechanisms suggested to play a role in the generation of free radicals following hypoxia-ischemia conditions are:

(i) **Mitochondrial dysfunction**, elevating superoxide anion levels during the hypoxic-ischemic period (Abramov et al. 2007).

(ii) **Xanthine Oxidase,** increasing levels of superoxide anion at the end of the hypoxic-ischemic and during the reperfusion-oxygenation period. The calcium overload induced by glutamate causes activation of calpain that activates xanthine oxidase, and its activity is favoured by the accumulation of hypoxanthine and xanthine during the hypoxic-ischemic period (Abramov et al. 2007).

(iii) **NADPH oxidase.** It is activated in neurons, microglia, neutrophils and macrophages, playing a main role during the reperfusion-oxygenation period, increasing anion superoxide levels, also contributing to oxidative damage due to its role in the release of glutamate,

increasing excitotoxicity during the reperfusion-oxygenation period (Abramov et al. 2007; Wang et al. 2013).

(iv) **Nitric Oxide Synthase (NOS)**. Endothelial NOS is activated by hypoxia-ischemia to maintain the cerebral blood flow. Neuronal NOS is also activated during hypoxia-ischemia and during the reperfusion-reoxygenation period. NO produced by overactivation of both nNOS and iNOS contributes to brain damage. The formed NO increases nitronium free radicals, yielding reactive species, such as peroxynitrite, nitrogen dioxide and nitronium ion (NO^{2+}), partly responsible of secondary neuronal damage. Also, NO can diffuse to neighbouring cells amplifying the damage (Pradeep et al. 2012)

(v) **Myeloperoxidase (MPO)**. It is a lysosomal enzyme secreted by leucocytes, as a response to oxidative stress. It generates hypochlorous acid (HOCl) that modifies lipids and proteins, causing local tissue damage and amplification of the inflammatory cascade. MPO is activated 48-72 h after reperfusion, promoting the dysfunction of the blood brain barrier, endothelium, and neurons (Matsuo et al. 1994; Like et al. 2002).

Thereby, a reperfusion-reoxygenation event after hypoxic-ischemia triggers a metabolic cascade generating oxidant molecules and free radicals, such as NO, superoxide anion, hydrogen peroxide, hydroxyl radicals and peroxynitrite. The redox imbalance caused by these molecules leads to oxidative stress in the brain of neonates, resulting in apoptosis, lipid peroxidation, DNA and proteins oxidation, as well as inflammation (Wong et al. 2008).

The immature antioxidant status of the brain contributes also to oxidative stress. As mentioned above the immature brain has low levels and low activity of antioxidant enzymes, since the maturation of the antioxidant system correlates with brain maturation (Galkina et al. 2009). Thus, studies performed in 10, 20 and 90 days old rats demonstrated that the activity of cytoplasmic superoxide dismutase (SOD1), glutathione (GSH), and glutathione peroxidase (Gpx) increased along development (Galkina et al. 2009).

Furthermore, the susceptibility of immature brain to oxidative stress is enhanced under the hypoxia-ischemia condition, due to the fact that oxidative stress induces downregulation of the expression of antioxidant enzymes, restricting the antioxidant defences of the immature

brain (Homi et al. 2002). The mechanism by which oxidative stress causes reduction of the expression of brain antioxidant enzymes is not well established, but it may be associated to epigenetic changes, as seen in myocardial and hepatic hypoxia-reperfusion models, in which a prolonged exposure to reactive oxygen species (ROS) causes downregulation of the expression of catalase, via hypermethylation of CpG islands in the catalase promoter (Quang et al. 2011). However, free radicals can also act directly on enzymes, modifying their activity, as evidenced by an oxidative stress model induced with cytokines in beta-pancreatic cells, in which increased NO levels inhibited the activity of catalase, causing apoptosis (Sigfrid et al. 2003).

Among several antioxidant systems (**Figure 2**), glutathione (GSH) is the main antioxidant of the brain, which is composed of three amino acids: glutamic acid, cysteine and glycine. GSH is found in the 2-3 mM concentration range in brain tissue, higher than in blood or cerebrospinal fluid (CSF) (Janaky et al. 2007). GSH levels increase along with brain development. Studies in cerebellum and neocortex showed low GSH levels at postnatal day 3 and a maximum at postnatal day 7. From postnatal day 10 a gradual increase has also been observed, up to adult levels (Khan et al. 2003). GSH scavenges multiple oxidative species, such as superoxide, NO, hydroxyl radicals, and peroxynitrite. GSH is also an essential cofactor for glutathione peroxidase (Gpx), found at higher than catalase concentration in the brain. GPx plays a role reducing hydrogen peroxide and oxidized lipids (Janaky et al. 2007).

In comparison with astrocytes, neurons are more susceptible to oxidative stress, due to lower levels of GSH. This led to the suggestion that astrocytes support the redox homeostasis of neurons, providing them with GSH and/or the precursors for the synthesis of GSH, such as cysteine, which enters into neurons via the excitatory amino acid carrier 1 (EAAC1), facilitating neuronal GSH synthesis (Langeveld et al. 1995). The GSH levels are decreased under ischemia-reperfusion, as shown by cerebral ischemia-reperfusion models in rats. GSH levels were decreased in the striatum and hippocampus during reperfusion, accompanied by an increase in the levels of malondialdehyde (MDA) and reactive oxygen species (Shivakumar et al. 1995). The decrease in GSH levels is explained by decreased cysteine uptake by EAAC1, which is impaired under oxidative stress (Nieoullon et al. 2006).

Superoxide dismutase (SOD) catalyses the dismutation of superoxide anion into H_2O_2. In mammals, there are three SOD isoforms, (i) cupper/zinc SOD (SOD1), present in the cytosol; (ii) manganese SOD (SOD2), present in the mitochondrial matrix, and (iii) extracellular SOD (SOD3), present in the extracellular space. In the immature brain, SOD1 is widely expressed by neurons, mainly in neocortex, hippocampus and hypothalamus, but also under hypoxia-ischemia events. Glutamate excitotoxicity causes downregulation of the expression of SOD1 in neurons, resulting in increased susceptibility to oxidative damage (Mc Donald et al. 1990; Peluffo et al. 2005). Thus, SOD1overexpression has emerged as a neuroprotective target, although at post-natal day 7 the overexpression of SOD1 causes accumulation of H_2O_2 levels in brain of rats subjected to hypoxia-ischemia before birth, producing apoptosis of neurons and oligodendrocytes, also reducing the activity of glutathione peroxidase (GPx) at 2-24h after hypoxia-ischemia (Sheldon et al. 2004). These results suggest a possible role of H_2O_2 in neuronal damage induced by hypoxia-ischemia events, also that the immature brain accumulates more H_2O_2 than the mature brain after a hypoxia-ischemia insults (Lafemina et al. 2006), which may be explained by low catalase activity in the immature brain. Indeed, catalase levels do not increase together with brain development, in contrast with other antioxidant enzymes (De(Addya) et al. 1986). A comparative study in human foetal brain with 20-27 weeks of gestation demonstrated that catalase activity did not change between 12 and 27 weeks of gestation, but yes at 28 weeks of gestation, decreased in brain, in contrast to that observed in liver and kidney, where the enzyme activity increases in parallel with the advancement of pregnancy. In the same study, the activity of SOD increased in brain, liver and kidney, together with gestational weeks (De(Addya) et al. 1986).

In hypoxia-reperfusion models performed in heart, liver and retina (Abou-El-Hassan et al. 2011; He et al. 2006; Chen et al. 2011), the overexpression of catalase reduced H_2O_2 levels, preventing lipid peroxidation, DNA damage and protein oxidation. Also, catalase enhanced the activity of SOD, resulting in lower levels of superoxide anion and suppression of the activation of transcription factors NF-kB and AP-1, reducing the inflammation induced by ischemia-reperfusion (He et al. 2006). Furthermore, catalase has been shown to play a role in several neurological diseases. Thus, in mice Alzheimer models, increased catalase levels resulted in reduction of peptide beta-amyloid and ROS levels (Kassmann et al. 2007). The

absence of catalase in peroxisomes causes severe neurological disorders, such as Zellweger syndrome (Sheikh et al. 1998), resulting in defects in peroxisomal enzymes, reduction in the activity of electron transport chain and increased mitochondrial ROS, leading to death cell (Walton et al. 2012).

1.6 Redox balance and energetic metabolism in neonatal brain under hypoxia-ischemia conditions

NAD^+ and $NADP^+$ are the main electron carriers sustaining cell metabolism and redox homeostasis (Massudi et al. 2012; Chong et al. 2003). NAD^+ is used to drive oxidative phosphorylation, maintaining ATP levels according with cell needs (Stein et al. 2012). NAD^+ also contributes to DNA repair by ADP-ribosylation mediated by PARP-1 (Houtkooper et al. 2012).

Oxidative stress induces DNA damage, leading to depletion of NAD^+ by over-activation of PARP-1 (Berger 1985; Virag and Szabo 2002; Ying et al. 2010; Neira-Peña et al. 2015), as a consequence of energetic cell failure and decreased ATP synthesis (Klaidmanet al. 2003; Liu et al. 2009), resulting in cell death (Turunc et al. 2013). The administration of NAD^+ precursors, such as nicotinamide ribose in a mouse sepsis model displayed prevention of oxidative stress and apoptosis by increasing NAD^+ levels, which resulted in SIRT1 activation (Hong et al. 2018).

NADPH contributes to cell redox balance and proliferative fate, maintaining the activity of antioxidant enzymes, GSH:GSSG ratio and sustained cell repair, including DNA repair systems (Stincone et al. 2015; Riganti et al. 2012; Ying et al. 2008). The synthesis of NADPH can also be driven to either (**i**) the pentose phosphate (PPP), or (**ii**) the salvage pathway (Ying et al. 2008; Chakrabarti et al. 2015).

The oxidative phase of the pentose phosphate pathway (**Figure 3**) starts with a shunt towards oxidation of glucose-6-phosphate to 6-phosphogluconolactone by glucose-6-phosphate dehydrogenase (G6PDH), resulting in the formation of NADPH. Then, 6-phosphogluconolactone is oxidised to 6-phosphogluconate, which, by oxidative decarboxylation mediated by 6-phosphogluconic dehydrogenase (6PGDH) produces a second molecule of NADPH, CO_2 and ribulose 5-phosphate, converted then into ribose 5-phosphate, required for the synthesis of nucleotides (Stincone et al. 2015). The NADPH

produced via this pathway is used as reduction molecule for lipid synthesis (fatty acid, cholesterol, and steroid hormones), detoxification, and also for maintaining the enzymatic activity of glutathione reductase (GR), an enzyme that reduces oxidized glutathione (GSSG) to yield reduced glutathione (GSH), therefore PPP contributes to maintain GSH levels (Stincone et al. 2015; Riganti et al. 2012).

Glucose-6-phosphate dehydrogenase (G6PDH) is the limiting enzyme of PPP. The activity of this enzyme is dependent of the $NADP^+$/NADPH ratio, so $NADP^+$ acts as an allosteric modulator stabilizing the active conformation of the enzyme, whereas NADPH de-stabilizes this conformation, inhibiting the activity of the enzyme (Stanton 2012). Under basal conditions, G6PDH has low activity, but it is increased under conditions of oxidative stress, lipid synthesis, DNA repair and synthesis, or detoxification, resulting in increased PPP flux (Cao et al. 2015).

The non-oxidative phase of the PPP (**Figure 3**) converts pentoses-5-phosphate to hexoses monophosphate and triose phosphate, reincorporating them into the glycolytic pathway, or reintroducing them into the PPP (Riganti et al. 2012). The ribose-5-phosphate and xylulose 5-phosphate are converted into glyceraldehyde 3-phosphate and sedoheptulose 7-phosphate by transketolase (TKT), subsequently, converted into fructose 6-phosphate and erythrose 4-phosphate by transaldolase (TALDO). The erythrose 4-phosphate produces fructose 6-phosphate and glyceraldehyde 3-phosphate, which can either be metabolized in the glycolytic pathway or reintroduced into the PPP (Stincone et al. 2015). TALDO is the rate-limiting enzyme of the non-oxidative PPP and its increased activity contributes to increase susceptibility to oxidative stress, reducing GSH and NADPH levels (Kuehne et al. 2015; Riganti et al. 2012).

Under hypoxia-ischemia conditions the shunt of glucose-6-phosphate to PPP is dependent upon TIGAR (Tp53-inducible glycolysis and apoptosis regulator) for yielding NADPH, identified as a p53-inducible gene (Bensaad et al. 2006; Li et al. 2014; Cao et al. 2015). TIGAR acts as a phosphofructokinase. It presents sequence homology with the bi-phosphatase domain (FBPase-2) of PFK-2/FBPase-2 (6-phosphofructo-2-kinase/fructose-2,6-bisphosphatase), which degrades fructose-2,6-bisphosphate (Fru-2,6-P2), inhibiting glycolysis, resulting in the glucose-6-phosphate shunt of the PPP (Bensaad et al. 2006). In brain hypoxia-ischemia, there is a high correlation between TIGAR and NADPH and GSH

levels, resulting in decreased susceptibility of cells to oxidative stress, apoptosis and DNA damage (Li et al. 2014; Chen et al. 2018; Yu et al. 2015). TIGAR expression decreases along development, achieving low levels in the adult brain, compared to the neonatal brain (P1 to P30), period showing the highest TIGAR levels (Li et al. 2014). In models of cerebral ischemia in adult mice, ROS has a role in the induction of TIGAR during reperfusion and/or reoxygenation. In a model of primary cortical neurons, the exposition to H_2O_2 (30 μM) up-regulated TIGAR, while NADPH blocked this effect (Sun et al. 2015). In contrast, neonatal brain exposed to hypoxia-ischemia displayed a reduced PPP activity after the insult, correlating with a reduction of glutathione reductase activity (by 50%) (Brekke et al. 2014).

The salvage pathway for NADPH synthesis (**Figure 4**) is coupled to NAD^+ synthesis from nicotinamide (Ying *et al*. 2008). Niacin (vitamin B3) exists as nicotinamide or nicotinic acid, available from dietary (Poljsak *et al*. 2016). In mammals, nicotinamide ribose is known as the only precursor supporting NAD^+ synthesis. NADPH generation can be driven by the NAD^+ salvage pathway via NAmPRT, which catalyses the transfer of the phosphoribosyl group from 5-phosphoribosyl-1-pyrophosphate to nicotinamide, forming nicotinamide mononucleotide and pyrophosphate. NAD^+ generation can then be coupled to NAD^+ kinase (NADK) activity to generate $NADP^+$ that can then be reduced to NADPH through the PPP pathway (Massudi et al. 2012).

Nicotinamide plays a role as a precursor of NAD^+ and $NADP^+$, replenishing exchangeable nucleoside phosphate pools. Both, nicotinamide and ribose analogues contribute to increase NAD^+ levels in brain models of cerebral ischemia (Park et al. 2016; Vaur et al. 2017). In models of oxidative stress *in vitro*, it has been demonstrated that nicotinamide can inhibit lipid peroxidation started by hydroxyl radicals and superoxide anions (Kamat et al. 2009). In consequence, intraperitoneal administration of nicotinamide for 7 days in a rat model of Alzheimer's disease has demonstrated a protective role, reducing oxidative stress and apoptosis induced by amyloid β peptide 1-42 (Turunc et al. 2013). A decrease of PARP1 over-activation, NF-κβ up-regulation and increased catalase and glutathione peroxidase enzymatic activity was found in hippocampus and neocortex from rats treated with nicotinamide 100 and 500 mg/Kg (Turunc et al. 2013). Similar results were found in diabetic rats orally treated with 200 mg/kg of nicotinamide, showing an increase in the

expression of antioxidant enzymes, such as SOD and catalase in liver (John et al. 2012). The neuroprotective effect of nicotinamide in perinatal asphyxia has been evaluated by intraperitoneal administration of repeated or a single dose of nicotinamide (0.8 mmol/kg, i.p.) 1h after asphyxia (Klawitter et al. 2006; 2007), yielding an intracerebral concentration of 10 µM of nicotinamide for approximately 5 hours, as monitored by *in vivo* microdialysis (Allende-Castro et al. 2013). In a model of global PA *in vivo*, nicotinamide produced a reduction of apoptosis and neuroinflammation, via decreasing PARP1 over-activation (Neira-Peña et al. 2015; Bustamante et al. 2003; Allende-Castro et al. 2013).

1.7 Purpose of Thesis

In hypoxia-ischemia models of neonatal brain, the activation of molecular events has been described to be associated to excitotoxicity, calcium overload and inflammation, contributing to the progression of brain damage. Although, all these consequences are associated to free radicals and redox misbalance, their contribution to brain damage have been described in most studies to occur during the first hours of the reperfusion-oxygenation period. Indeed, the neonatal brain is highly susceptible to oxidative stress and antioxidant therapies have been proposed to restore the redox balance and death cell in ischemia models.

In this Thesis, the effect of perinatal asphyxia on redox homeostasis associated to the progression of brain damage has been studied, using a model of perinatal asphyxia in rat characterized by global asphyxia, producing severe hypoxia, simulating a clinical condition affecting human babies.

The following aims have been proposed:

(**i**) The first aim was to determine whether severe perinatal asphyxia in rat produces an alteration of redox homeostasis, sustained along the time, affecting brain areas described as highly susceptible to hypoxia-ischemia. Hereby, focusing on mesencephalon, hippocampus and telencephalon, showing differences in maturation timing and susceptibility to hypoxia insults. Redox homeostasis was studied from P1 to P14, a time period under which perinatal asphyxia induces delayed cell death in rat neonatal brain, determining a relationship between redox homeostasis and delayed cell death.

(**ii**) The second aim of this Thesis was to determine the contribution of redox balance to brain damage induced by perinatal asphyxia, focusing on hippocampus, a brain area highly susceptible to oxidative stress. The impaired redox homeostasis was restored by nicotinamide, a precursor of NAD^+/$NADP^+$. The effect of nicotinamide on the consequences of perinatal asphyxia was evaluated at P1 and P14.

1.7.1 Hypothesis

The progression of brain damage during a delayed cell death period in vulnerable brain areas of animals exposed to perinatal asphyxia is associated with sustained oxidative stress along development, impairing redox homeostasis. Nicotinamide enhances the response of glutathione-dependent enzymes by a pentose phosphate dependent pathway, preventing the progression of asphyxia-dependent brain damage.

1.7.2 General Aims

(**a**) To determine whether perinatal asphyxia induces a sustained oxidative stress during a period of delayed cell death in vulnerable brain areas.

(**b**) To determine whether perinatal asphyxia and nicotinamide induces a modulation of glutathione dependent-antioxidant and brain damage cell responses in hippocampus.

1.7.3 Specific Aims

(i) To evaluate oxidative stress in the brain of rats exposed to global perinatal asphyxia, measuring GSSG:GSH ratio and iron reducing capacity (FRAP), focusing on mesencephalon, hippocampus and telencephalon at postnatal days 1, 3, 7 and 14.

(ii) To evaluate the removal of peroxide hydrogen in brain of rats exposed to global perinatal asphyxia, measuring the expression and activity of catalase, focusing on mesencephalon, hippocampus and telencephalon at postnatal days 1, 3, 7 and 14.

(iii) To evaluate delayed cell death in brain of rats exposed to global perinatal asphyxia, measuring caspase-3 protein levels, focusing on mesencephalon, hippocampus and telencephalon at postnatal days 1, 3, 7 and 14.

(iv) To evaluate the effect of perinatal asphyxia and nicotinamide on glutathione, measuring reduced and oxidized glutathione levels, determining the GSSG:GSH ratio as an index of oxidative stress in the hippocampus of neonatal rats 1 and 14 days after birth.

(v) To evaluate the effect of perinatal asphyxia and nicotinamide on the removal of hydrogen peroxide, measuring glutathione peroxidase activity together with protein levels and enzymatic activity of catalase in the hippocampus of neonatal rats 1 and 14 days after birth.

(vi) To evaluate the effect of perinatal asphyxia and nicotinamide on the pentose phosphate pathway, measuring TIGAR protein levels and glutathione reductase activity in the hippocampus of neonatal rats 1 and 14 days after birth.

(vii) To evaluate the effect of perinatal asphyxia and nicotinamide on cell damage, measuring XRCC1 protein levels and calpain activity in the hippocampus of neonatal rats at 1 and 14 days after birth.

Chapter 2

Materials and Methods

2.1 Materials

2.1.1 Reagents and solvents

Acetic Acid, ACS for analysis. WINKLER; Product code: AC-0030; Lot: LTBP111017; FW: 60.05 g/mol; Purity: ≥ 99.7 %.

40% Acrylamide/Bis Solution, 19:1. BIORAD; cat: 1610154; control: 64061776.

Alkylphenoxypolyethoxy ethanol (Triton X-100). New England Nuclear; Product code: NEF-936; Lot: 054TX1.

Ammonium persulfate (APS), for molecular biology. WINKLER; Product code: BM-0250; Lot: K4398301; FW 228.19 g/mol; Purity: 98.7%.

2-β Mercaptoethanol, for molecular biology. WINKLER; Product code: BM-1200; Lot: 2571C508; FW: 78.13 g/mol; Purity: ≥ 99.5 %; Humidity: 0.25%.

β-Nicotinamide adenine dinucleotide 2-phosphate reduced tetrasodium salt hydrate (NADPH). SIGMA ALDRICH; Product code: N1630; Lot: SLBM0996V; FW: 833.35 g/mol; Purity (hplc): ≥ 93 %.

β-Nicotinamide adenine dinucleotide 2-phosphate reduced tetrasodium salt hydrate (NADPH). MP Biomedicals LCC; Product code: 151742; Lot: QR10019; FW: 833.4 g/mol; Purity (hplc): ≥ 93 %.

Bovine Serum Albumine, for molecular biology. WINKLER; Product code: BM.0150; Lot: 1262C458; Purity: 100 %; Humidity: 0.4267%.

Butanol, HPLC grade. MERCK; Product code: 9628; Lot: 6931513; FW: 74.12 g/mol; Density: 0.81 kg/l.

Brilliant Blue R, pure. SIGMA-ALDRICH; Product code: B7920; Lot: MKBS9408V; FW 825.97 g/mol; Purity (HPLC) ≥ 70 %.

Bromophenol blue, analytical grade. WINKLER; Product code: AZ-0395; Lot: WE1029; FW 60.06 g/mol.

Chloride acid (HCl), ACS for analysis. WINKLER; Product code: AC-0065; Lot: 507141; Density: 1.184 kg/l; Purity: ≥ 37.3 %.

Chloride acid (HCl), ACS for analysis. WINKLER; Product code: AC-0065; Lot: 729141; Density: 1.184 kg/l; Purity: ≥ 36.5-38 %.

Deoxycholic Acid, Sodium Salt (C24H39O4Na), for molecular biology. WINKLER; Product code: BM-0035; Lot: 3341C100; FW 414.57 g/mol; Purity: 103.7 %; Humity: max. 5.0%.

Dithiothreitol (DTT), molecular biology grade. WINKLER; Product code: BM-0665; Lot: 6N012910; FW 154.25 g/mol; Purity: 99.5%.

5,5 Dithiobis(2-nitrobenzoic acid) DTNB, ≥ 98 %, Bioreagent. SIGMA-ALDRICH; Product code: D8130; Lot: SHBF3784V; FW 396.35 g/mol.

Ethylenediaminetetraacetic acid (EDTA), for molecular biology. WINKLER; Product code: BM-0680; Lot: 20072568; FW 372.24 g/mol; Purity: 100.0 %.

Ethylene glycol-bis(β-aminoethyl ether)-N,N,N′,N′-tetraacetic acid (EGTA), for molecular biology. WINKLER; Product code: BM-0693; Lot: 1499B506; FW 380.35 g/mol; Purity: 99.12%; Humity: 0.8848%.

Glycerol, EMSURE Reagent PhEur for analysis. MERCK; Product code: 1.04094.1000; Lot: Z0313094406; Density: 1.23 kg/l; Purity (GC): ≥ 84.5-85.5 %; Humidity: 14.5-15.5%.

Glycine (Gly), for molecular biology. WINKLER; Product code: BM-0820; Lot: 7T011330/0544c518; FW 75.07 g/mol; Purity: min 99.6 %.

Hydrogen peroxide 30% (H_2O_2), Perhydrol p.a. Pro analysis. MERCK; Product code: 1072010.1000; Lot: K36414310704; Density: 1.11 g/cm^3.

Iron(III) Chloride anhydrous for synthesis. MERCK; Product code: 803945; FW 162.20 g/mol; Purity: ≥ 98%.

L-glutathione oxidized (GSSG). SIGMA ALDRICH; Product code: G4376; Lot: SLBM9313V; FW: 612.63 g/mol; Purity (hplc): ≥ 98 %.

L-glutathione reduced (GSH). SIGMA ALDRICH; Product code: G4251; Lot: SLBH7927V; FW: 307.32 g/mol; Purity (hplc): ≥ 98 %.

Meta-Phosphoric acid, ACS reagent chips, 35.5-36.5 %. SIGMA-ALDRICH; Product code: 239275; Lot: MKBT0873V; FW 79.98 g/mol.

Metanol, EMSURE for analysis. MERCK; Product code: 1.06009.2511; Lot: I865309701; FW: 32.04 g/mol; Density: 0.792 kg/l.

Niacinamide (Nicotinamide). SIGMA Aldrich; Product code: N-3376; Lot: 111K0026; FW 122.1 g/mol; Purity (HPLC) ≥98%.

N, N, N′, N′-Tetramethylethylenediamine (TEMED), for molecular biology. WINKLER; Product code: BM-1970; Lot: 0304C531/0430C516; FW 116.21 g/mol; Purity: 99.9%.

Polyoxyethylenesorbitanmonolaurate (TWEEN 20), molecular biology reagent. MP Biomedicals, LLC; Product code: 11TWEEN201; Lot: Q1831; FW 116.21 g/mol; Purity: 99.9%; Water Content: 2.2%; Density (25°C): 1.11 g/ml.

Ponceau S, practical grade. SIGMA-ALDRICH; Product code: P3504; Lot: MKBB2133; FW 760.58 g/mol.

Potassium phosphate monobasic (KH_2PO_4), for molecular biology. WINKLER; Product code: PO-1290; Lot: 004404; FW 136.09 g/mol; Purity: min 99.3 %; Humidity: 0.01%.

Potassium phosphate dibasic anhydride (K_2HPO_4), for analysis. Mallinckrodt; Product code: 7092; Lot: 7092V33D07; FW 174.18 g/mol; Purity: min 99.6 %; Humidity: 0.08%.

Potassium Ferricyanide ($K_3Fe(CN)_6•3H_2O$) grade I. SIGMA ALDRICH; Product code: P-8131; Lot: 14C2730; FW:329.3 g/mol ; Purity: 99 %.

Potassium Ferrocyanide ($K_4Fe(CN)_6•3H_2O$). SIGMA ALDRICH; Product code: 455989; Lot: 470527; FW:422.39 g/mol ; Purity: 99.95 %.

Phenylmethylsulfonyl fluoride (PMSF: C7H7FO2S), for molecular biology. WINKLER; Product code: 713482; Lot: 1382C519; FW 174.19 g/mol; Purity: 99.9%.

Sodium Chloride (NaCl), for analysis. WINKLER; Product code: SO-1455; Lot: IB-1601009; FW 58.44 g/mol; Purity: min 99.0 %.

Sodium dodecyl sulfate (SDS), for molecular biology. WINKLER; Product code: BM-1650; Lot: 0264C513; FW 288.38 g/mol; Purity: min 99.0 %.

Sodium hydroxide (NaOH), for molecular biology. WINKLER; Product code: 105470; Lot: BH20100608; FW 40 g/mol; Purity: min 99.0 %.

Sodium Fluoride (NaF), for analysis. MERCK; Product code: 6449; Lot: 538174; FW: 42 g/mol; Purity (GC): ≥ 84.5-85.5 %; Humidity: 0.1%.

Sodium orthovanadate (Na_3VO_4), for molecular biology. SIGMA Aldrich; Product code: S6508; Lot: 096K0122; FW 183.91 g/mol; Minimum 90% titration.

Sodium phosphate dibasic (Na_2HPO_4), for molecular biology. WINKLER; Product code: SO-1490; Lot: 206917; FW 141. 96 g/mol; Purity: min 99.53 %; Humidity: 0.017%.

Sodium phosphate dibasic ($Na_2HPO_4 \cdot 12H_2O$), for molecular biology. WINKLER; Product code: SO-1497; Lot: 293276; FW 358.14 g/mol; Purity: min 99.7 %; Humidity: 57.0-61.0%.

Sodium phosphate monobasic ($NaH_2PO_4 \cdot H_2O$), for molecular biology. WINKLER; Product code: SO-1500; Lot: 831201; FW 137.99 g/mol; Purity: min 99.4 %; Humidity: 57.0-61.0%.

Trichloroacetic acid, ACS reagent ≥ 99.0 %. SIGMA-ALDRICH; Product code: T6399; Lot: STBF5881V; FW 163.39 g/mol.

Triethanolamine, GR for analysis. MERCK; Product code: 1.08379.1000; Lot: K46623479528; FW 149.19 g/mol; Purity (GC): ≥ 99.0 %; Humidity: 0.2%.

Tris(hidroximetil)aminometano (Tris), for molecular biology. WINKLER; Product code: BM-2000; Lot: 2837C166; FW 121.14 g/mol; Purity: 100.0 %; Humity: 0.1%.

4-Vinylpyridine, contains 100 ppm hydroquinone as inhibitor. SIGMA-ALDRICH; Product code: V3704; Lot: STBD7497V; FW 105.14 g/mol; Purity (GC): ≥ 94.5 %.

2.1.2 Antibodies and Proteins

α-tubulin, alpha tubulin monoclonal antibody DM1A. Thermo Fisher Scientific, Product: 62204.

Albumin Standard from bovine serum albumin. Thermo Scientific; Product code: 23209; Lot: OG189315; 2.0 mg/ml in a 0.9% aqueous NaCl solution containing sodium azide.

β-actin, **beta actin loading control anti-mouse monoclonal antibody BA3R**. Thermo Fisher Scientific. Product: MA515739; Lot: RE233986.

Catalase from bovine liver, lyophilized powder. SIGMA ALDRICH; Product code: C9322; Lot: SLBG1321V; 2000-3000 units/ mg protein.

Catalase Rabbit polyclonal antibody. Thermo Fisher scientific; Product: PA5-23246; Lot: RJ2282482A and Lot: SG2423797.

Complete Tablets EDTA-free, EASYpack, Protease Inhibitor Cocktail Tables. Roche; Product code: 04693132001; Lot: 15205300.

Goat anti-Rabbit IgG (H+L) Secondary Antibody, HRP. PIERCE THERMO SCIENTIFIC. Prod: 31460; Lot: QC214563.

Goat anti-Mouse IgG (H+L) Secondary Antibody, HRP. PIERCE THERMO SCIENTIFIC. Prod: 31430; Lot: QB213868.

Glutathione reductase from baker's yeast (S. cerevisae), Ammonium sulphate suspension**.** SIGMA ALDRICH; Product code: G3664; Lot: SLBK1185V; 100-300 units/mg protein (biuret); 0.28 ml; 9.5 mg protein/ ml (biuret); 189 units/ mg protein.

Procaspase-3 and cleaved caspase-3 (Rabbit mAb 9665S). Cell signalling technology; Product code: 8G10; Lot: 7; Ref: 08/2016.

Protease Inhibitor Cocktail Set III, EDTA-free Calbiochem; Product code: 539134; Lot: D00163193.

TIGAR Rabbit polyclonal. Thermo Fisher scientific. Product: PA5-20346; Lot: TF2587492.

XRCC1 Rabbit polyclonal. Abcam. Product: ab58465; Lot: 372659.

2.1.3 Other materials and software

AccuRuler RGB PLUS Prestained protein Ladder, 10-250 kDa. MAESTROGEN; Product code: 02102-250; Lot: 10008762 rev C.

Bench Mark Prestained Protein Ladder, 10-250 kDa. Invitrogen; Product code: 10748-010; Lot: 1671922

Catalase specific activity assay kit. ABCAM; Product code: ab118184; Lot: GR166857-13; GR236418-5.

Calpain activity fluorometric assay kit. SIGMA ALDRICH; Product code: MAK228-1KT; Lot: SLBZ9179.

Mini Trans-Blot Filter paper. Biorad; Product code: 1703932; Lot: 110371.

PageRuler Plus Prestained Protein Ladder 10-250 kDa. Thermo Scientific; Product code: 26619; Lot: 00321631; 00311589.

Pierce BCA Protein Assay reagent B. Thermo scientific; Product code: 23224; Lot: QF217388.

Pierce BCA Protein Assay reagent A. Thermo scientific; Product code: 23223; Lot: QL226800.

Precision Plus Protein Western C Standards, 10-250 kDa. BioRad; Product code: 161-0376; Lot: 10008762 rev C.

Protan Whatman Pure Nitrocellulose Transfer and immobilization membrane. Perkin Elmer; Product code: NBA083C001EA; Lot: G4032136; Pore size: 0.2 µm.

Protan™ Pure Nitrocellulose membrane. Perkin Elmer; Product code: NBA085C001EA; Lot: A10052898; Pore size: 0.45 µm.

WT PLUS ECL Enhanced chemiluminescence substrate. Perkin Elmer. Lot: 203-15021; Nº NEL104001EA.

XLSTAT software, version 2018. 20.1.49878 (ADDINSOFT SARL, Paris, France).

2.1.4 Instruments and equipment

ChemiScope 3400. ClinX Sciences Instruments Co, Ltd. Model Nº 3400; Serial Nº 89348.

Electrophoresis Chamber. BIORAD; model Mini PROTEAN Tetra Cell; Serial Nº: 552BR174397.

Magnetic Stirrer. IKA LABORTECHNIK; Model JK RCT basic Nº 00.037175; Serie 79219.

Multispin. BIOSCAN Model MSC6000; Nº 010211-1204-0058.

Multiplate Reader Synergy HT equipment. Biotek Instruments, Inc. Serial Nº 269167

Orbit™ LS Low Speed Orbital Shaker. S2030-LS-B.

pH meter. HANNA Instruments; Model HI111 pH/ORP meter; Serie A57760.

Select Heat dry block heater. Select Bioproducts. Model SBD110-2; Serial Nº SA1127326.

Transfer chamber. BIORAD; model Mini PROTEAN 3 Cell; Serial Nº: 525BR061820.

Waterbath. Memmert; Type WB14; Nº 14011587.

Newborn rat brain slicer. Zivic Instruments Pittsburgh, PA 15237.

2.2 Methods

2.2.1 Animals

Wistar albino rats from the animal station of the Molecular & Clinical Pharmacology Programme, ICBM, Faculty of Medicine, University of Chile, Santiago, Chile, were used along the experiments. The animals were kept on a temperature- and humidity-controlled environment with a 12/12-h light/dark cycle, with access to water and food ad libitum when not used in the experiments, monitoring permanently the wellbeing of the animals by qualified personnel.

2.2.2 Ethic Statement

All procedures were conducted in accordance with the animal care and use protocol established by a Local Ethics Committee for experimentation with laboratory animals at the Medical Faculty, University of Chile (Protocol CBA# 0722 FMUCH) and by an ad-hoc commission of the Chilean Council for Science and Technology Research (CONICYT), endorsing the principles of laboratory animal care (NIH; No. 86-23; revised 1985). Animals were permanently monitored (on 24 h basis) regarding well-being, following the ARRIVE guidelines for reporting animal studies (www.nc3rs.org.uk/ARRIVE).

2.2.3 Perinatal asphyxia Model

Pregnant Wistar rats within the last day of gestation (G22) were euthanized by neck dislocation and hysterectomised. One or two pups per dam were removed immediately and used as non-asphyxiated caesarean-delivered controls (CS). The remaining foetuses-containing uterine horns were immersed into a water bath at 37 °C for 21 min (asphyxia-exposed rats, AS). Following asphyxia, the uterine horns were incised and the pups removed, stimulated to breathe and, after an approximately 40 min observation period on a warming pad, evaluated with an Apgar scale for rats, according to Dell'Anna *et al*. 1997 and nurtured by a surrogate dam. The Apgar parameters were monitored up to P14, comparing the same CS and AS cohorts.

2.2.4 Nicotinamide Treatment

One hour after birth, asphyxia-exposed and control rats were divided into 6 experimental groups: Control (CS), Control+Vehicle (CS Veh.), Control +Nicotinamide (CS Nicot.), Asphyxia (AS), Asphyxia+Vehicle (AS Veh.) and AS+Nicotinamide (AS Nicot.).

The nicotinamide group (CS Nicot. and AS Nicot.) was injected intraperitoneally with a single dose of nicotinamide (Sigma, St. Louis, MO, USA) 0.8 mmol/kg, i.p. (diluted in 0.9% NaCl) in a volume of 0.1 mL/ kg body weight. The vehicle group (CS Veh and AS Veh) received 0.9 % NaCl in a volume of 0.1 mL/ kg body weight, injected intraperitoneally.

2.2.5 Tissue sampling

AS and CS rats (females and males) were euthanized at postnatal days (P) 1, 3, 7 or 14. The brain was quickly removed for dissecting out mesencephalon, hippocampus and telencephalon. For experiments evaluating the effect of nicotinamide on redox homeostasis the animals were euthanized at postnatal days (P) 1 and 14 by rapid decapitation. The brain was quickly removed for dissecting out the hippocampus. The procedure was performed on ice, using a newborn rat brain slicer (Zivic Instruments Pittsburgh, PA 15237 USA). The samples were stored at − 80 °C for further experiments.

2.2.6 Glutathione determination

Sample preparation. The hippocampus was homogenized in 40 μL 0.1 M potassium phosphate buffer with 5 mM EDTA disodium salt, pH 7.5. The recollected supernatant was deproteinated by adding 20 μL of previously cold 5% metaphosphoric acid and 10 μL of 10% trichloroacetic acid. The mixture was kept on ice for 5 min and centrifuged at 5,000 rpm, 4°C, for 5 min. The supernatant was transferred to fresh Eppendorf tubes and used for total GSH and GSSG determination during the same day.

Total GSH measurement by recycling method. Twenty microliters of de-proteinated samples were added to a microplate of 96 wells containing 200 μL of incubation buffer (500 μL 20% β-NADPH, 200 μL 6 mM DTNB and 300 μL H2Od) to allow the oxidation of GSH by DTNB, resulting in the formation of GSSG and TNB. Then, 5 μL of glutathione reductase (266 U/ml, adding baker's yeast S. cerevisiae 100–300 units/mg protein, Sigma

Aldrich, Saint Louis, MO, USA) were added to allow the recycling of GSSG to GSH. The absorbance of TNB was measured at 412 nm each 10 s for 1 min in a Multi-Mode Microplate Reader (Synergy HT Biotek Instruments, Inc., Winooski, VT, USA). The rate of TNB formation is directly proportional to the recycling reaction which is directly proportional to total GSH in samples.

GSSG measurement by derivatization. Fifty microlitres of de-proteinated samples were mixtured with 1 μL 4-vinylpyridine (1:10 in phosphate buffer) to allow the derivatization of GSH, leaving only GSSG for quantification. The derivatization mixture was vigorously stirred in a vortex and incubated for 1 h under dark at room temperature and stirring. Then, 3 μL triethanolamine (1:100 in phosphate buffer) was added to each sample, mixed vigorously in a vortex and incubated at room temperature for 10 min while stirring, leading to neutralization of excess of 4-vinylpyridine. Then, twenty microliters of the derivatized samples were added to a microplate of 96 wells containing 200 μL of incubation buffer, and 5 μL of glutathione reductase (to reduce GSSG and to allow recycling reaction). The absorbance of TNB was measured at 412 nm each 10 s for 1 min in a Multi-Mode Microplate Reader as above. The rate of formation TNB is directly proportional to the recycling reaction which is directly proportional to GSSG in samples.

Analysis. Standard curves were set up for GSH, 5–60 μM and GSSG, 0.25–3.0 μM. (Sigma-Aldrich, Saint Louis, MO, USA). The change of absorbance (ΔA412nm) over 1 minute was calculated for standard solutions and samples by linear regression (A vs time), the corrected ΔA412nm was obtained by subtraction of ΔA412nm blank sample. The corrected ΔA412nm was used to determine the concentration of total GSH and GSSG by interpolation into respective standard curves (ΔA412nm vs concentration). Total GSH and GSSG concentration was expressed in micromole per milligram of total protein. GSH (total GSH-2GSSG) was determined to calculate the GSSG:GSH ratio.

2.2.7 Reducing power Assay (Potassium Ferricyanide Reducing Assay, FRAP).

The effect of PA on glutathione levels and oxidative stress can be associated with antioxidant reduction capacity. Thus, global antioxidant capacity, FRAP, was assessed by spectrophotometry (Benzie and Strain 1996; Perez-Lobos et al. 2017). The antioxidant potential of each brain sample was determined by a reducing power assay (Oyaizu 1986). Brain samples were homogenised in 0.1 M phosphate buffered saline (PBS), 5 mM EDTA, 1 mM EGTA, 10 mM NaF and a protease inhibitory cocktail, CALBIOCHEM set III). The homogenised samples were incubated for 20 min on ice, centrifuged at 10,000 rpm, 4 °C, for 10 min and the supernatant was transferred to fresh Eppendorf tubes. Fifty microlitres of the supernatant was added to 300 µL 0.1M phosphate buffer pH 6.6 and 300 µL 1% potassium ferricyanide (K3Fe(CN)6•3H2O). The mixture was incubated at 50 °C for 25 min. Then, 300 µL 10% trichloroacetic acid was added to the mixture and incubated on ice for 5 min. The supernatant was obtained by centrifugation at 14,000 rpm, 4 °C, for 10 min. Five hundred microliters of the supernatant was mixed with 60 µL 0.1% chloride ferric and 300 µL distilled water. The mixture was vigorously stirred in a vortex and incubated for 5 min at room temperature. The absorbance was measured at 700 nm in a Multi-Mode Microplate Reader (Synergy HT Biotek Instruments, Inc. Winooski, VT, USA). Aqueous solutions of a known Fe (II) concentration, in a range of 100–1000 µM (potassium ferrocyanide $K_4Fe(CN)_6•3H_2O$), were used for the calibration curve. The absorbance of blank was subtracted from the absorbance of each sample. The corrected absorbance values were interpolated to the calibration curve. The values were expressed as micromolar of Fe (II) equivalents per microgram of total protein. All measurements were performed in triplicates for each tissue homogenate.

2.2.8 Glutathione Reductase Activity

Sample preparation. Brain samples were homogenized in 100µL 0.2 M potassium phosphate buffer pH 7.6 with 2mM EDTA, supplemented with 2 µL protease inhibitor cocktail (1 mM sodium orthovanadate; 1 mM PMSF; 5mMEDTA; 1mMEGTA; 10mMNaF, and protease inhibitors, CALBIOCHEM set III). A syringe attached to 27 gauge needles was used for lysing the tissue on ice. Samples were centrifuged at 14,000 rpm, for 10 min at 4 °C. Supernatant was collected to fresh Eppendorf tubes and used for

Glutathione reductase activity determination during the same day.

Glutathione reductase activity by spectrophotometry assay. Twenty microliters of samples were added to a microplate of 96 wells containing 100 µL of potassium phosphate buffer pH 7.6; 10 µL of 20 mM GSSG and 10 µL 2 mM NADPH. The absorbance was measured at 340 nm in 15 s intervals for 5 min at 25ºC in a Multi-Mode Microplate Reader (Synergy HT Biotek Instruments, Inc. Winooski, VT, USA).

Analysis. Standard solutions of Glutathione reductase among 5–25 mU/mL (266 U/ml, adding baker's yeast S. cerevisiae 100–300 units/mg protein, Sigma Aldrich, Saint Louis, MO, USA) were prepared into 0.2 M potassium phosphate buffer pH 7.6 with 2mM EDTA. The absorbance values at 340 nm were obtained according procedure applied for samples. The change in absorbance (ΔA340nm) over 5 min for each standard solution was obtained for setting up a calibration curve between ΔA340nm and glutathione reductase activity (5–25 mU/mL). For samples the ΔA340nm over 5 min were obtained and by linear regression in calibration curve, the GR activity was determined into samples expressed as mU/mL per microgram of total protein.

2.2.9 Glutathione Peroxidase Activity

Sample preparation. Brain samples were homogenized in 100µL 50 mM potassium phosphate buffer pH 7.4 with 5mM EDTA (assay buffer) supplemented with 2 µL protease inhibitor cocktail (1 mM sodium orthovanadate; 1 mM PMSF; 5mMEDTA; 1mMEGTA; 10mMNaF, and protease inhibitors, CALBIOCHEM set III). A syringe attached to 27 gauge needles was used for lysing the tissue on ice. Samples were centrifuged at 14,000 rpm, for 10 min at 4 °C. Supernatant was collected to fresh Eppendorf tubes and used for Glutathione peroxidase activity determination during the same day.

Glutathione peroxidase activity measurement. 100 microliters of sample or NADPH standard solution (10–120 nmol) was added to a microplate of 96 wells containing 50 µL of reaction buffer (20 µL 40 mM NADPH; 2 µL Glutathione reductase 5 mU/mL; 2 µL 2 mM GSH and 33 µL assay buffer). The plate was incubated for 15 minutes at room temperature.

Thereafter 100 μL 3% H_2O_2 was added. The absorbance was measured at 340 nm in 5 minute intervals for 30 minutes at 25ºC in a Multi-Mode Microplate Reader (Synergy HT Biotek Instruments, Inc. Winooski, VT, USA).

Analysis. The change of absorbance (ΔA340nm) over 30 minutes for each NADPH standard solution was determined and the calibration curve between ΔA340nm and concentration of NADPH in nmol was set up. The ΔA340nm for samples was used to determine the glutathione peroxidase activity by linear regression in calibration curve. The glutathione peroxidase activity was expressed as nmol NADPH/min/mL per microgram of total protein.

2.2.10 Protein extraction and protein content determination

Brain tissue was homogenised in RIPA lysis buffer (50mMTris-HCl, pH 7.2, 0.15 M NaCl, 1.0 mM EDTA, 0.1% SDS, 1.0% Triton X-100, 1.0% sodium deoxycholate) supplemented with phosphatase and protease inhibitors (1 mM sodium orthovanadate, 1 mM PMSF, 5 mM EDTA, 1 mM EGTA, 10 mM NaF and a protease inhibitor cocktail, CALBIOCHEM set III). Tissue was lysed, by passing it through 21 and then 27-gauge needles, ten times. The lysates were incubated on ice for 20 min and centrifuged at 13,500 rpm, 4 °C, for 20 min. The supernatant was transferred to fresh Eppendorf tubes, and stored at -80°C pending further experiments. Protein concentration was determined using a commercially available bicinchoninic acid (BCA) assay kit from Pierce (Thermo Scientific, Rockford, IL USA). Absorbance was measured at 562 nm in a Multi-Mode Microplate Reader (Synergy HT Biotek Instruments, Inc. Winooski, VT, USA).

2.2.11 Catalase Western blots

Proteins were separated by electrophoresis onto SDS polyacrylamide gels. Percentage of stacking (4%) and separating (10%) gels were used for separation of catalase. Samples were mixed with loading buffer (30% glycerol, 6% SDS, 15% DTT, 0.2% bromophenol blue, and 120 mM Tris-HCl buffer pH 6.8) and immediately heated at 95°C for 5 min. The loaded sample amount onto the wells was according to linear dynamic range of catalase in different brain regions (35 μg for mesencephalon; 15 μg for telencephalon; 25 μg for

hippocampus). Protein extracts from rat liver (P1) (lane liver) and purified catalase (catalase from bovine liver, Sigma Aldrich, Saint Louis, MO, USA) (lane catalase) were loaded as positive controls. A protein extract from cerebellum (P1) (Lane C) was loaded to control variations in transference.

Gels were run at constant 40 V for the stacking gel and at 80 V for the separating gel. After electrophoresis, proteins were electroblotted on BioTrace TM pure nitrocellulose membranes 0.45 µm (Pall Corporation, Pensacola, FL, USA) at 250 mA, 4 °C, for 90 min. Ponceau red solution was used to visualise transferred proteins onto the membranes and images were digitalized to estimate total protein, as loading control. Thereafter, Ponceau red was removed with water and the blotted membranes were blocked with 5% BSA dissolved in TBST (Tris-buffered saline containing 0.1% Tween-20) at room temperature for 1 h.

The incubation with primary antibodies was performed at 4 °C overnight. The dilution used for catalase was 1:500 (Rabbit polyclonal, ThermoFisher scientific, Rockford, IL, USA). After incubation with primary antibodies, the membranes were washed with TBST three times for 15 min and incubated with HRP conjugated rabbit secondary antibody (Thermo Scientific Pierce, Rockford, IL, USA) at 1:10,000 dilution in 1% BSA and TBST for 1 h, under constant shaking at room temperature. Then, the membranes were washed with TBST five times for 10 min under constant shaking at room temperature. For visualisation of proteins, the membranes were incubated in an enhanced chemiluminescence solution prepared according to manufacturer's instructions (Perkin Elmer Life Sciences, Boston, MA). Chemiluminescence was captured by a ChemiScope 3400 (ClinX Sciences Instruments Co, Ltd, Shangai, China).

The same membranes were stripped for reproving β-actin used as loading control for quantification of catalase in chapter 4. Membranes were incubated in stripping buffer pH 2.2 (0.2 mM glycine, 3.47 mM SDS and 1% v/v Tween 20) for 5 min twice, and then were washed in PBS twice for 10 min and in TBST, twice for 5 min. The membrane was blocked with 2.5% non-fat dry milk for 1 hour at room temperature. The incubation with β-actin was performed at 4°C overnight. The dilution used for β-actin (Thermo Fisher Scientific, Rockford, IL, USA) was 1:2,500. Thereafter, the membranes were washed with TBST three times for 15 min and incubated with HRP conjugated mouse secondary antibody (Pierce

Thermo Scientific, Rockford, IL, USA) at 1:10,000 dilution in 1% BSA and TBST for 1 hour, under constant shaking at room temperature. Then, the membranes were washed with TBST five times for 10 min under constant shaking at RT for detection of β-actin by chemiluminescence.

2.2.13 Catalase Specific Activity and ELISA

Catalase activity and protein levels were measured according to Mueller et al. (1997), using a catalase specific activity kit (ab118184 Abcam, Cambridge, UK). Brain samples from animals at P1, 3, 7 and 14 were processed according to the protocol provided by the kit. Catalase was immunocaptured and H_2O_2 levels, no removed by catalase, were immediately assayed by luminescence in a Synergy HT equipment (Biotek Instruments, Inc. Winooski, VT, USA) every 5 min for 30 min. The quantity of protein was then measured at 600 nm. The absorbance value for each sample was divided by total protein (determined by the BCA method), obtaining relative catalase protein levels. Liver protein extract from neonatal rat (P1) and purified catalase protein (catalase from bovine liver, Sigma Aldrich, Rockford, IL USA) were loaded as positive controls. Catalase activity was determined according to the exponential decay of H_2O_2. The rate constant (k), reflecting catalase activity, was determined from the luminescence data according to the equation: $k = \ln (S1/S2)/dt$, where dt is the measured time interval; S1 and S2 are H_2O_2 concentrations at time t_1 and t_2, respectively. The specific catalase activity was obtained by dividing the rate constant (k) by absorbance values of catalase and total protein, expressed in milligrams.

2.2.14 Procaspase and cleavage caspase-3 Western blots

Proteins were separated by electrophoresis onto SDS polyacrylamide gels. Percentage of stacking (4%) and separating (12%) gels were used for separation of caspase-3. Samples were mixed with sampling buffer (30% glycerol, 6% SDS, 15% DTT, 0.2% bromophenol blue, and 187.5 mM Tris-HCl buffer pH 6.8) and immediately heated at 95 °C for 5 min.

The loaded sample [amount] onto the wells was according to the linear dynamic range of caspase-3 (40 µg for mesencephalon; 15 µg for telencephalon; 20 µg for hippocampus). A liver protein extract from rat (P1) was loaded as a positive control (lane liver). Total protein

from cerebellum (P1) was loaded as an internal control for monitoring variations in transference (lane C).

Gels were run at constant 60 V for the stacking gel and at 100 V for the separating gel. After electrophoresis, proteins were electro blotted to BioTrace TM pure nitrocellulose membranes 0.2µm (Pall Corporation, Pensacola, FL, USA), 250 mA at 4 °C for 60 min. Ponceau red solution was used to visualise and digitalize the image of transferred proteins onto the membranes, using total protein as loading control. Thereafter, Ponceau red was removed with water and the blotted membranes were blocked with 2.5% BSA dissolved in TBST at room temperature for 1 h.

The incubation with primary antibody was performed at 4 °C overnight. The dilution required for detection of procaspase-3 and cleaved caspase-3 (Cell signalling Technology, Inc. Danvers, MA, USA) was 1:500, according to the validation. After primary antibody incubation, the membranes were washed with TBST three times for 15 min and incubated with HRP conjugated rabbit secondary antibody (Thermo Scientific Pierce, Rockford, IL, USA) at 1:10,000 dilution in 1% BSA and TBST under constant shaking at room temperature for 1 h. Then, the membranes were washed with TBST five times under constant shaking at room temperature for 10 min. For visualisation of proteins, the membrane was incubated in an enhanced chemiluminescence solution prepared according to manufacturer's instructions (Perkin Elmer Life Sciences, Boston, MA). Chemiluminescence was captured by a ChemiScope 3400 (ClinX Sciences Instruments Co, Ltd, Shangai, China).

2.2.15 TIGAR Western blots

Proteins were separated by electrophoresis onto SDS polyacrylamide gels. Percentage of stacking (4%) and separating (12%) gels were used for separation of proteins. Samples were mixed with loading buffer (30% glycerol, 6% SDS, 15% DTT, 0.2% bromophenol blue, and 120 mM Tris-HCl buffer pH 6.8) and immediately heated at 95 °C for 5 min. The loaded sample amount onto the wells was according to linear dynamic range in hippocampus (15 µg at P1 and 35 µg at P14). A protein extract from cerebellum (P1) (Lane C) was loaded to control variations in transference.

Gels were run at constant 40 V for the stacking gel and at 80 V for the separating gel. After electrophoresis, proteins were electro blotted on BioTrace TM pure nitrocellulose membranes 0.2μm (Pall Corporation, Pensacola, FL, USA) at 250 mA, 4 °C, for 60 min. Ponceau red solution was used to visualise transferred proteins onto the membranes and images were digitalized to estimate total protein, as loading control. Thereafter, Ponceau red was removed with water and the blotted membranes were blocked with 5% BSA dissolved in TBST (Tris-buffered saline containing 0.1% Tween-20) at room temperature for 1 h.

The incubation with primary antibody was performed at 4 °C overnight. The dilution used for TIGAR (Rabbit polyclonal, PA5-20346 Thermo Fisher scientific, Rockford, IL, USA) was 1:250. After incubation with primary antibody, the membranes were washed with TBST three times for 15 min and incubated with HRP conjugated rabbit secondary antibody (Thermo Scientific Pierce, Rockford, IL, USA) at 1:10.000 dilution in 1% BSA and TBST for 1 h, under constant shaking at room temperature. Then, the membranes were washed with TBST five times for 10 min under constant shaking at room temperature. For visualization of proteins, the membranes were incubated in an enhanced chemiluminescence solution prepared according to manufacturer's instructions (Perkin Elmer Life Sciences, Boston, MA). Chemiluminescence was captured by a ChemiScope 3400 (ClinX Sciences Instruments Co, Ltd, Shangai, China).

The same procedure described for catalase was used for incubation with secondary antibody, with the exception that after incubation with TIGAR, the membranes were washed with TBST three times for 10 min. The same membranes were stripped (same protocol for catalase Western blots) for reproving β-actin, to be used as loading control for quantification of TIGAR.

2.2.16 XRCC1 (X-ray repair cross-complementing protein 1) Western blots

XRCC1 was monitored by Western blots, evaluating whether oxidative stress induced changes in the scaffolding protein XRCC1, reflecting DNA damage. Proteins were separated by electrophoresis onto SDS PAGE. Percentage of stacking (4%) and separating (8%) gels were used for separation of XRCC1. Samples were mixed with loading buffer (30% glycerol, 6% SDS, 15% DTT, 0.2% bromophenol blue, and 120 mM Tris-HCl buffer

pH 6.8) and immediately heated at 95 °C for 5 min. The amount of loaded sample onto the wells was according to the linear dynamic range of XRCC1 in hippocampus (30-40μg). A protein extract from liver (P1) was loaded to control variations in transference.

Gels were run at constant 40 V for the stacking gel and at 80 V for the separating gel. The proteins into the gel were electroblotted and detected as described above. The transference was at 250 mA, 4°C, for 100 min. The blocking solution for membranes was 2.5% BSA. The same procedure described above was carried out for incubation with XRCC1, diluted at 1:500 (Rabbit polyclonal, Abcam, Cambridge, UK). The same procedure for washing and incubation described for TIGAR Western blots was carried out for detection of XRCC1 by chemiluminescence. The same membranes were stripped for reproving α-tubulin (alpha tubulin monoclonal antibody DM1A, 62204, Thermo Fisher Scientific, Rockford, IL, USA) used as loading control for quantification of XRCC1, following the same procedure described above.

2.2.17 Calpain activity assay

Calpain was measured using a calpain activity kit (MAK228; Sigma-Aldrich, St Louis, MO, USA). Brain samples from animals at P1 and P14 were processed according to the protocol provided by the kit. The calpain activity was quantified by fluorescence in a Synergy HT equipment (Synergy HT Biotek Instruments, Winooski, VT, USA). The Ac-LLY-AFC is cleaved by calpain releasing AFC which emits a yellow-green fluorescence (max= 505 nm). Calpain activity was obtained by interpolation of fluorescence intensity in a calibration curve for calpain I (0.1-0.8 units), expressed as enzymatic units and normalized per milligram of total protein present in each sample. The MAK228 kit provides an estimation of total calpain activity, only.

2.2.18 Image Acquisition and Densitometry

For visualisation of target protein detected by Western blots, the membranes were incubated in an enhanced chemiluminescence solution prepared according to manufacturer's instructions (Perkin Elmer Life Sciences, Boston, MA). Chemiluminescence was captured by a ChemiScope 3400 (ClinX Sciences Instruments Co, Ltd. Shangai, China) and images were digitalized and processed by an ImageJ software

(National Institutes of Health, USA). The background was subtracted using a rolling ball algorithm. The image for quantification was chosen within the linear range of time exposition, the measurement area was obtained as signal for each protein band. The area values were normalised by the Sum of all Data Points in replicate (Degasperi et al. 2014). According the experiment three loading controls were used for determination of normalised target protein levels (Taylor et al. 2014) corresponding to total protein (Ponceau staining) and β-actin or α-tubulin as housekeeping. The values obtained from loading controls were analysed for statistical analysis.

2.2.19 Statistical analysis

All results are expressed as means ± standard error of the means (SEM). To determine statistic differences on the effect of PA, postnatal days and treatment an unbalanced and balanced ANOVA analysis was performed for unequal and equal sample sizes, respectively. Benjamini-Hochberg was used as a post hoc test for reducing the false discovery rate (type I error) for multiple comparisons. ANOVA results are expressed as F ratio value, the freedom degrees corresponding to n-1 (n: number of groups in comparison) and N-1 (N: number of replicas of each group) respectively, given in parenthesis.

Principal factor method was used for multivariate analysis, determining the main variables contributing to changes along postnatal days in CS and AS groups. Pearson method was set up for determining the correlation among variables with principal factors.

The probability value (P) is indicated when proper. For statistically significant differences, the probability of error was set up to less than 5% for all analysis.

All data analysis was performed with a XLSTAT software, version 2018. 20.1.49878 (ADDINSOFT SARL, Paris, France).

Chapter 3

Redox Homeostasis and Delayed Cell Death in the brain of rats subjected to perinatal asphyxia

3.1 Results

3.1.1 Apgar and Postnatal Evaluation

Table 1 shows the outcome of global perinatal asphyxia (PA) evaluated by an Apgar scale applied 40 min after delivery (the time of the uterine excision), and that evaluation was repeated at P1, P3, P7 and P14. Asphyxia-exposed neonates (AS) are compared to sibling neonates delivered by the caesarean section without any asphyxia (CS). The rate of survival shown by AS neonates was approximately 60%, while it was practically 100% among control (CS) neonates. Surviving AS neonates showed decreased respiratory frequency supported by gasping, decreased vocalisation, cyanotic skin, rigidity and akinesia, indicating a severe metabolic insult.

The animals were observed up to P14, monitoring reception by the surrogate dam, body weight, respiratory frequency, fur and skin colour and motility. While reception and survival was equivalent for both CS and AS neonates, there were signs of a sustained physiological deficit mainly affecting respiratory and cardiovascular parameters. AS neonates showed a decreased respiratory frequency (by approximately 40% along the monitored postnatal days), compared to that shown by CS neonates. The effect of PA on respiratory frequency was accompanied by a change in skin colour, CS neonates showed a pink healthy colour along the monitored period, while AS neonates showed a pink-blue (PB) colour and opaque fur, suggesting a reduced blood perfusion and/or decreased oxygenation, as well as decreased cleaning behaviour.

3.1.2 Effect of Perinatal Asphyxia on Glutathione (GSH, GSSG) and GSSG:GSH Ratio Evaluated in Mesencephalon, Telencephalon and Hippocampus of Asphyxia-Exposed and Control Rat Neonates.

Table 2 (**A, B y C**) summarises the effect of PA on GSH and GSSG levels, evaluated in mesencephalon (**Table 2A**), telencephalon (**Table 2B**) and hippocampus (**Table 2C**) from CS and AS rat neonates at P1, 3, 7 and 14. The GSSG:GSH ratio was calculated for each group, as an index of oxidative stress.

The comparison between CS and AS rat neonates showed a reduction of GSH levels induced by PA, both in mesencephalon and hippocampus, but only at P14 (**Figure 5a and 7a**). In telencephalon GSH levels were increased at P7 and P14 (**Figure 6a**).

The effect of PA on GSSG levels indicated that PA produced an increase of GSSG levels in both mesencephalon and hippocampus along P1 to P14 (**Figure 5b and 7b**). In telencephalon, a statistically significant increase of GSSG levels was only observed at P1 (**Figure 6b**).

The GSSG:GSH ratio was calculated to determinate oxidative stress along P1 to 14. An increase of GSSG:GSH ratio both in mesencephalon and hippocampus from AS rat compared to CS rat neonates was observed (**Figure 5c and 7c**). The highest effect induced by PA on the GSSG:GSH ratio was observed in mesencephalon and hippocampus at P14, a 3- fold increase, when compared with CS neonates at the same time after birth. In telencephalon, the GSSG:GSH ratio increased significantly only at P1 in AS compared to CS rat neonates (**Figure 6c**).

3.1.3 Effect of Perinatal Asphyxia on Tissue Reducing Capacity (FRAP) Evaluated in Mesencephalon, Telencephalon and Hippocampus of Asphyxia-Exposed and Control Rat Neonates

Table 3 summarises the effect of PA on FRAP evaluated in mesencephalon, telencephalon and hippocampus at P1, 3, 7 and 14, of CS and AS rat neonates.

Figure 8 shows that FRAP capacity increased along development, both in CS and AS animals, but FRAP levels were lower in AS compared to CS animals, an effect sustained along postnatal days in mesencephalon (**Figure 8a**) and hippocampus (**Figure 8c**). In telencephalon, however, FRAP levels were increased in AS at P7 and P14, compared to CS animals (**Figure 8b**).

3.1.4 Effect of Perinatal Asphyxia on Catalase levels in the Neonatal Rat Brain

Figure 9 shows representative catalase immunoblots and Ponceau Red stained membranes, assaying protein extracts from mesencephalon (A), telencephalon (B) and hippocampus (C) of CS and AS neonates sampled at P1, 3, 7 and 14. Catalase was identified as a unique band at 60 kDa. Purified catalase protein (lane catalase) and a liver sample (lane liver) taken at P1 were used as positive controls, and protein extract from cerebellum (P1) (lane C) loaded to control transference variation. Densitometry of the intensity of the protein bands for CS and AS rats is shown in **Table 4**, summarising the effect of PA and postnatal days on catalase protein levels (expressed as arbitrary units, a.u.).

The comparison between CS and AS did not show any significant differences in mesencephalon and telencephalon (**Figure 9a, b and 9c, d**), with exception of hippocampus at P3 ($p< 0.001$), where an increase of catalase protein was found in AS neonates in comparison to controls (**Figure 9e, f**). Similar results were obtained for relative catalase protein levels measured by ELISA, used for determination of catalase activity. A significant increase was found in hippocampus at P3 ($p < 0.0001$) in AS neonates in comparison with the controls (**Figure 10e**). Also, in mesencephalon the catalase protein relative levels showed a decrease in AS rat neonates in comparison to controls at P3 ($p<0.001$) (**Figure 10a**).

Catalase activity was calculated for each individual, determining the k value for the decomposition of hydrogen peroxide, normalised by catalase relative levels and total protein. Catalase activity in mesencephalon and hippocampus, decreased when compared to the controls along postnatal days. In mesencephalon, PA decreased catalase activity at P1

and P3 (**Figure 10b**). In hippocampus, catalase activity decreased by 70% in AS, compared to samples from CS animals at P14. However, catalase activity increased in AS versus CS hippocampus at P3 (**Figure 10f**). No significant differences between CS and AS neonates were detected in telencephalon along postnatal days (**Figure 10 c, d**).

3.1.5 Effect of Perinatal Asphyxia on Caspase-3 Assayed in the Neonatal Rat Brain

Figure 11 shows representative immunoblots for procaspase-3 and cleaved caspase-3 expression in mesencephalon (**Figure 11A**), telencephalon (**Figure 11C**) and hippocampus (**Figure 11E**). The blots for caspase-3 displayed a double band at 35/36 kDa, corresponding to procaspase-3, while cleaved caspase-3 fragments were at 19, 17 and 12 kDa. A caspase-3 fragment was observed at 30 kDa at P7, but only in hippocampus (**Figure 11E**), reported to correspond to a fragment cleaved by calpain (Blomgren et al. 2001), increased in AS, as compared to that from CS samples. Table 5 summarises procaspase-3 and cleaved caspase-3 levels in mesencephalon (**Table 5A**), telencephalon (**Table 5B**) and hippocampus (**Table 5C**) of CS and AS animals at P1, 3, 7 and 14, expressed as arbitrary units. Procaspase-3 protein levels did not show significant changes between CS and AS rat neonates along the analysed postnatal days (**Table 5**).

Only, in mesencephalon (**Figure 11A, B**) and hippocampus (**Figure 11E, F**), there was an increase in cleaved caspase-3 levels, as compared to the corresponding controls. Cleaved caspase-3 levels increased at P1, P3 and P14 in mesencephalon (**Figure 11B**), and at P3 and P7 in hippocampus (**Figure 11F**). No significant change on cleaved caspase-3 was observed in telencephalon between CS and AS (**Figure 11 C, D**).

3.1.6 Progression of brain damage and redox environment in the neonatal rat brain

The progression of brain damage induced by PA was monitored by changes in redox environment and activation of apoptosis, as a molecular mechanism for delayed cell death. Multivariate analysis was used to determinate the main variables contributing to differences along postnatal days in CS and AS groups in different brain areas.

In mesencephalon (**Figure 12A**), the main changes along postnatal days in the CS group are explained by the first principal component F1 in a 49.13%, composed by cleaved

caspase-3 (*r*: 0.898); FRAP (*r*: -0.723); catalase activity (*r*: 0.712) and GSSG:GSH ratio (*r*: 0.711). While in the AS group (**Figure 12B**), catalase activity (*r*: 0.964), FRAP (*r*: -0.811), cleaved caspase-3 (*r*: 0.784) contribute to F1 and explain variations along postnatal days in a 50,22%.

For telencephalon (**Figure 13A**) catalase activity (*r*: 0.983) and caspase-3 (*r*: 0.628) is the main variable correlated with the first principal factor F1 in CS group, which explains variations along postnatal days in a 41.34%. In AS group (**Figure 13B**), the first principal factor F1 explains the variations among postnatal days in a 39.54%, being FRAP (*r*: 0.923) and GSSG:GSH ratio (*r*: -0.884) the main variables that contribute to F1.

In hippocampus (**Figure 14A)** the first principal factor F1 in the CS group contributed to variation along postnatal days in a 56.36%, being FRAP (*r*: 0.990); catalase activity (*r*: -0.907) and cleaved caspase-3 (*r*: -0.712) the main variables explaining the differences. In AS group (**Figure 14B**), both the first principal factor F1 and the second F2 explain the variations along postnatal days in a 33.501% and 28.85%, respectively. The variables GSSG:GSH ratio (*r*: 0.898, for F1) and cleaved caspase-3 (*r*: 0.899 for F2), explain the main variations along postnatal days.

3.2 Discussion of Chapter 3

The present study provides evidence that redox homeostasis is impaired in a regionally specific manner in the neonatal rat brain subjected to global PA, showing a delayed effect up to P14 on (i) GSSG/GSH; (ii) tissue reducing capacity (FRAP); (iii) catalase activity, and (iv) cleaved caspase-3 levels, mainly affecting mesencephalon and hippocampus, suggesting a sustained oxidative stress induced by global perinatal asphyxia.

The study focused on a short postnatal period, up to 14 days, characterized by intensive neuritogenesis, synaptogenesis and synaptic integration, affecting in particular dopaminergic pathways. Indeed, while the rat brain shows a similar number of dopamine cell bodies at P1 as at adulthood, axon projection and synaptogenesis occurs along the first weeks, the distribution of dopaminergic fibers reaching a near-adult feature only at P13-20 (Voorn et al. 1988). Furthermore, there is a process of naturally occurring cell death, affecting dopamine neurons with a first peak at P2/3, and a second peak at P14 (Oo &

Burke 1997; Jackson-Lewis et al. 2000), involving members of the Bcl-2 protein family, regulating cytochrome release from mitochondria and activation of caspase cascades. Selective nuclear fragmentation has been observed in brain of rat neonates, naive and subjected to PA, depending upon the stage of development and brain region (Dell'Anna et al. 1997). At P1, apoptosis-like cell fragmentation was observed in para- and presubiculum of both PA-exposed and control rat neonates, while in neostriatum it was only observed in PA-exposed neonates, but at P8 (Dell'Anna et al. 1997; Neira-Peña et al. 2014). In mesencephalon and hippocampus, TUNEL-positive cell death was observed at P1 and P7, increased in animals subjected to PA (Morales et al. 2008; Neira-Peña et al. 2014, 2015). In hippocampus, delayed cell death was observed to be increased in AS compared to that in CS rats up to 30 days (Morales et al. 2010).

PA implies a long-term metabolic insult, triggered by the length of the induced hypoxia-ischemia, the resuscitation/reoxygenation manoeuvres, but also by the developmental stage of the affected brain regions, and the integrity of cardiovascular and respiratory physiological functions, which are fundamental for warrantying a proper development.
The role of oxidative stress on cell damage has be extensively studied in models of hypoxia/ischemia at P7, implying vessels ligation and hypoxic chambers, focusing on the reperfusion-oxygenation period (Bågenholm et al. 1997; Ikeda et al. 2002), also following global asphyxia (Capani et al. 2001, 2003). A relationship between duration of asphyxia and ROS production has been demonstrated both in animal and clinical studies (Kumar et al. 2007). It has been proposed that oxidative stress markers predict the severity of damage induced by PA (Seema et al. 2014; Perrone et al. 2010; Bahuhali et al. 2013). A metabolic recovery period has, however, been observed after the insult in neonates exposed to PA, (Shah et al. 2003), also in brain damage progression, associated with oxidative stress, ROS playing a key molecular mechanism (Morken et al. 2013).

In the present study, the effect of PA on redox homeostasis was monitored in mesencephalon, telencephalon and hippocampus, brain areas shown to be susceptible to hypoxia and ischemic insults (Bielke et al. 1991; Dell'Anna et al. 1997; Homi et al. 2002). The GSSG:GSH ratio was calculated as a marker of oxidative stress, based on the fact that

reduced glutathione (GSH) is the major non-enzymatic antioxidant regulating redox homeostasis (Aquilano et al. 2014). There was an increase in the GSSG:GSH ratio in mesencephalon and hippocampus, confirming that PA induces long-term oxidative stress (Capani et al. 2003), in contrast to what was previously reported by Lubec et al. (1997a), who concluded that there was no evidence for the involvement of active oxygen species, radical adducts or energy depletion, using the same experimental model as reported here, but evaluating oxidative stress in total brain 10 min after delivery, without considering any regional compartmentalization.

Redox homeostasis can be impaired by increased ROS production or by decreased antioxidant defences (Day et al. 2014). The synthesis of glutathione is modulated by Nrf-2, a transcriptional factor responding to moderate ROS levels, increasing the transcription of genes coding for antioxidant enzymes of phase II metabolism (Zhang et al. 2013). Increased ROS levels induce degradation of Nrf-2, by ubiquitination, decreasing antioxidant enzymes expression (Bryan et al. 2013). Glutathione reductase (GTx) belongs to phase II enzymes, restoring GSH levels by reduction of GSSG (Dringen et al. 2000; Franco et al. 2009). The activity of this enzyme is NADPH dependent, hence from glucose and ATP availability, promoting the pentose phosphate pathway (PPP), maintaining NADPH physiological levels (Bolaños et al. 2008). In models of hypoxia/ischemia in postnatal rats, PPP showed a reduced activity after a hypoxic/ischemic insult, leading to reduced NADPH levels and decreased glutathione reductase (GTx) activity (Brekke et al. 2014; Fullerton et al. 1998), also implying mitochondrial hypo-metabolism (Wallin et al. 2000). A long-term energetic deficit induced by PA has been demonstrated in organotypic cultures from asphyxia exposed animals, showing a 6-fold increase of the ADP/ATP ratio at DIV 21-22, potentiated by high H_2O_2 exposure (Perez-Lobos et al. 2017). Therefore, the results observed in mesencephalon and hippocampus indicate GSSG accumulation, suggesting reduced GTx activity, linked to decreased NADPH levels, contributing to a sustained oxidative stress, affecting the synthesis *de novo* of GSH, regulated by the Nrf-2 pathway (Itoh et al. 1999).

The effect of PA on the GSSG:GSH ratio was supported by that on FRAP, showing a decreased antioxidant capacity after PA, both in mesencephalon and hippocampus. FRAP is directly associated with reducing molecules availability, such as ascorbic acid, tocopherol, ubiquinone, NADPH, L-carnitine, and free thiols (Benzie et al. 1996). Hence, decreased FRAP levels supports the idea of a decreased synthesis of NADPH, favouring the GSSG accumulation observed during the P1-14 period, leading to oxidative stress, explaining the delayed response on decreased GSH levels observed at P14, in mesencephalon and hippocampus after PA. No effects were observed in telencephalon, where FRAP was increased by PA at P7, compared to control neonates, indicating a local, instead of a generalized effect, supporting the idea that oxidative stress depends upon the generation of free radical species, as well as upon the intrinsic defences against the insult.

Catalase is a major cell protecting enzyme against oxidative damage and reactive oxygen species. Its main function is to decompose hydrogen peroxide to water and molecular oxygen, controlling H_2O_2 levels (Veal et al. 2007; Nicholls et al. 2012). There is a direct relationship between the decomposition of H_2O_2 levels by catalase and resistance to oxidative stress and hypoxia-ischemia (Fullerton et al. 1998; Argomida et al. 2011). At high levels H_2O_2 is detrimental to the cells, leading to activation of cell death cascades and GSH depletion (Veal et al. 2007), favouring oxidative modifications of proteins (Spolarics et al. 1997; Ibi et al. 1999; Hohnholt et al. 2014).

Catalase protein levels were analysed by Western blots and ELISA, estimating the enzymatic activity by the constant (k) from the exponential degradation of H_2O_2, normalized by catalase relative levels, finding that catalase activity was decreased up to P14, in both mesencephalon and hippocampus from AS, compared to CS neonates. The maximum effect was observed in hippocampus at P14. No significant changes were observed in telencephalon, which has been shown to be more resilient against hypoxia and ischemia induced at early neonatal stages (Homi et al. 2002), probably reflecting a delayed postnatal development (Voorn et al. 1988). The antioxidant system of the neonatal brain also matures along development, a main factor of vulnerability compared to that shown by the adult brain (Khan et al. 2003). It has been reported that the neonatal brain (P7)

accumulates more H_2O_2 levels than the adult brain (P42) up to 5 days after a postnatal hypoxic-ischemic insult (Lafemina et al. 2006). At the first hours after a hypoxic-ischemic insult, catalase activity is not changed in the neonatal brain (Weis et al. 2011), but it is increased in the adult brain (Homi et al. 2002). In the present study, however, catalase activity was decreased in mesencephalon and hippocampus, up to 14 days after PA, but not in telencephalon.

Western blot and ELISA did not show changes in catalase protein levels in any of the studied brain areas, only in hippocampus at P3, associated with increased catalase activity in the AS group. At P7 and P14, there was however a decrease in catalase activity in hippocampus, without changes in expression, suggesting that oxidative stress induced by PA is long-lasting, because of reduced catalase activity, not affecting protein expression. In the same region and same period, there was a >2-fold increase of the GSSG/GSH ratio, indicating elevated oxidative stress. Similar results have been reported, based on different experimental models, showing that catalase activity is decreased by oxidative stress, without inducing changes in protein expression, explained by post-transductional modifications (Chakravarty et al. 2015; Krych-Madej et al. 2015). Similarly, in a model of asthma, oxidative stress led to nitrosylation and oxidation of catalase residues, decreasing enzymatic activity, but not protein expression (Ghosh et al. 2006).

Delayed cell death has been observed after PA (Dell'Anna et al. 1997), and at the reperfusion-oxygenation period in models of postnatal hypoxia-ischemia (Northington FJ et al. 2001a; Northington FJ, et al. 2001b), characterized by activation of apoptotic mechanisms (Ferrer et al. 1997), explaining the reported neuronal progressive death after PA (Benjelloun et al. 1999; Hudome et al., 1997; Morales et al. 2005; Winerdal et al. 2012). An increase of molecular mediators of apoptosis has been reported, associated to caspase-dependent cascades, and TUNEL positive cell death (Morales et al. 2008; Neira-Peña et al. 2015; Tapia-Bustos et al. 2016). Several studies have reported that both oxidative and nitrosative stress cause DNA fragmentation and mitochondrial dysfunction, leading to activation of caspase-dependent cell death (Chen et al. 2011; Ikonomidou et al. 2011). Hence increased cleaved caspase-3 levels in mesencephalon and hippocampus,

confirming that PA induces apoptotic cell death, which is sustained along development, in parallel with changes in redox balance, observed in vulnerable brain areas. Cleaved caspase-3 levels were increased in mesencephalon of PA neonates at P1-14, while in hippocampus that increase was only observed at P3-7. No effect was observed in telencephalon, indicating a regional co-variance with postnatal development.

The multivariate analysis was performed to understand the interplaying of the main variables explaining the progression of brain damage along postnatal days following perinatal asphyxia, affecting mesencephalon, hippocampus and telencephalon. In mesencephalon, hippocampus and telencephalon the differences along postnatal days in animals CS was associated with changes on cleaved caspase-3 and catalase activity. In regards to AS animals, the pattern of variables contributing to differences observed along postnatal days showed variations among mesencephalon, hippocampus and telencephalon. Changes on cleaved caspase-3 and GSSG:GSH ratio explain differences along postnatal days in hippocampus. In telencephalon, FRAP and GSSG:GSH ratio, the variables contributing to the differences along postnatal days were those induced by asphyxia. However, in mesencephalon there was not any clear pattern contributing to differences along postnatal days between AS and CS group, although catalase activity was the variable with the strongest contribution in AS group. These results confirm that progression of brain damage induced by perinatal asphyxia in brain areas susceptible to asphyxia is associated with changes on apoptosis mechanisms mediated by cleaved caspase-3, together with changes in GSSG:GSH ratio and catalase. Whereas in telencephalon, changes in FRAP and GSSG:GSH ratio along postnatal days contribute to a major resistant to PA.

3.3 Conclusion of Chapter 3

The present study provides evidence that redox homeostasis is impaired in a regionally specific manner in the neonatal brain of rats subjected to global PA, showing a delayed effect up to P14, mainly affecting mesencephalon and hippocampus, suggesting a sustained oxidative stress after a hypoxia-ischemia period. It is proposed that PA implies a long-term metabolic insult, triggered by (i) the length of asphyxia; (ii) the resuscitation/reoxygenation manoeuvres, but also by (iii) the developmental stage of the affected brain regions, and (iv)

the integrity of cardiovascular and respiratory physiological functions, which are fundamental for warrantying a proper development, suggesting novel targets and an expanded therapeutic window against the long-term effects induced by global perinatal asphyxia.

Chapter 4

Restoring of redox homeostasis by nicotinamide in the hippocampus of rats subjected to global perinatal asphyxia

4.1 RESULTS

4.1.1 Global Perinatal asphyxia

Perinatal asphyxia was performed by immersing caesarean removed foetus-containing uterine horns from on term rat dams into a water bath at 37^{o}C for 21 min, using sibling caesarean-delivered foetuses for comparisons. The rate of survival shown by AS neonates was approximately 60%, while it was 100% for control (CS) neonates (**Table 6**). Surviving AS neonates showed decreased respiratory frequency supported by gasping, decreased vocalization, cyanotic skin, rigidity and akinesia, indicating a severe metabolic insult. Asphyxia-exposed and control neonates were, however, nurtured well by surrogate dams up to postnatal (P) day P1 or P14, when they were euthanized for dissecting samples from hippocampus to be assayed for glutathione, glutathione reductase (GR), glutathione peroxidase (GPx), catalase, TIGAR, calpain and XRCC1. A series of asphyxia-exposed and control neonates was injected with either 100 µl saline or 0.8 mmol/kg nicotinamide, i.p., one hour after delivery.

4.1.2 Effect of perinatal asphyxia and nicotinamide on glutathione (GSH, GSSG; and GSSG:GSH ratio) levels in hippocampus from neonatal rats.

In section A of Table 7, the effect of PA on GSH and GSSG levels, and GSSG:GSH ratio evaluated in hippocampus from CS and AS rat neonates at P1 and 14 is summarized. Unbalanced two-way ANOVA indicated a significant effect of PA and postnatal days on GSH and GSSG levels and GSSG:GSH ratio. PA increased GSSG levels (~2-fold) at P1 and P14 (**Figure 15B**), while GSH levels were decreased by 36% in PA-exposed animals, compared to the corresponding controls, but only at P14 (**Figure 15A**). The GSSG:GSH ratio increased in hippocampus of AS versus that in CS neonates, ~2-fold at P1 and >4-fold at P14, compared to that observed in CS neonates at the same age (**Figure 15C**).

In section B of Table 7, the effect of neonatal nicotinamide treatment is summarized. Unbalanced two-way ANOVA indicated a significant effect of PA by nicotinamide treatment. Nicotinamide increased GSH levels (~2-fold) at P1 and P14, both in control and asphyxia-exposed neonates (**Figure 15A**), and the GSSG:GSH ratio was decreased in all

cases, at P1 and P14 (**Figure 15C**). Nicotinamide treatment also decreased GSSG levels, but only in asphyxia exposed-animals (**Figure 15B**).

4.1.3 Effect of perinatal asphyxia and nicotinamide on glutathione reductase (GR) activity in hippocampus from neonatal rats.

The enzymatic activity of GR in hippocampus at P1 and P14 was determined by absorbance at 340 nm. In section A of Table 8, the effect of PA on GR activity evaluated in hippocampus from CS and AS rat neonates at P1 and 14 is summarized. Unbalanced two-way ANOVA indicated a significant effect of PA on GR activity ($F(1, 40) = 112.408$, $P < 0.0001$). The comparison between AS and CS rat neonates showed a reduced enzymatic activity on GR in hippocampus of AS animals, both at P1 and P14 (**Figure 16**).

In section B of Table 8, the effect of nicotinamide treatment on GR activity is summarized. Unbalanced two-way ANOVA indicated a significant effect of nicotinamide on GR levels ($F_{(3, 69)} = 24.239$, $P < 0.0001$). Nicotinamide treatment increased GR activity, both in CS and AS animals, at P1 and P14, compared to the corresponding group treated with vehicle. The effect of nicotinamide was particularly prominent in AS neonates at P1 (Table 8; **Figure 16**).

4.1.4 Effect of perinatal asphyxia and nicotinamide on glutathione peroxidase (GPx) activity in hippocampus from neonatal rats.

In section A of Table 9 the effect of PA on GPx activity is shown, measured by absorbance at 340 nm in hippocampus of CS and AS rat neonates at P1 and P14. Unbalanced two-way ANOVA indicated a significantly effect of PA on GPx ($F_{1, 23}=149.002$; $P < 0.0001$). The enzymatic activity of GPx was decreased in AS in comparison with CS animals at both P1 and P14 (**Figure 17**).

In section B of Table 9 the effect of nicotinamide on GPx activity is summarized. Unbalanced two-way ANOVA indicated a significant effect of nicotinamide ($F_{(3, 49)}= 54.039$, $P < 0.0001$) on GPx activity. Nicotinamide increased GPx activity in both CS and AS neonates, compared with the corresponding vehicle-treated control. The effect was particularly prominent on AS neonates, both at P1 and P14, while in CS neonates the effect of nicotinamide was only observed at P14 (**Figure 17**).

4.1.5 Effect of perinatal asphyxia and nicotinamide on catalase protein levels and catalase activity in hippocampus from neonatal rats.

Immunoblots for catalase were assayed in hippocampus at P1 and P14. In **Figure 18A and C**, a band protein at 60kDa was detected for catalase, using as positive controls liver lysate and catalase protein purified from liver, shown in the same immunoblots. Ponceau staining was used as loading control for normalization and quantification of catalase protein. No significant differences were observed when AS and CS rat neonates were compared regarding levels measured by immunoblots at P1 (**Figure 18B and 19A**) and P14 (**Figure 18D and 19A**). Nevertheless, a significant decrease produced by PA was observed when measuring protein levels by ELISA (**Figure 19C**).

In section A of Table 10, the effect of PA on catalase levels and catalase activity in hippocampus is shown at P1 and P14 (**Figure 19B and C**). Unbalanced two-way ANOVA indicated a significant effect of PA on both protein ($F_{1, 39}$= 62.197; P < 0.0001) and activity ($F_{1, 13}$= 40.626; P < 0.0001). In section B of Table 10 the effect of nicotinamide on catalase protein and catalase activity is shown. Unbalanced two-way ANOVA indicated a significant effect of nicotinamide treatment on catalase activity ($F_{3, 29}$= 10.959; P < 0.0001), increased in both groups at P1, and also at P14, but only in AS neonates.

4.1.6 Effect of perinatal asphyxia and nicotinamide on pentose phosphate pathway monitored by the expression of TIGAR in hippocampus from neonatal rats.

The pentose phosphate pathway (PPP) was evaluated by the TIGAR expression, a regulator promoting a shift of glucose, from oxidative phosphorylation toward the pentose phosphate pathway, promoting cell survival. **In Figure 20** representative immunoblots for TIGAR expression in hippocampus are shown, at P1 (**Figure 20A and B**) and at P14 (**Figure 20C and D**). The corresponding experimental groups to evaluate the effect of perinatal asphyxia and nicotinamide are indicated. TIGAR appeared as a band at 30 kDa. The corresponding loading controls for β-actin and total protein (Ponceau Stained) are also shown. Table 11 shows TIGAR protein quantification expressed as arbitrary units (a.u.) obtained by densitometry of immunoblots.

Section A of Table 11 shows the effect of PA on TIGAR levels at P1 and P14. TIGAR levels were decreased in hippocampus of asphyxia-exposed neonates at P1, but were increased at P14 (**Figure 21**), compared with the controls, an effect that was prevented by nicotinamide (section B of Table 11). Nicotinamide also produced a slight, but significant decrease of TIGAR levels in hippocampus of control neonates at P14 (**Figure 21**).

4.1.7 Effect of perinatal asphyxia and nicotinamide on XRCC1 protein levels in hippocampus from rats exposed to perinatal asphyxia

The effect of perinatal asphyxia on DNA integrity was estimated by XRCC1 protein expression, a scaffold protein that forms part of the DNA base excision repair (BER) pathway. Downregulation of this DNA repair pathway has been associated with brain damage produced by ischemia-reperfusion in models of stroke in adult brain.

Representative immunoblots for XRCC1 are shown in Figure 20. Full length XRCC1 was identified in hippocampus at P1 (**Figure 22A and B**) and P14 (**Figure 22C and D**), as a band at 96 kDa. α-Tubulin and total protein (Ponceau Stained) are used as loading controls. Table 12 shows full length XRCC1 protein quantification, expressed as arbitrary units (a.u.) obtained by densitometry. Data illustrate the effect of PA on XRCC1, shown in section A of Table 12, as well as the effect of nicotinamide on XRCC1, shown in section B of Table 12. PA induced a significant increase of XRCC1 protein levels, but only at P1 (**Figure 23)**, compared with CS animals. The effect of nicotinamide on XRCC1 protein levels is shown in section B of Table 12, decreasing the enhancement induced by PA at P1. Nicotinamide treatment had not any significant effect on XRCC1 protein levels in hippocampus at P14, comparing vehicle versus nicotinamide-treated animals (**Figure 23)**.

4.1.8 Effect of perinatal asphyxia and nicotinamide on calpain activity in hippocampus from rats exposed to perinatal asphyxia

In section A of Table 13, the effect of PA on hippocampus calpain activity is shown at P1 and P14 (**Figure 24)**. There was a 2-fold increase in calpain activity in PA-exposed, compared with CS animals at P14 (**Figure 24)**. As shown in section B of Table 13,

nicotinamide did not have any effect in CS animals, but it decreased calpain activity, compared to saline-treated AS animals at P14 (by 60%).

4.2 Discussion of Chapter 4

The present study evaluates the effect of PA on redox regulation in rat hippocampus at P1 and P14, evaluating also the effect of intraperitoneal administration of nicotinamide one hour after delivery. It was found that global PA produced: (i) a sustained increase of GSSG levels and GSSG:GSH ratio at P1 and P14; (ii) a decrease of GR, GPx and catalase activity at P1 and P14; (iii) a decrease of TIGAR levels at P1, followed by an increase at P14; (iv) an increase of XRCC1 levels, but only at P1; (v) an increase of calpain activity at P14; (vi) Nicotinamide prevented the effect of PA on GSSG levels and GSSG:GSH ratio, and on GR, GPx and catalase activity, also on TIGAR levels, XRCC1 protein levels and calpain activity observed at P14.

The study demonstrates that PA induces oxidative stress in hippocampus, observed at P1 and at P14, associated with a shift towards a TIGAR-dependent PPP, affecting glutathione availability for maintaining the activity of glutathione dependent enzymes, leading to alteration of redox homeostasis, and activation of cell damage mechanisms leading to death cell. Nicotinamide, a precursor of $NAD^{+/}NADP^{+}$, could modulate redox homeostasis by a PPP independent mechanism, restoring NADPH levels. As consequence, nicotinamide enhanced the activity of glutathione dependent enzymes, by transcriptional upregulation, decreasing cell damage associated with oxidative stress.

It was observed that TIGAR, a fructose-2, 6 bisphosphate, is rapidly up-regulated in response to postnatal ischemia/reperfusion (Li et al. 2014), letting the glucose metabolism enter into the PPP (Ros et al. 2013; Li et al. 2014), enhancing its flux, generating NADPH, reducing GSSG to GSH, decreasing ROS levels (Fico et al. 2004; Bensaad et al. 2006). The shunt of glucose-6-phosphate to the PPP occurs by the fructose-2, 6-bisphosphatase activity of TIGAR, decreasing fructose-2, 6-biphosphate levels, inhibiting phosphofructokinase 1 (PFK1), a rate-limiting enzyme of glycolysis (Bensaad et al. 2006, Okar et al. 2001, Li et al. 2014). Also, TIGAR could re-localise to the outer mitochondrial membrane, increasing

the activity of hexokinase 2 (HK2) to maintain mitochondrial membrane potential, reducing ROS levels, preventing caspase-depending apoptosis (Cheung et al. 2012; da-Silva et al. 2004). In postnatal models of brain ischemia, TIGAR has been shown to be up-regulated, reaching a peak at 3 h post reperfusion, declining thereafter toward basal levels (Li et al. 2014, Cao et al. 2015). In the present study, it was found that TIGAR levels were decreased in hippocampus from AS animals at P1, but increased at P14. The decrease of TIGAR levels observed at P1 occurred together with a decrease of GR, GPx and catalase activity, at a time when the GSSG:GSH ratio was increased ~2-fold. At P14, however, TIGAR levels were increased in PA-exposed animals, when the GSSG:GSH ratio was increased >4-fold in AS compared with CS animals, while GPx and catalase activity was remarkable decreased (by more than 50%). The downregulation of TIGAR observed at P1 suggests a failure of the cell system to shunt glucose-6-phosphate to the PPP for producing NADPH during the postnatal period, probably because of a reduced glutathione reductase (GTx) activity, also observed in models of postnatal brain hypoxia/ischemia, reducing PPP in brain from unilaterally clamped carotid arteries, correlating with a reduction of GTx activity, 2 hours after the insult (Brekke et al. 2014). The increase of TIGAR expression observed at P14, together with a reduction of GR activity, suggests a compensatory delayed mechanism, increasing PPP. However, NADPH levels resulting from this pathway did not appear to enhance the activity of NADPH-dependent enzymes, since the oxidative stress was sustained, evidenced by a high GSSG:GSH ratio still observed at P14. These results suggest that the NADPH produced by PPP in AS animals is used to generate instead superoxide anion by the action of NADPH oxidase, because there is *in vitro* evidence (Lu et al. 2012; Kleikers et al. 2012; Gupte et al. 2006, Balteau et al. 2011) indicating that superoxide anion production is dependent upon glucose metabolism, via the hexose monophosphate shunt to generate NADPH after ischemia-reperfusion (Suh et al. 2008; Kuehne et al. 2015). A low NADPH availability and a decreased GR activity observed at P1 and P14 after PA can explain the GSSG accumulation observed in hippocampus from AS animals up to P14, indicating that PA impairs the GR-dependent salvage pathway for GSH recycling. The salvage pathway reduces GSSG to GSH, maintaining the GSH dependent activity of antioxidant enzymes (Lushchak et al. 2012). The changes observed in GSH levels (decreased by ~36% in AS animals at P14) can imply a failure of *de novo*

synthesis of GSH, associated to metabolic deregulation of cysteine, glycine and/or glutamate, precursors of GSH synthesis by astrocytes (Hertz et al. 2004).

Another issue addressed by the present study was to evaluate whether the enzymatic activity of GPx is affected by PA, since a reduced catalase activity was reported in AS animals, suggesting H_2O_2 accumulation following hypoxia and re-oxygenation (Lespay-Rebolledo et al. 2018), in agreement with a cooperative function shown between both enzymes under oxidative stress conditions (Baud et al. 2004). The present results show a decrease of around 50% in GPx activity, together with more than 60% decrease of catalase activity in AS animals at P14. GPx is the enzyme removing hydro- and lipid-peroxides, performed by two steps: (i) an oxidative reaction by which H_2O_2 binds to the catalytic site of GR, reduced to H_2O by GSH, and (ii) a reductive reaction, by which the GSSG formed in the first step is reduced to GSH. Although, the second step is dependent of GSH, the catalytic activity of this enzyme depends upon the H_2O_2 concentration (Deponte et al. 2013). Both GPx and catalase cooperatively act to remove H_2O_2 (Baud et al. 2004, Lardinois et al. 1996). At high concentrations of H_2O_2 (>100 µM) catalase is auto-inactivated by irreversible inhibition, prevented by GPx, removing H_2O_2, to be maintained at low levels (>1 µM), allowing the functioning of catalase (Baud et al. 2004). Therefore, the decreased GPx activity observed under AS conditions suggests that is a consequence of high accumulation of catalase-regulated H_2O_2. High GSH levels can activate catalase, as shown by studies carried out with astrocytes, demonstrating that GSH deprivation induces auto-inactivation of catalase (Dringen et al. 1997, Sokolova et al. 2001). However, as also shown in a previous study (Lespay-Rebolledo et al. 2018), PA induced a decrease of GSH levels at P14, suggesting that at early stages following PA a decrease of catalase activity is not a consequence of low GSH levels, but it is achieved by other mechanisms, increasing H_2O_2 levels, perhaps due to overactivation of SOD and /or NADPH oxidase (Kinouchi et al. 1998; Lu et al. 2012; Kleikers et al. 2012).

An important issue was to evaluate the effect of nicotinamide, reversing the redox impairment induced by PA. Nicotinamide has been shown to play a fundamental role as a biological precursor for the synthesis of NAD^+ and $NADP^+$ (Kamat et al. 1999, Chong et al.

2004), preventing oxidative stress (Turunc et al. 2014). Indeed, NAD^+ can be yielded by two pathways: (i) the kynurenine (from dietary tryptophan) and (ii) the salvage pathway from nicotinamide by the enzymes nicotinamide phosphoribosyl transferase and NMNAT nicotinamide deamidase (Houtkooper et al. 2010; Massudi et al. 2012; Poljsak et al. 2016). The synthesis of NADPH can be then driven by re-routing glycolysis to the PPP pathway (Chakrabarti et al. 2015), but also by the NAD^+ salvage pathway (Massudi et al. 2012), which, via NAMPT, contributes to NADPH synthesis by transference of the phosphoribosyl group from 5-phosphoribosyl-1-pyrophosphate to nicotinamide, forming nicotinamide mononucleotide (NMN), and pyrophosphate. The coupling with NAD^+ kinase (NADK) to generate $NADP^+$ from NAD^+ contributes to NADPH synthesis (Massudi et al. 2012). Thus, nicotinamide administration probably contributes to restore the redox homeostasis under a sustained oxidative stress induced by PA, increasing $NADP^+$, acting on the NAD^+ salvage pathway. It was previously shown that a single injection of nicotinamide (0.8 mmol/kg, i.p.) yields cerebral nicotinamide concentration above the 10 μM range, lasting for longer than 5 hours (Allende-Castro et al. 2012).

It is suggested here that nicotinamide enhances NADPH levels probably via a PPP-independent mechanism, since TIGAR expression was downregulated by nicotinamide (by approximately 40%) in AS animals at P14, showing increased GR activity (2 fold) at P14. However, at P1 TIGAR expression was not changed by nicotinamide, while GR activity was increased in both AS (4-fold) and CS (2-fold) animals, indicating that, indeed, nicotinamide causes a reversion of the PPP flux to basal levels and a shift to other mechanisms for producing NADPH, such as the NAD^+ salvage pathway.

The increase of GR activity in AS animals produced by nicotinamide at P1 and P14 led to a decrease in GSSG (by 40%) and an increase in GSH levels (2-3 fold), resulting in a decreased GSSG:GSH ratio, also observed in nicotinamide-treated CS animals. The effect of nicotinamide on GSSG:GSH ratio suggests a decrease of oxidative stress and activation of mechanisms of the *de novo* synthesis of GSH, since nicotinamide-treated CS animals showed increased GSH basal levels without any changes in GSSG levels. The high GSH availability implies an increased GPx and catalase activity in AS treated with nicotinamide animals at P1 and P14, a maximal effect observed at P14.

The increased enzymatic activity induced by nicotinamide on GR, GPx and catalase can be associated with allosteric mechanisms mediated by substrate and products (Ramos-Martinez, 2017). Post-transductional modifications mediated by oxidative stress contribute to enzyme inactivation (Miyamoto et al. 2003; Gosh et al. 2006). A transcriptional control causes up-regulation of protein expression, resulting in increased enzymatic activity (Franco-Enzástiga et al. 2017). The nicotinamide effect on GR and GPx activity, above basal levels observed in CS and AS animals suggests up-regulation by increased transcriptional-dependent protein levels (Franco-Enzástiga et al. 2017). Although, a statistical significant increase in catalase expression was observed in nicotinamide-treated CS and AS animals at P1 and P14, that slightly increaseed, had no effect on basal catalase activity, suggesting that the increased enzymatic activity observed is due to a decrease of post-transductional modifications mediated by ROS.

Finally, it was investigated whether oxidative stress induced by PA produced activation of cell damage, in agreement with hippocampus cell damage observed following PA, shown in Chapter 3 of this thesis. PA induced caspase-dependent cell death at P3 and P7, but not at P1 or at P14, suggesting others molecular mechanisms for the delayed cell death observed in hippocampus, perhaps associated to progression of brain damage. Thus, both XRCC1 and calpain were used as markers of cell damage, activated by oxidative stress.

An increase of XRCC1 levels was only observed at P1 after PA, in agreement with previous observations regarding PARP-1 overexpression, restricted in hippocampus to the first hours after delivery (Neira-Peña et al. 2014, 2015), prevented, however, by neonatal nicotinamide treatment (Allende-Castro et al. 2012; Neira-Peña et al. 2015) and selective siRNA PARP-1 knockdown (Vio et al. 2018). The increase in XRCC1 levels induced by PA was also prevented by nicotinamide, reducing XRCC1 protein to basal levels. In ischemia-reperfusion postnatal models, in which oxidative stress induces DNA strand breaks (SSBR), it was observed that polyADP ribosylation sites accumulated XRCC1 (El-Khamisy et al. 2003; Wei et al. 2013), interacting with DNA ligase III, polymerase DNA and PARP-1, probably for DNA repairing (London, 2015). Also, the down-regulation of XRCC1 expression has been associated with brain damage in ischemia (Fujimura et al.

1999; Ghosh et al. 2015), and now also induced by perinatal asphyxia, as previously reported (Chiappe-Gutierrez et al. 1998).

The effect of PA on calpain activity, increased at P14, has also been observed in HI brain neonatal models, associated with fragmentation of dendritic processes and neuronal degeneration (Neumar et al. 2001), showing an initial activation of calpain 1, short after the insult, decreased at 2-48h, but again increased at P14 to P21 (Ostwald et al. 1993; Blomgren et al. 1999), leading to apoptosis independent cell death, associated to caspase 7, 8 and 9 (Chua et al. 2000; Neumar et al. 2003). In the present study, the increase in calpain activity and the effect of nicotinamide observed at P14 also indicates a role of oxidative stress on calpain, implying increased cytosolic Ca^{+2} levels, mitochondrial dysfunction, and/or endoplasmic reticulum-stress (Ermak et al. 2002), producing activation of calpain 1 (Yamada et al. 2012). Whether calpain mediates the cell damage induced by PA in hippocampus, via necrosis or programmed necrosis, is something that requires further investigation, including evaluation of the role of AIF release and/or TNF-α signalling, as shown by Neira-Peña et al. (2015) and Cheng et al. (2018). The effect of PA on calpain activity was observed at P14, a time at which an increase in caspase-3 levels was no longer observed (Lespay-Rebolledo et al. 2018), suggesting a caspase-3 independent, but bax-dependent delayed cell death, as previously proposed, showing mitochondrial impairment to precede neuronal death (D'Orsi et al. 2012).

Thus, the present results support the idea that brain damage continues long after the re-oxygenation period, extending to days (P1) and/or weeks (P14) after PA, implying changes in metabolism, redox homeostasis and suppression and/or over-activation of gene expression. Apoptosis has been observed by DNA fragmentation assays in hippocampus of PA-exposed animals along periods extending one month, being a primary mechanism for progression of brain damage induced by PA (Morales et al. 2010). In this study, the activation of differential mechanisms of cell damage was demonstrated, at P1 depending upon DNA fragmentation, reflected by decreased XRCC1 levels. But at P14, cell death depended upon calpain activation, playing a role in the progression of brain damage induced PA.

4.3 Conclusion of Chapter 4

The sustained oxidative stress induced by PA causes a reduced antioxidant response in hippocampus, leading to increased GSSG:GSH ratio, in parallel with decreased GR, GPX and catalase activity, at P1 and P14. PA triggers activation of survival pathways, to reduce oxidative stress, increasing NADPH, TIGAR and XRCC1 availability, shifting to PPP flux and DNA repair, attenuating, but not avoiding the effect of severe PA on cell death observed in hippocampus at P14, associated with increased calpain activity, indicating a caspase-independent mechanism for delayed cell death.

Nicotinamide, as a NAD^+/$NADP^+$ precursor, increased the activity of antioxidant enzymes, restoring GSH, decreasing cell damage in hippocampus. These effects, induced by nicotinamide, suggest a metabolic modulation towards restoring redox homeostasis, which is fundamental for preventing the neurological damage observed in adolescent rats suffering PA. Therefore, nicotinamide can play a fundamental therapeutic role to prevent the progression of brain damage and the long-term neurological deficits affecting neonates surviving PA.

5. Final conclusion

The immature neonatal brain exposed to PA undergoes a progression of damage known as delayed death cell, which is relevant for the motor and cognitive outcome of neonates surviving PA. It well known that apoptosis is the main mechanism involved in delayed death cell associated with ATP deficits within the 24 first hours period when over-activation of PARP-1 occurs, worsening cell damage. It is poorly understood, however, how the temporal changes in redox mechanisms, contributing to delayed death cell. In mature brain exposed to ischemia insults there is a contribution lasting 1-2 hours, without evidence for a long-term period associated to delayed death.

The results obtained in this Thesis support the hypothesis that: *the progression of brain damage during a delayed cell death period in vulnerable brain areas of animals exposed to perinatal asphyxia is associated with sustained oxidative stress along development, impairing redox homeostasis. Nicotinamide enhances the response of glutathione-dependent enzymes by a pentose phosphate dependent pathway, preventing the progression of asphyxia-dependent brain damage.*

The present Thesis contributes to demonstrate that redox mechanisms are altered by PA, leading to a sustained oxidative stress during a delayed death cell period, evaluated here from P1 to P14 in susceptible brain areas, mesencephalon, hippocampus and telencephalon. A role for cleaved caspase-3, GSSG:GSH ratio and catalase activity was demonstrated, supporting the progression of damage associated with the antioxidant response and apoptosis occurring along a postnatal period following recovering from PA. Thus, an increase of reduced glutathione, together with an increase of catalase activity will lead to enhanced resistant to apoptotic-like mechanisms.

The relevance of glutathione for the damage induced by PA was evaluated in hippocampus, demonstrating that the response of glutathione-dependent enzymes is controlled by the pentose phosphate dependent pathway (PPP), preventing asphyxia-dependent brain damage. Thus, precursors of NAD/NADP, like nicotinamide, have the ability of induce changes in redox environment by mechanisms modulating the PPP increasing NADPH, to maintain the functioning of cell redox, activating mechanisms of repairing.

The understanding the molecular mechanisms involved in the progression of brain damage during a delayed death cell period, and the contribution of redox systems leads

to selective therapeutic approaches, but also to increase a window of opportunities to prevent PA-induced damage.

6. References

Abou-El-Hassan MA, Rabelink MJ, van der Vijgh WJ, Bast A, Hoeben RC. (2003). A comparative study between catalase gene therapy and the cardioprotectormonohydroxyethylrutoside (MonoHER) in protecting against doxorubicin-induced cardiotoxicity in vitro. Br. J. Cancer 89(11): 2140 – 2146.

Abramov AY, Scorziello A, and Duchen MR. (2007). Three Distinct Mechanisms Generate Oxygen Free Radicals in Neurons and Contribute to Cell Death during Anoxia and Reoxygenation. J Neurosci. 27(5):1129-38.

Aliyu I, Lawal TO, Onankpa B. (2018). Hypoxic-ischemic encephalopathy and the Apgar scoring system: The experience in a resource-limited setting. J Clin Sci. 15:18-21

Almeida MFB, Kawakami MD, Moreira LMO, Santos RMVD, Anchieta LM, Guinsburg R. (2017). Early neonatal deaths associated with perinatal asphyxia in infants ≥2500g in Brazil. J Pediatr (Rio J). 93(6):576-584.

Alonso-Spilsbury M, Mota-Rojas D, Villanueva-García D, Martínez-Burnes J, Orozco H, Ramírez-Necoechea R, Mayagoitia AL, Trujillo ME. (2005). Perinatal asphyxia pathophysiology in pig and human: A review.AnimReprod Sci. 90(1-2):1-30.

Allende-Castro C, Espina-Marchant P, Bustamante D, Rojas-Mancilla E, Neira T, Gutierrez-Hernandez MA, Esmar D, Valdes JL, Morales P, Gebicke-Haerter PJ, Herrera-Marschitz M (2012) Further studies on the hypothesis of PARP-1 inhibition as strategy for lessening the long-term effects produced by perinatal asphyxia: effects of nicotinamide and theophylline on PARP-1 activity in brain and peripheral tissue. Neurotox Res 22:79–90.

An C, Shi Y, Li P, Hu X, Gan Y, Stetler RA, Leak RK, Gao Y, Sun BL, Zheng P, Chen J. (2014). Molecular dialogs between the ischemic brain and the peripheral immune system: dualistic roles in injury and repair. ProgNeurobiol. 115:6-24.

Antonucci R, Porcella A, Pilloni MD. (2014). Perinatal asphyxia in the term newborn. J PediatrNeonat Individual Med. 3(2):e030269.

Aquilano K, Baldelli S, Ciriolo MR. (2014). Glutathione: new roles in redox signaling for an old antioxidant. Front Pharmacol. 5:196.

Ariff S, Lee AC, Lawn J, Bhutta ZA. (2016). Global burden, epidemiologic trends, and prevention of intrapartum-related deaths in low-resource settings. ClinPerinatol. 43:593-608.

Armogida M, Spalloni A, Amantea D, Nutini M, Petrelli F, Longone P, Bagetta G, Nisticò R, Mercuri NB. (2011). The protective role of catalase against cerebral ischemia in vitro and in vivo. Int J Immunopathol Pharmacol. 24(3):735-47.

Arnaez J, García-Alix A, Arca G, Valverde E, Caserío S, Moral MT, Benavente-Fernández I, Lubián-López S; Grupo de Trabajo EHI-ESP. (2018). Incidence of hypoxic-ischaemic encephalopathy and use of therapeutic hypothermia in Spain. AnPediatr (Barc). 89(1):12-23.

Aslam HM, Saleem S, Afzal R, Iqbal U, Saleem SM, Shaikh MWA et al. (2014). Risk factors of birth asphyxia and quot. Italian J Pediatr. 40:94.

Azzopardi D, Robertson NJ, Bainbridge A, Cady E, Charles-Edwards G, Deierl A, Fagiolo G, Franks NP, Griffiths J, Hajnal J, Juszczak E, Kapetanakis B, Linsell L, Maze M, Omar O, Strohm B, Tusor N, Edwards AD. (2016). Moderate hypothermia within 6 h of birth plus inhaled xenon versus moderate hypothermia alone after birth asphyxia (TOBY-Xe): a proof-of-concept, open-label, randomised controlled trial. Lancet Neurol. 15(2):145-153.

Balteau M, Tajeddine N, de Meester C, Ginion A, Des Rosiers C, Brady NR, Sommereyns C, Horman S, Vanoverschelde JL, Gailly P, Hue L, Bertrand L, Beauloye C (2011) NADPH oxidase activation by hyperglycaemia in cardiomyocytes is independent of glucose metabolism but requires SGLT1.Cardiovasc Res. 92 (2):237-46.

Bahubali D Gane, Nandakumar S, Vishnu Bhat B, Ramachandra Rao, Adhisivam B, Rojo Joy, Prasad P, Shruti S. (2013). Biochemical marker as predictor of outcome in perinatal asphyxia. Curr Pediatr Res. 17 (2): 63-66.

Bågenholm R, Nilsson UA, Kjellmer I. (1997). Formation of free radicals in hypoxic ischemic brain damage in the neonatal rat, assessed by an endogenous spin trap and lipid peroxidation. Brain Res. 773(1-2):132-8.

Barkhuizen M, van den Hove DL, Vles JS, Steinbusch HW, Kramer BW, Gavilanes AW. 25 years of research on global asphyxia in the immature rat brain. (2017). NeurosciBiobehav Rev. 75:166-182.

Baud O, Greene AE, Li J, Wang H, Volpe JJ, Rosenberg PA (2004). Glutathione peroxidase-catalase cooperativity is required for resistance to hydrogen peroxide by mature rat oligodendrocytes. J Neurosci. 24 (7):1531-40.

Benjelloun, N., Renolleau, S., Represa, A., Ben-Ari, Y. and Charriaut-Marlangue, C. (1999). Inflammatory responses in the cerebral cortex after ischemia in the P7 neonatal rat. Stroke. 30 (9):1916-23

Bensaad K, Tsuruta A, Selak MA, Vidal MN, Nakano K, Bartrons R, Gottlieb E, Vousden KH (2006) TIGAR, a p53-inducible regulator of glycolysis and apoptosis. Cell. 126 (1):107-20.

Bentle MS, Reinicke KE, Bey EA, Spitz DR, Bootman DA (2006) Calcium dependent modulation of Poly(ADP-ribose) polymerase 1 alters cellular metabolism and DNA repair. J Biol Chem. 281(44):33684-96.

Benzie IF, Strain JJ. (1996).The Ferric Reducing Ability of Plasma (FRAP) as a Measure of ‘‘Antioxidant Power’’: The FRAP Assay. Anal Biochem. 239(1):70-6.

Berger NA. Poly(ADP-ribose) in the cellular response to DNA damage (1985). Radiat. Res.101:4–15.

Berman DR, Mozurkewich E, Liu Y, Barks J. (2009). Docosahexaenoic acid pretreatment confers neuroprotection in a rat model of perinatal cerebral hypoxia-ischemia. Am J Obstet Gynecol. 200:305, e301–306.

Bolaños JP, Delgado-Esteban M, Herrero-Mendez A, Fernandez-Fernandez S, Almeida A. (2008) Regulation of glycolysis and pentose–phosphate pathway by nitric oxide: Impact on neuronal survival. Biochim Biophys Acta. 1777(7-8):789-93.

Bordone L, Campbell C (2002) DNA ligase III is degraded by calpain during cell death induced by DNA-damaging agents. J Biol Chem. 277(29): 26673-80.

Bustamante D, Goiny M, Astrom G, Gross J, Andersson K, Herrera-Marschitz M. (2003). Nicotinamide prevents the long-term effects of perinatal asphyxia on basal ganglia monoamine systems in the rat. Exp Brain Res. 148:227–232

Blomgren K, Hallin U, Andersson AL, Puka-Sundvall M, Bahr BA, McRae A, Saido TC, Kawashima S, Hagberg H (1999). Calpastatin is up-regulated in response to hypoxia and is a suicide substrate to calpain after neonatal cerebral hypoxia-ischemia. J Biol Chem. 274(20):14046-52.

Blomgren K, Zhu C, Wang X, Karlsson JO, Leverin AL, Bahr BA, Mallard C, Hagberg H (2001) Synergistic activation of caspase-3 by m-calpain after neonatal hypoxia-ischemia: a mechanism of "pathological apoptosis"? J Biol Chem. 276(13):10191-8.

Blomgren K and Hagberg H (2005) Free radicals, mitochondria, and hypoxia-ischemia in the developing brain. Brain Pathol. 15(3):234-40.

Blomgren, K. and Hagberg, H. (2006). Free radicals, mitochondria, and hypoxia-ischemia in the developing brain. Free RadicBiol Med. 2006 Feb 1;40(3):388-97.

Bryce J, Boschi-Pinto C, Shibuya K, Black RE; WHO Child Health Epidemiology Reference Group. WHO estimates of the causes of death in children. Lancet. 2005 Mar 26-Apr 1;365(9465):1147-52.

Brekke EM, Morken TS, Widerøe M, Håberg AK, Brubakk AM, Sonnewald U (2014) The pentose phosphate pathway and pyruvate carboxylation after neonatal hypoxic-ischemic brain injury. J Cereb Blood Flow Metab. 34 (4):724-34.

Brookes PS, Yoon Y, Robotham JL, Anders MW, Sheu SS. (2004). Calcium, ATP, and ROS: a mitochondrial love-hate triangle. Am J Physiol Cell Physiol 287: C817–C833.

Bjelke B, Andersson K, Ögren SÖ, Bolme P (1991) Asphyctic lesion: proliferation of tyrosine hydroxylase immunoreactive nerve cell bodies in the rat substantia nigra and functional changes in dopamine neurotransmission. Brain Res 543: 1–9.

Bryan HK, Olayanju A, Goldring CE, Park BK. (2013) . The Nrf2 cell defence pathway: Keap1-dependent and -independent mechanisms of regulation. Biochem Pharmacol. 15;85(6):705-17.

Cao L, Chen J, Li M, Qin YY, Sun M, Sheng R, Han F, Wang G, Qin ZH (2015) Endogenous level of TIGAR in brain is associated with vulnerability of neurons to ischemic injury. Neurosci Bull. 31 (5):527-40.

Capani F, Loidl CF, Aguirre F, Piehl L, Facorro G, Hager A, De Paoli T, Farach H, Pecci-Saavedra J. (2001). Changes in reactive oxygen species (ROS) production in rat brain during global perinatal asphyxia: an ESR study. Brain Res. 914(1-2):204-7.

Capani F, Loidl CF, Piehl LL, Facorro G, De Paoli T, Hager A. (2003). Long term production of reactive oxygen species during perinatal asphyxia in the rat central nervous system: effects of hypothermia. Intern. J. Neuscience 113(5): 641-654.

Cerio F. G. D., Lara-Celador I., Antonia A., Enrique H. (2013). Neuroprotective therapies after perinatal hypoxic-ischemic brain injury. Brain Sci. 3 191–214.

Chakrabarti G, Gerber DE, Boothman DA (2015) Expanding antitumor therapeutic windows by targeting cancer-specific nicotinamide adenine dinucleotide phosphate-biogenesis pathways. ClinPharmacol. 7: 57-68.

Chakravarti R, Gupta K, Majors A, Ruple L, Aronica M, Stuehr DJ. (2015). Novel insights in mammalian catalase heme maturation: Effect of NO and thioredoxin-1. Free Radic Biol Med. 82:105-13.

Chen B and Tang L (2011). Protective effects of catalase on retinal ischemia/reperfusion injury in rats. Exp Eye Res 93: 599-606.

Chen J, Zhang DM, Feng X, Wang J, Qin YY, Zhang T, Huang Q, Sheng R, Chen Z, Li M, Qin ZH. (2018). TIGAR inhibits ischemia/reperfusion-induced inflammatory response of astrocytes. Neuropharmacology 131: 377e388.

Cheng SY, Wang SC, Lei M, Wang Z, Xiong K (2018) Regulatory role of calpaìn in neuronal death. Neural RegenRes.13(3): 556-562.

Cheung EC, Ludwig RL, Vousden KH (2012) Mitochondrial localization of TIGAR under hypoxia stimulates HK2 and lowers ROS and cell death. ProcNatlAcadSci U S A. 109 (50):20491-6.

Chiappe-Gutierrez M, Kitzmueller E, Labudova O, Fuerst G, Hoeger H, Hardmeier R, Nohl H, Gille L, Lubec B (1998) mRNA levels of the hypoxia inducible factor (HIF-1) and DNA repair genes in perinatal asphyxia of the rat. Life Sci. 63 (13):1157-67.

Chong ZZ, Lin SH, Maiese K (2004) The NAD+ Precursor Nicotinamide Governs Neuronal Survival During Oxidative Stress Through Protein Kinase B Coupled to FOXO3a and Mitochondrial Membrane Potential. J Cereb Blood Flow Metab. 24 (7):728-43.

Chua BT, Guo K, Li P. (2000) Direct cleavage by the calcium-activated protease calpain can lead to inactivation of caspases. J Biol Chem. 275 (7):5131-5.

da-Silva WS, Gómez-Puyou A, de Gómez-Puyou MT, Moreno-Sanchez R, De Felice FG, de Meis L, Oliveira MF, Galina A (2004) Mitochondrial bound hexokinase activity as a preventive antioxidant defense: steady-state ADP formation as a regulatory mechanism of

membrane potential and reactive oxygen species generation in mitochondria. J Biol Chem. 279 (38):39846-55.

Day BJ. Antioxidant therapeutics:Pandora′s box. (2014). Free Radic Biol Med. 66:58-64.

De(Addya) K, Sengupta D. (1986). Ontogeny of human fetal catalase, superoxide dismutase and lipid peroxidation: A comparative study. J. Biosci. 10(3): 319-22.

Degasperi A, Birtwistle MR, Volinsky N, Rauch J, Kolch W, Kholodenko BN. (2014). Evaluating strategies to normalise biological replicates of Western blot data. PLoS One. 27;9(1):e87293.

Dell'Anna E, Chen Y, Engidawork E, Andersson K, Lubec G, Luthman J, Herrera-Marschitz M. (1997). Delayed neuronal death following perinatal asphyxia in rat. Exp Brain Res. 115:105–115

Deponte M (2013) Glutathione catalysis and the reaction mechanisms of glutathione-dependent enzymes. BiochimBiophysActa. 1830 (5):3217-66.

Dingley J, Tooley J, Porter H, Thoresen M. (2006). Xenon provides short-term neuroprotection in neonatal ratswhen administered after hypoxia-ischemia. Stroke. 37:501–506

Dirnagl U, Iadecola C, Moskowitz MA. (1999). Pathobiology of ischaemic stroke: an integrated view. Trends in Neurosci 22(9):391-7.

D'Orsi B, Bonner H, Tuffy LP, Düssmann H, Woods I, Courtney MJ, Ward MW, Prehn JH (2012) Calpains are downstream effectors of bax-dependent excitotoxic apoptosis. J Neurosci. 32(5):1847-58.

Dringen R, Hamprecht B (1997) Involvement of glutathione peroxidase and catalase in the disposal of exogenous hydrogen peroxide by cultured astroglial cells. Brain Res. 759(1):67-75.

Dringen R (2000) Metabolism and functions of glutathione in brain. ProgNeurobiol. 62(6):649-71.

Edwards AD, Brocklehurst P, Gunn AJ, Halliday H, Juszczak E, Levene M, Strohm B, Thoresen M, Whitelaw A, Azzopardi D. (2010). Neurological outcomes at 18 months of age after moderate hypothermia for perinatal hypoxic ischaemic encephalopathy: synthesis and meta-analysis of trial data. BMJ. 340:c363.

Eicher DJ, Wagner CL, Katikaneni LP, Hulsey TC, Bass WT, Kaufman DA, Horgan MJ, Languani S, Bhatia JJ, Givelichian LM, Sankaran K, Yager JY. (2005). Moderate hypothermia in neonatal encephalopathy: efficacy outcomes. Pediatr Neurol. 32(1):11-7.

Elmahdy H, El-Mashad AR, El-Bahrawy H, El-Gohary T, El-Barbary A, Aly H. (2010). Human recombinant erythropoietin in asphyxia neonatorum: pilot trial. Pediatrics. 125(5):e1135-42.

El-Khamisy SF, Masutani M, Suzuki H, Caldecott KW (2003) A requirement for PARP-1 for the assembly or stability of XRCC1 nuclear foci at sites of oxidative DNA damage. Nucleic Acids Res. 31(19): 5526-33.

Ermak G, Davies KJ (2002) Calcium and oxidative stress: from cell signaling to cell death. MolImmunol. 38:713–721.

Ferrer I, Pozas E, Lopez E, Ballabriga J (1997) Bcl-2, Bax and Bcl-x expression following hypoxia-ischemia in the infant rat brain. Acta Neuropathol 94: 583-589

Fico A, Paglialunga F, Cigliano L, Abrescia P, Verde P, Martini G, Iaccarino I, Filosa S (2004) Glucose-6-phosphate dehydrogenase plays a crucial role in protection from redox-stress-induced apoptosis. Cell Death Differ. 11 (8):823-31.

Finer NN, Robertson CM, Richards RT, Pinnell LE, Peters KL. (1981). Hypoxic-ischemic encephalopathy in term neonates: perinatal factors and outcome. J Pediatr. 98(1):112-7.

Fujimura M, Morita-Fujimura Y, Sugawara T, Chan PH (1999) Early decrease of XRCC1, a DNA base excision repair protein, may contribute to DNA fragmentation after transient focal cerebral ischemia in mice. Stroke 30(11): 2456-63.

Fullerton HJ, Ditelberg JS, Chen SF, Sarco DP, Chan PH, Epstein CJ, Ferriero DM (1998) Copper/zinc superoxide dismutase transgenic brain accumulates hydrogen peroxide after perinatal hypoxia ischemia. Ann Neurol. 44:357–364.

Fleiss B, Gressens P. (2012). Tertiary mechanisms of brain damage: a new hope for treatment of cerebral palsy? Lancet Neurol. 11:556–66.

Franco R, Cidlowski JA. (2009). Apoptosis and glutathione: beyond an antioxidant. Cell Death Differ. 16(10):1303-14.

Franco‐Enzástiga U, Santana‐Martínez RA, Silva‐Islas CA, Barrera‐Oviedo D, Chánez‐Cárdenas ME, Maldonado PD (2017) Chronic Administration of S-Allylcysteine Activates Nrf2 Factor and Enhances the Activity of Antioxidant Enzymes in the Striatum, Frontal Cortex and Hippocampus. Neurochem Res. 42:3041–3051.

Galkina O. V., Putilina F. E., Romanova A. A., and Eshchenko N. D. (2009). Changes in lipid peroxidation and antioxidant system of the brain during early postnatal development in rats. Neurochem. J. 3:93-97.

Golubnitschaja O., Yeghiazaryan K., Cebioglu M., Morelli M. and Herrera-Marschitz M. (2011). Birth asphyxia as the major complication in newborns: moving towards improved individual outcomes by prediction, targeted prevention and tailored medical care. EPMA J. 2:197–210.

Gunn AJ, Gluckman PD, Gunn TR. (1998). Selective head cooling in newborn infants after perinatal asphyxia: a safety study. Pediatrics. 102(4 Pt 1):885-92.

Gupte SA, Levine RJ, Gupte RS, Young ME, Lionetti V, Labinskyy V, Floyd BC, Ojaimi C, Bellomo M, Wolin MS, Recchia FA (2006) Glucose-6-phosphate dehydrogenase-derived NADPH fuels superoxide production in the failing heart. J Mol Cell Cardiol. 41 (2):340-9.

Ghosh S, Janocha AJ, Aronica MA, Swaidani S, Comhair SA, Xu W, Zheng L, Kaveti S, Kinter M, Hazen SL, Erzurum SC (2006) Nitrotyrosine proteome survey in asthma identifies oxidative mechanism of catalase inactivation. J Immunol 176(9):5587–5597.

Ghosh S, Canugovi C, Yoon JS, Wilson DM 3rd, Croteau DL, Mattson MP, Bohr VA (2015) Partial loss of the DNA repair scaffolding protein, Xrcc1, results in increased brain damage and reduced recovery from ischemic stroke in mice. Neurobiol Aging, 36(7): 2319-2320.

Hagberg H, David Edwards A, Groenendaal F (2016) Perinatal brain damage: The term infant. Neurobiol Dis. 92(Pt A):102-12.

Hankins GD, Speer M. (2003). Defining the pathogenesis and pathophysiology of neonatal encephalopathy and cerebral palsy. Obstet Gynecol. 102(3):628-36.

Hassell KJ, Ezzati M, Alonso-Alconada D, Hausenloy DJ, Robertson NJ. (2015). New horizons for newborn brain protection: enhancing endogenous neuroprotection. Arch Dis Child Fetal Neonatal Ed. 100(6):F541-52.

Herrera-Marschitz M., Morales P., Leyton L., Bustamante D, Klawitter V, Espina-Marchant P, Allende C, Lisboa F, Cunich G, Jara-Cavieres A, Neira T, Gutierrez-Hernandez MA, Gonzalez-Lira V, Simola N, Schmitt A, Morelli M, Andrew Tasker R, Gebicke-Haerter PJ. (2011). Perinatal asphyxia: current status and approaches towards neuroprotective strategies, with focus on sentinel proteins. Neurotox. Res. 19(4):603-27.

Herrera-Marschitz M, Neira-Pena T, Rojas-Mancilla E, Espina-Marchant P, Esmar D, Perez R, Muñoz V, Gutierrez-Hernandez M, Rivera B, Simola N, Bustamante D, Morales P, Gebicke-Haerter PJ (2014) Perinatal asphyxia: CNS development and deficits with delayed onset. Front Neurosci. 8: 47.

Hertz L, Zielke HR (2004) Astrocytic control of glutamatergic activity: astrocytes as stars of the show. Trends Neurosci. 27 (12):735-43.

He SQ, Zhang YH, Venugopal SK, Dicus CW, Perez RV, Ramsamooj R, Nantz MH, Zern MA, Wu J. (2006). Delivery of Antioxidative Enzyme Genes Protects Against Ischemia/Reperfusion–Induced Liver Injury in Mice. Liver Transpl. 12:1869-1879.

Hobson A., Baines J. and Weiss M.D. (2013). Beyond Hypothermia: Alternative Therapies for Hypoxic Ischemic Encephalopathy. The Open Pharmacology Journal 7: 26-40.

Hohnholt MC, Dringen R. (2014). Short time exposure to hydrogen peroxide induces sustained glutathione export from cultured neurons. Free Radic Biol Med. 70:33-44.

Homi HM, Freitas JJ, Curi R, Velasco IT, Junior BA. (2002). Changes in superoxide dismutase and catalase activities of rat brain regions during early global transient ischemia/reperfusion. Neurosci. Lett. 333(1):37-40.

Hong G, Zheng D, Zhang L, Ni R, Wang G, Fang GC, Lu Z, Peng T. (2018). Administration of nicotinamide riboside prevents oxidative stress and organ injury in sepsis. Free Radical Biology and Medicine 123: 125–137.

Houtkooper RH, Cantó C, Wanders RJ, Auwerx J (2010) The secret life of NAD+: an old metabolite controlling new metabolic signaling pathways. Endocr Rev. 31 (2):194-223.

Hudome, S., Palmer, C., Roberts, R.L., Mauger, D., Housman, C. and Towfighi, J. (1997). The role of neutrophils in the production of hypoxic-ischemic brain injury in the neonatal rat. Pediatr Res. 41(5):607-16.

Huang BY, Castillo M. (2008). Hypoxic-ischemic brain injury: imaging findings from birth to adulthood. Radiographics. 28(2):417-39; quiz 617. doi: 10.1148/rg.282075066.

Ibi M, Sawada H, Kume T, Katsuki H, Kaneko S, Shimohama S, Akaike A. (1999). Depletion of Intracellular Glutathione Increases Susceptibility to Nitric Oxide in Mesencephalic Dopaminergic Neurons. J Neurochem. 73(4):1696-703.

Ikeda T, Xia YX, Kaneko M, Sameshima H, Ikenoue T. (2002). Effect of the free radical scavenger, 3-methyl-1-phenyl-2-pyrazolin-5-one (MCI-186), on hypoxia-ischemia-induced brain injury in neonatal rats. Neurosci Lett. 329(1):33-6.

Ikonomidou C, Kaindl AM.. Neuronal Death and Oxidative Stress in the Developing Brain (2011). Antioxid Redox Signal. 14(8):1535-50.

Itoh K, Wakabayashi N, Katoh Y, Ishii T, Igarashi K, Engel JD, Yamamoto M. (1999). Keap1 represses nuclear activation of antioxidant responsive elements by Nrf2 through binding to the amino-terminal Neh2 domain. Genes Dev. 1;13(1):76-86.

Jacobs SE, Berg M, Hunt R, Tarnow-Mordi WO, Inder TE, Davis PG. (2013). Cooling for newborns with hypoxic ischaemic encephalopathy. Cochrane Database Syst Rev. (1):CD003311.

Jackson-Lewis V, Vila M, Djaldetti R, Guenan C, Liberatore G, Liu J, O'Malley K, Burke K, Przedbobrski S (2000) Developmental cell death in dopaminergic neurons of the substantia nigra in mice. J Comp Neurol 424: 476-488,

Janáky R., Cruz-Aguado R., Oja S.S., Shaw C.A. (2007) 15 Glutathione in the Nervous System: Roles in Neural Function and Health and Implications for Neurological Disease. In:

Jin R, Yang G and Li G. (2010). Inflammatory mechanisms in ischemic stroke: role of inflammatory cells. J LeukocBiol 87(5):779-89.

John CM, Ramasamy R, Al Naqeeb G, Al-Nuaimi AHD. and Adam A. (2012). Nicotinamide Supplementation Protects Gestational Diabetic Rats by Reducing Oxidative Stress and Enhancing Immune Responses. Current Medicinal Chemistry. 19, 5181-5186.

Johnston MV, Trescher WH, Ishida A, Nakajima W. (2001). Neurobiology of hypoxic-ischemic injury in the developing brain. Pediatr Res. 49(6):735-41.

Kamat JP, Devasagayam TP (1999) Nicotinamide (vitamin B3) as an effective antioxidant against oxidative damage in rat brain mitochondria. Redox Rep. 4 (4):179-84.

Karim, R., and M. A. Mannan. (2006). Alpha-Tocopherol Reduces Oxidative Stress in Perinatal Asphyxia. Bangladesh Journal of Pharmacology, Vol. 1, no. 1, 1, pp. 5-9.

Kassmann CM, Lappe-Siefke C, Baes M, Brügger B, Mildner A, Werner HB, Natt O, Michaelis T, Prinz M, Frahm J, Nave KA. (2007). Axonal loss and neuroinflammation caused by peroxisome-deficient oligodendrocytes. Nat Genet 39: 969-976.

Kinouchi H, Kamii H, Mikawa S, Epstein CJ, Yoshimoto T, Chan PH (1998) Role of superoxide dismutase in ischemic brain injury: a study using SOD-1 transgenic mice. Cell MolNeurobiol. 18(6): 609-620.

Kuehne A, Emmert H, Soehle J, Winnefeld M, Fischer F, Wenck H, Gallinat S, Terstegen L, Lucius R, Hildebrand J, Zamboni N (2015) Acute Activation of Oxidative Pentose Phosphate Pathway as First-Line Response to Oxidative Stress in Human Skin Cells. Mol Cell. 59 (3):359-71.

Kumar A, Mittal R, Khanna HD, Basu S. (2008). Free Radical Injury and Blood-Brain Barrier Permeability in Hypoxic-Ischemic Encephalopathy. Pediatrics 122(3):e722–e727.

Khan JY and Black SM. (2003). Developmental changes in murine brain antioxidant enzymes. Pediatr Res. 54(1):77-82.

Klawitter V, Morales P, Bustamante D, Goiny M, Herrera-Marschitz M. (2006). Plasticity of the central nervous system (CNS) following perinatal asphyxia: Does nicotinamide provide neuroprotection?. Amino Acids. 31(4):377-84.

Klawitter V, Morales P, Bustamante D, Gomez-Urquijo S, Hökfelt T, Herrera-Marschitz M. (2007). Plasticity of basal ganglia neurocircuitries following perinatal asphyxia: effect of nicotinamide. Exp Brain Res. 180(1):139-52.

Klaidman L, Morales M, Kem S, Yang J, Chang ML, Adams JD Jr. (2003). Nicotinamide Offers Multiple Protective Mechanisms in Stroke as a Precursor for NAD+, as a PARP Inhibitor and by Partial Restoration of Mitochondrial Function. Pharmacology. 69(3):150-7

Kleikers PW, Wingler K, Hermans JJ, Diebold I, Altenhöfer S, Radermacher KA, Janssen B, Görlach A, Schmidt HH (2012) NADPH oxidases as a source of oxidative stress and molecular target in ischemia/reperfusion injury. J Mol Med (Berl). 90 (12):1391-406.

Krych-Madej J, Gebicka L. (2015). Do pH and flavonoids influence hypochlorous acid-induced catalase inhibition and heme modification? Int J Biol Macromol. 80:162-9.

Lai MC and Yang SN (2011). Perinatal Hypoxic-Ischemic Encephalopathy. J. Biomed Biotechnol. Volume 2011, Article ID 609813, 6 pages.

Lafemina MJ, Sheldon RA and Ferriero DM. (2006). Acute hypoxia-ischemia results in hydrogen peroxide accumulation in neonatal but not adult mouse brain. Pediatr Res. 59(5):680-3.

Langeveld CH, Jongenelen CA, Schepens E, Stoof JC, Bast A and Drukarch B. (1995). Cultured rat striatal and cortical astrocytes protect mesencephalic dopaminergic neurons against hydrogen peroxide toxicity independent of their effect on neuronal development. NeurosciLett 192(1):13-6.

Lawn JE, Cousens S, Zupan J. (2005). 4 million neonatal deaths: when? where? why?. Lancet 365:891-900.

Lardinois OM, Mestdagh MM, Rouxhet PG (1996) Reversible inhibition and irreversible inactivation of catalase in presence of hydrogen peroxide. BiochimBiophysActa. 1295 (2):222-38.

Lespay-Rebolledo C, Perez-Lobos R, Tapia-Bustos A, Vio V, Morales P, Herrera-Marschitz M (2018) Regionally Impaired Redox Homeostasis in the Brain of Rats Subjected to Global Perinatal Asphyxia: Sustained Effect up to 14 Postnatal Days. Neurotox Res. 34(3):660-676.

Li M, Sun M, Cao L, Gu JH, Ge J, Chen J, Han R, Qin YY, Zhou ZP, Ding Y, Qin ZH (2014) A TIGAR-regulated metabolic pathway is critical for protection of brain ischemia. J Neurosci. 34 (22):7458-71.

Like W., Xiaojuan W., Xueming S. (2002). Post ischemia-reperfusion MPO activity changes in the brain and the observa. Journal of Brain and Nervous Diseases 2: 98-100.

Liu F and McCullough LD. (2013). Inflammatory responses in hypoxic ischemic encephalopathy. Acta Pharmacol Sin. 34: 1121–1130.

Liu D, Gharavi R, Pitta M, Gleichmann M, Mattson MP. (2009). Nicotinamide Prevents NAD+ Depletion and Protects Neurons AgainstExcitotoxicity and Cerebral Ischemia: NAD+ Consumption by SIRT1 may Endanger Energetically Compromised Neurons. Neuromolecular Med. 11(1):28-42.

London RE (2015) The structural basis of XRCC1-mediated DNA repair. DNA repair (Amst.) 30:90-103.

Lorek A, Takei Y, Cady EB, Wyatt JS, Penrice J, Edwards AD, Peebles D, Wylezinska M, Owen-Reece H, Kirkbride V, et al. (1994). Delayed ("secondary") cerebral energy failure after acute hypoxia-ischemia in the newborn piglet: continuous 48-hour studies by phosphorus magnetic resonance spectroscopy. Pediatr Res 36(6):699-706.

Lubec B, Labudova O, Hoeger H, Kirchner L, Lubec G (2002) Expression of transcription factors in the brain of rats with perinatal asphyxia. Biol Neonate 81: 266–278.

Lu Q, Wainwright MS, Harris VA, Aggarwal S, Hou Y, Rau T, Poulsen DJ, Black SM (2012) Increased NADPH oxidase-derived superoxide is involved in the neuronal cell death induced by hypoxia-ischemia in neonatal hippocampal slice cultures. Free RadicBiol Med. 53 (5):1139-51.

Lushchak VI. (2012) Glutathione homeostasis and functions: potential targets for medical interventions. J Amino Acids. 2012:736837.

Massudi H, Grant R, Guillemin GJ, Braidy N (2012) NAD+ metabolism and oxidative stress: the golden nucleotide on a crown of thorns. Redox Rep. 17 (1):28-46.

Matsuo Y, Onodera H, Shiga Y, Nakamura M, Ninomiya M, Kihara T, Kogure K. (1994) Correlation between myeloperoxidase-quantified neutrophil accumulation and ischemic brain injury in the rat. Effects of neutrophil depletion. Stroke. 25(7):1469-75.

Miyamoto Y, Koh YH, Park YS, Fujiwara N, Sakiyama H, Misonou Y, Ookawara T, Suzuki K, Honke K, Taniguchi N (2003) Oxidative stress caused by inactivation of glutathione peroxidase and adaptive responses. Biol Chem. 384 (4):567-74.

Mc Donald JW and Johnston MV. (1990). Physiological and pathophysiological roles of excitatory amino acids during central nervous system development. Brain Res Rev 15 (1); 41:70

Morales P, Reyes P, Klawitter V, Huaiquín P, Bustamante D, Fiedler J, and Herrera-Marschitz M. (2005) Effects of perinatal asphyxia on cell proliferation and neuronal phenotype evaluated with organotypic hippocampal cultures. Neuroscience 135(2):421-31.

Morales P, Fiedler JL, Andres S, Berrios C, Huaiquin P, Bustamante D, Cardenas S, Parra E, Herrera-Marschitz M (2008) Plasticity of hippocampus following perinatal asphyxia: effects on postnatal apoptosis and neurogenesis. J Neurosci Res. 86 (12):2650-62.

Morales P, Simola N, Bustamante D, Lisboa F, Fiedler J, Gebicke-Haerter PJ, Morelli M, Tasker RA, Herrera-Marschitz M. (2010) Nicotinamide prevents the long-term effects of perinatal Asphyxia on apoptosis, non-spatial working memory and anxiety in rats. Exp Brain Res 202:1–14.

Morken TS, Widerøe M, Vogt C, Lydersen S, Havnes M, Skranes J, Goa PE, Brubakk AM. (2013). Longitudinal diffusion tensor and manganese-enhanced MRI detect delayed cerebral gray and white matter injury after hypoxia-ischemia and hyperoxia. Pediatr Res.73(2):171-9.

Nelson, K.B. and Ellenberg, J.H. (1981). Apgar scores as predictors of chronic neurologic disability. Pediatrics 68: 38–44.

Neira-Peña, P. Espina-Marchant, E. Rojas-Mancilla, D. Esmar, C. Kraus, V. Munoz, R. Perez, B. Rivera, D. Bustamante, J. L. Valdes, M. Hermoso, P. Gebicke-Haerter, P. Morales, M. Herrera-Marschitz. (2014) Molecular, Cellular, and Behavioural Effects Produced by Perinatal Asphyxia: Protection by Poly (ADP-Ribose) Polymerase 1 (PARP-1) Inhibition. In: Kostrzewa R. (eds) Handbook of Neurotoxicity pp 2075-2098. Springer, New York, NY.

Neira-Peña T, Rojas-Mancilla E, Munoz-Vio V, Perez R, Gutierrez-Hernandez M, Bustamante D, Morales P, Hermoso MA, Gebicke-Haerter P, Herrera-Marschitz M (2015) Perinatal asphyxia leads to PARP-1 overactivity, p65 translocation, IL-1β and TNF-α overexpression, and apoptotic-like cell death in mesencephalon of neonatal rats: prevention by systemic neonatal nicotinamide administration. Neurotox Res. 27 (4):453-65.

Neumar RW, Meng FH, Mills AM, Xu YA, Zhang C, Welsh FA, Siman R (2001) Calpain activity in the rat brain after transient forebrain ischemia. Exp Neurol. 170(1):27-35.

Neumar RW, Xu YA, Gada H, Guttmann RP, Siman R (2003) Cross-talk between calpain and caspase proteolytic systems during neuronal apoptosis. J Biol Chem. 278(16):14162-7.

Nguyen HX, O'Barr TJ and Anderson AJ. (2007). Polymorphonuclear leukocytes promote neurotoxicity through release of matrix metalloproteinases, reactive oxygen species, and TNF-alpha. J Neurochem 102(3) 900-912.

Nieoullon A, Canolle B, Masmejean F, Guillet B, Pisano P, Lortet S. (2006). The neuronal excitatory amino acid transporter EAAC1/EAAT3: does it represent a major actor at the brain excitatory synapse? J. Neurochem. 98: 1007–1018.

Nicholls P. (2012) Classical catalase: Ancient and modern Arch Biochem Biophys. 15; 525(2):95-101.

Nortley R, Korte N, Izquierdo P, et al. (2019). Amyloid β oligomers constrict human capillaries in Alzheimer´s disease via signalling pericytes. Science. 365 (6450), eaav9518.

Northington FJ, Ferriero DM, Graham EM, Traystman RJ, Martin LJ. (2001). Early Neurodegeneration after Hypoxia-Ischemia in Neonatal Rat Is Necrosis while Delayed Neuronal Death Is Apoptosis. Neurobiol Dis. 8(2):207-19.

Northington FJ, Ferriero DM, Martin LJ. (2001) Neurodegeneration in the thalamus following neonatal hypoxia-ischemia is programmed cell death. Dev Neurosci. 23(3):186-91.

Okar DA, Manzano A, Navarro-Sabatè A, Riera L, Bartrons R, Lange AJ (2001) PFK-2/FBPase-2: maker and breaker of the essential biofactor fructose-2, 6-bisphosphate. Trends Biochem Sci. 26 (1):30-5.

Oo TF, Burke RE (1997). The time course of developmental cell death in phenotypically defined dopaminergic neurons of the substantia nigra. Dev Brain Res 98: 191-196.

Ostwald K, Hagberg H, Andiné P, Karlsson JO (1993) Upregulation of calpain activity in neonatal rat brain after hypoxic-ischemia. Brain Res. 630(1-2):289-94.

Osredkar D, Thoresen M, Maes E, Flatebø T, Elstad M, Sabir H. (2014) Hypothermia is not neuroprotective after infection-sensitized neonatal hypoxic-ischemic brain injury. Resuscitation 85(4):567-72.

Park JH, Long A, Owens K, Kristian T. (2016). Nicotinamide mononucleotide inhibits post-ischemic NAD+ degradation and dramatically ameliorates brain damage following global cerebral ischemia. NeurobiolDis. 95:102-10.

Peluffo H, Acarin L, Faiz M, Castellano B, Gonzalez B. (2005). Cu/Zn superoxide dismutase expression in the postnatal rat brain following an excitotoxic injury. J. Neuroinflammation 2(1):12.

Perez-Lobos R, Lespay-Rebolledo C, Tapia-Bustos A, Palacios E, Vío V, Bustamante D, Morales P, Herrera-Marschitz M. (2017). Vulnerability to a Metabolic Challenge Following Perinatal Asphyxia Evaluated by Organotypic Cultures: Neonatal Nicotinamide Treatment. Neurotox Res. 32(3):426-443.

Perrone S, Szabó M, Bellieni CV, Longini M, Bangó M, Kelen D, Treszl A, Negro S, Tataranno ML, Buonocore G. (2010). Whole Body Hypothermia and Oxidative Stress in Babies with Hypoxic-Ischemic Brain Injury. Pediatr Neurol. 43(4):236-40.

Polin RA, Randis TM and Sahni R. (2007) Systemic hypothermia to decrease morbidity of hypoxic-ischemic brain injury. J. Perinatology 27: S47–S58.

Poljsak B, Milisav I (2016) NAD+ as the Link Between Oxidative Stress, Inflammation, Caloric Restriction, Exercise, DNA Repair, Longevity, and Health Span. Rejuvenation Res. 19 (5):406-415.

Pradeep H, Diya JB, Shashikumar S, and Rajanikant GK. (2012). Oxidative stress – assassin behind the ischemic stroke. Folia Neuropathol 50 (3): 219-230.

Quang X, Lim SO, and Jung G. (2011). Reactive oxygen species downregulate catalase expression via methylation of a CpG Island in the Oct-1 promoter. FEBS Lett. 585: 3436–344.

Ramos-Martinez JI (2017) The regulation of the pentose phosphate pathway: Remember Krebs. Archives of Biochemistry and Biophysics 614, 50e52.

Riganti C, Gazzano E, Polimeni M, Aldieri E, Ghigo D. (2012). The pentose phosphate pathway:An antioxidant defense and across road in tumor cell fate. Free RadicalBiologyandMedicine 53: 421–436

Robertson NJ, Cox IJ, Cowan FM, Counsell SJ, Azzopardi D, Edwards AD. (1999). Cerebral intracellular lactic alkalosis persisting months after neonatal encephalopathy measured by magnetic resonance spectroscopy. Pediatr Res. 46(3):287-96.

Robertson NJ, Tan S, Groenendaal F, van Bel F, Juul SE, Bennet L, Derrick M, Back SA, Valdez RC, Northington F, Gunn AJ, Mallard C. (2012). Which neuroprotective agents are ready for bench to bedside translation in the newborn infant? J Pediatr. 160(4):544-552.e4.

Ros S, Schulze A (2013) Balancing glycolytic flux: the role of 6-phosphofructo-2-kinase/fructose 2, 6-bisphosphatases in cancer metabolism. Cancer Metab. 1(1):8.

Ryan M. McAdams and Sandra E. Juul (2012). The Role of Cytokines and Inflammatory Cells in Perinatal Brain Injury. Neurology Research International, vol. 2012, Article ID 561494, 15 pages.

Seema Shah, Kumar Goel Anil, Mamta Padhy, Sumitra Bhoi. (2014). Correlation of oxidative stress biomarker and serum marker of brain injury in hypoxic ischemic encephalopathy. International journal of medical and applied sciences. 3(1):106-115

Sigfrid LA, Cunningham JM, Beeharry N, Lortz S, Tiedge M, Lenzen S, Carlsson C, Green IC. (2003). Cytokines and nitric oxide inhibit the enzyme activity of catalase but not its protein or mRNA expression in insulin-producing cells. J MolEndocrinol. 31(3):509-18.

Sokolova T, Gutterer JM, Hirrlinger J, Hamprecht B, Dringen R (2001) Catalase in astroglia-rich primary cultures from rat brain: immunocytochemical localization and inactivation during the disposal of hydrogen peroxide. NeurosciLett. 297(2):129-32.

Stanton RC. (2012). Glucose-6-phosphate dehydrogenase, NADPH, and cell survival, IUBMB Life 64: 362–369.

Stincone A, Prigione A, Cramer T, Wamelink MM, Campbell K, Cheung E, Olin-Sandoval V, Grüning NM, Krüger A, TauqeerAlam M, Keller MA, Breitenbach M, Brindle KM, Rabinowitz JD, Ralser M. (2015) The return of metabolism: biochemistry and physiology of the pentose phosphate pathway. Biol Rev CambPhilos Soc. 90(3):927-63.

Suh SW, Shin BS, Ma H, Van Hoecke M, Brennan AM, Yenari MA, Swanson RA (2008) Glucose and NADPH Oxidase Drive Neuronal Superoxide Formation in Stroke. Ann Neurol. 64 (6):654-63.

Suganuma H, Arai Y, Kitamura Y, Hayashi M, Okumura A, Shimizu T. (2010). Maternal docosahexaenoic acid-enriched diet prevents neonatal brain injury. Neuropathology. 30:597–605.

Sun M, Li M, Huang Q, Han F, Gu JH, Xie J, Han R, Qin ZH, Zhou Z. (2015). Ischemia/reperfusion-induced upregulation of TIGAR in brain is mediated by SP1 and modulated by ROS and hormones involved in glucose metabolism. Neurochem Int. 80:99-109.

Shah PS, Raju NV, Beyene J, Perlman M. (2003). Recovery of metabolic acidosis in term infants with postasphyxial hypoxic-ischemic encephalopathy. Acta Paediatr. 92(8):941-7.

Shah PS. (2010). Hypothermia: a systematic review and meta-analysis of clinical trials. Semin Fetal Neonatal Med. 15(5):238-46.

Sheldon RA, Jiang X, Francisco C, Christen S, Vexler ZS, Täuber MG and Ferriero DM. (2004). Manipulation of Antioxidant Pathways in Neonatal Murine Brain. Pediatr Res 56(4): 656-62.

Sheikh FG, Pahan K, Khan M, Barbosa E, Singh I. (1998). Abnormality in catalase import into peroxisomes leads to severe neurological disorder. Proc. Natl. Acad. 95(6):2961-6.

Shin DH, Bae YC, Kim-Han JS, Lee JH, Choi IY, Son KH, Kang SS, Kim WK and Han BH. (2006). Polyphenol amentoflavone affords neuroprotection against neonatal hypoxic-ischemic brain damage via multiple mechanisms. J Neurochem. 96(2):561-72

Shivakumar BR, Kolluri SV, and Ravindranath V. (1995) Glutathione and protein thiol homeostasis in brain during reperfusion after cerebral ischemia. J PharmacolExpTher 274(3):1167-73.

Spolarics Z, Wu JX. (1997). Role of glutathione and catalase in H2O2 detoxification in LPS-activated hepatic endothelial and Kupffer cells. Am. J. Physiol. 273(6 Pt 1):G1304-11.

Stein LR, Imai S. (2012). The dynamic regulation of NAD metabolism in mitochondria. Trends EndocrinolMetab. 23(9):420-8.

Stincone A, Prigione A, Cramer T, Wamelink MM, Campbell K, Cheung E, Olin-Sandoval V, Grüning NM, Krüger A, TauqeerAlam M, Keller MA, Breitenbach M, Brindle KM, Rabinowitz JD, Ralser M. (2015) The return of metabolism: biochemistry and physiology of the pentose phosphate pathway. Biol Rev CambPhilos Soc. 90(3):927-63.

Stone BS, Zhang J, Mack DW, Mori S, Martin LJ, Northington FJ. (2008). Delayed Neural Network Degeneration after Neonatal Hypoxia-Ischemia. Ann Neurol. 64(5): 535–546

Swarte R, Lequin M, Cherian P, Zecic A, van Goudoever J, Govaert P. (2009). Imaging patterns of brain injury in term-birth asphyxia. ActaPaediatr. 98(3):586-92.

Tapia-Bustos A, Perez-Lobos R, Vío V, Lespay-Rebolledo C, Palacios E, Chiti-Morales A, Bustamante D, Herrera-Marschitz M, Morales P. (2017) Modulation of Postnatal Neurogenesis by Perinatal Asphyxia: Effect of D1 and D2 Dopamine Receptor Agonists. Neurotox Res. 31(1):109-121.

Taylor SC, Posch A (2014) The design of a quantitative western blot experiment. Biomed Res Inter. Vol 2014 ID 361590.

Turunc Bayrakdar E, Uyanikgil Y, Kanit L, Koylu E, Yalcin A (2014) Nicotinamide treatment reduces the levels of oxidative stress, apoptosis, and PARP-1 activity in A b (1–42)-induced rat model of Alzheimer's disease. Free Radic Res. 48 (2):146-58.

Thornberg E, Thiringer K, Odeback A, Milsom I. (1995). Birth asphyxia: incidence, clinical course and outcome in a Swedish population. ActaPaediatr. 84(8):927-32.

Thoresen M, Penrice J, Lorek A, Cady EB, Wylezinska M, Kirkbride V, Cooper CE, Brown GC, Edwards AD, Wyatt JS, et al. (1995). Mild Hypothermia after Severe Transient Hypoxia-Ischemia Ameliorates Delayed Cerebral Energy Failure in the Newborn Piglet. Pediatr Res. 37: 667–670

Thoresen M, Hobbs CE, Wood T, Chakkarapani E, Dingley J. (2009). Cooling combined with immediate or delayed xenon inhalation provides equivalent long-term neuroprotection after neonatal hypoxia-ischemia. J Cereb Blood Flow Metab. 29:707–714

Tsunoda T, Takagi T. (1999). Estimating transcription factor bindability on DNA. Bioinformatics. 15(7-8):622-30.

Vannucci RC, Towfighi J, Vannucci SJ. (2004). Secondary Energy Failure After Cerebral Hypoxia–Ischemia in the Immature Rat. J Cereb Blood Flow Metab. 24(10):1090-7.

Vasiljević B, Maglajlić-Djukić S, Gojnić M, Stanković S. (2012). The Role of Oxidative Stress in Perinatal Hypoxic-Ischemic Brain Injury. SrpArhCelokLek. 140(1-2):35-41

Vaur P, Brugg B, Mericskay M, Li Z, Schmidt MS, Vivien D, Orset C, Jacotot E, Brenner C, Duplus E. (2017). Nicotinamide riboside, a form of vitamin B3, protects against excitotoxicity-induced axonal degeneration. FASEB J. 31(12):5440-5452.

Veal EA, Day AM, Morgan BA. Hydrogen Peroxide Sensing and Signaling. Mol Cell. 13; 26(1):1-14.

Virág L, Szabó C. The therapeutic potential of poly(ADP-ribose) polymerase inhibitors (2002). Pharmacol Rev. Sep;54(3):375-429.

Vio V, Riveros AL, Tapia-Bustos A, Lespay-Rebolledo C, Perez-Lobos R, Muñoz L, Pismante P, Morales P, Araya E, Hassan N, Herrera-Marschitz M, Kogan MJ (2018) Gold

nanorods/siRNA complex administration for knockdown of PARP-1: a potential treatment for perinatal asphyxia Int J Nanomedicine. 13: 6839-6854.

Voorn P, Kalsbeek A, Jorritsma-Byham B, Goenewegen HJ (1988) The pre- and postnatal development of the dopaminergic cell groups in the ventral mesencephalon and the dopaminergic innervation of the striatum of the rat. Neuroscience 25: 857-887.

Wakabayashi-Ito Noriko and Nagata Shigekazu (1994). Characterization of the Regulatory Elements in the Promoter of the Human Elongation Factor-la Gene. The Journal of Biological Chemistry. 269 (47): 29831-29837.

Walton PA, and Pizzitelli M. (2012). Effects of peroxisomal catalase inhibition on mitochondrial function. Front Physiol. 23; 3:108.

Wallin C, Puka-Sundvall M, Hagberg H, Weber SG, Sandberg M. (2000) Alterations in glutathione and amino acid concentrations after hypoxia–ischemia in the immature rat brain. Brain Res Dev Brain Res. 29; 125(1-2):51-60.

Wang Z, Wei X, Liu K, Zhang X, Yang F, Zhang H, He Y, Zhu T, Li F, Shi W, Zhang Y, Xu H, Liu J, and Yi F. (2013). NOX2 deficiency ameliorates cerebral injury through reduction of complexin II mediated glutamate excitotoxicity in experimental stroke. Free RadicBiol Med. 65: 942–951

Wei L, Nakajima S, Hsieh CL, Kanno S, Masutani M, Levine AS, Yasui A, Lan L (2013) Damage response of XRCC1 at sites of DNA single strand breaks is regulated by phosphorylation and ubiquitylation after degradation of poly(ADP-ribose). J Cell Sci. 126(Pt 19): 4414-23

Weis SN, Schunck RV, Pettenuzzo LF, Krolow R, Matté C, Manfredini V, do Carmo R Peralba M, Vargas CR, Dalmaz C, Wyse AT, Netto CA. (2011). Early biochemical effects after unilateral hypoxia-ischemia in the immature rat brain. Int. J. Dev Neuroscience 29(2):115–120.

Winerdal M, Winerdal ME, Kinn J, Urmaliya V, Winqvist O, Adén U.(2012). Long Lasting Local and Systemic Inflammation after Cerebral Hypoxic ischemia in Newborn Mice. PLoS One 7(5):e36422.

Wintermark P, Boyd T, Gregas MC, Labrecque M, Hansen A. (2010). Placental pathology in asphyxiated newborns meeting the criteria for therapeutic hypothermia. Am J Obstet Gynecol. 203(6):579.e1-9.

Wong CH, Crack PJ. (2008). Modulation of Neuro-Inflammation and Vascular Response by Oxidative Stress Following Cerebral Ischemia-Reperfusion Injury. Curr Med Chem. 15(1):1-14.

Yamada KH, Kozlowski DA, Seidl SE, Lance S, Wieschhaus AJ, Sundivakkam P, Tiruppathi C, Chishti I, Herman IM, Kuchay SM, Chishti AH (2012) Targeted gene inactivation of calpain-1 suppresses cortical degeneration due to traumatic brain injury and neuronal apoptosis induced by oxidative stress. J Biol Chem. 287 (16):13182-93.

Ying W. (2008). NAD+/NADH and NADP+/NADPH in Cellular Functions and Cell Death: Regulation and Biological Consequences. Antioxid Redox Signal.10(2):179-206.

Ying W, Xiong ZG (2010). Oxidative Stress and NAD+ in Ischemic Brain Injury: Current Advances and Future Perspectives. Curr Med Chem. 17(20):2152-8.

Yu HP, Xie JM, Li B, Sun YH, Gao QQ, Ding ZD, Wu HR, Qin. ZH. (2015). TIGAR regulates DNA damage and repair through pentose phosphate pathway and Cdk5-ATM pathway. SCIENTIFIC REPORTS: 5 : 9853

Zhang M, An C, Gao Y, Leak RK, Chen J, Zhang F. (2013). Emerging roles of Nrf2 and phase II antioxidant enzymes in neuroprotection. Prog Neurobiol. 100:30-47.

Zhu C, Kang W, Xu F, Cheng X, Zhang Z, Jia L, Ji L, Guo X, Xiong H, Simbruner G, Blomgren K, Wang X. (2009). Erythropoietin improved neurologic outcomes in newborns with hypoxic-ischemic encephalopathy. Pediatrics. 124(2):e

7. Tables

Table 1. Apgar and postnatal evaluation. Apgar scale evaluating the consequences of PA induced by immersing foetus-containing uterine horns (removed from ready to delivery rat dams) into a water bath at 37 °C for 21 min. The Apgar scale was applied 40 min after delivery to both asphyxia-exposed (AS) and sibling caesarean delivered neonates, used as controls (CS). The following parameters were also monitored at postnatal day 1 (P1), P3, P7 and P14 after delivery: (**a**) survival (yes/no, following intensive resuscitation manoeuvres for at least 5 min; in% of the corresponding litter). (**b**) Body weight (g). (**c**) Presence of gasping (yes/no; in % of the corresponding litter). (**d**) Respiratory frequency (events/min). (**e**) Skin colour (pink to blue, P, PB, BP or B). (**f**) Spontaneous movements (0–4; 0 = no movements; 4 = coordinated movements of forward and hind legs, as well as head and neck). (**g**) Vocalisation (yes/no; in % of the corresponding litter). Data is expressed as means ± SEM, whenever the parameters are monitored by continuous scales, or by % of the corresponding litter in cases of qualitative no continuous scales (n, number of pups; m, number of dams).

CS (Caesarean delivered; 0 min asphyxia) (*n*= 76; *m*=5)					
Parameters	**40 min**	**P1**	**P3**	**P7**	**P14**
Survival (%)	100	100	100	100	100
Body weight (g)	6.08 ± 0.12	5.31 ± 0.58	8.55 ± 0.37	13.7 ± 0.49	17.58 ±1.79
Gasping (%)	0.06 ± 0.06	0	0	0	0
Respiratory frequency (events/min)	78.51±1.43	77.76 ± 2.32	80.56 ± 1.28	93.85 ± 2.68	98.0 ± 2.89
Skin colour (P-B; %)	P (99.16 ± 0.83)	P (100)	P (100)	P (100)	P (100)
Spontaneous Movements (4-0)	3.99 ±0.07	4	4	4	4
Vocalizations (%)	99.24± 0.75	100	100	100	100
AS (21 min asphyxia) (*n* = 44; *m* = 5)					
Parameters	**40 min**	**P1**	**P3**	**P7**	**P14**
Survival (%)	**62.16 ± 2.23 (by 36%)******	100	100	100	100
Body weight (g)	5.89 ± 0.11	4.94 ± 0.74	8.15 ± 0.43	14.14 ± 0.87	16.87 ± 1.92

Gasping (%)	**47.50 ± 8.69 (>7 X)******	0	0	0	0
Respiratory frequency (events/min)	**31.81 ± 2.74 (by 60%)******	**41.3 ± 5.71 (by 47%)******	**37.38 ± 3.92 (by 54%)******	**58.88 ± 6.66 (by 37%)******	**58.18 ± 5.37 (by 41%)******
Skin colour (P-B; %)	**PB (89.83 ± 4.07)***** **BP (24.27 ± 8.30)*****	P (50 ± 25) **PB (50 ± 25)****	P (80±12.24) PB (20±12.24)	P (25 ± 28.86) **PB (75 ± 28.86)*****	P (30 ± 14.58) **PB (70 ± 14.58)******
Spontaneous Movements (4-0)	**0.53 ± 0.12 (by 87%)*****	4	4	4	4
Vocalizations (%)	**44.75 ± 7.26 (by 55%)*****	100	100	100	100

Unbalanced two-way ANOVA was used for testing the significant effects of PA and postnatal days on (**a**) *survival*: ($F_{(9, 39)}$ = 34.119, P < 0.0001); effect of PA ($F_{(1, 39)}$ = 6.5, P = 0.015); effect of postnatal day: ($F_{(4, 39)}$ = 72.055, P < 0.0001) and effect of interaction ($F_{(4, 39)}$ = 3.087, P = 0.027). (**b**) *body weight* ($F_{(9, 110)}$ = 129.618, P < 0.0001); effect of PA ($F_{(1, 110)}$ = 621.577, P < 0.0001); effect of postnatal day: ($F_{(4, 110)}$ = 131.847, P < 0.0001) and effect of interaction ($F_{(4, 110)}$ = 4.398, P = 0.002). (**c**) *gasping* ($F_{(9, 39)}$ = 66.813, P < 0.0001); effect of PA ($F_{(1, 39)}$ = 51.838, P < 0.0001); effect of postnatal day: ($F_{(4, 39)}$ = 75.165, P < 0.0001) and effect of interaction ($F_{(4, 39)}$ = 62.205, P < 0.0001). (**d**) *respiratory frequency* ($F_{(9,110)}$ = 37.254, P < 0.0001); effect of PA ($F_{(1, 110)}$ = 253.067, P < 0.0001); effect of postnatal day: ($F_{(4, 110)}$ = 19.822, P < 0.0001) and effect of interaction ($F_{(4, 110)}$ = 0.733, P = 0.571). (**e**) *pink colour skin* ($F_{(9, 39)}$ = 14, P < 0.0001); effect of PA ($F_{(1, 39)}$ = 6.499, P = 0.015); effect of postnatal day: ($F_{(4, 39)}$ = 25.322, P < 0.0001) and effect of interaction ($F_{(4, 39)}$ = 4.636, P = 0.004). (**f**) *pink-blue colour skin* ($F_{(9, 39)}$ =13.925, P < 0.0001); effect of PA ($F_{(1, 39)}$ = 71.774, P < 0.0001); effect of postnatal day: ($F_{(4, 39)}$ = 11.376, P < 0.0001) and effect of interaction ($F_{(4, 39)}$= 2.011, P = 0.112). (**g**) *blue-pink colour skin* ($F_{(9, 39)}$ = 4.446, P < 0.001); effect of PA ($F_{(1, 39)}$ = 3.449, P = 0.071); effect of postnatal day: ($F_{(4, 39)}$ = 5.002, P = 0.002) and effect of interaction ($F_{(4, 39)}$ = 4.139, P = 0.007). (**h**) *spontaneous movements* ($F_{(9, 39)}$ = 32.933, P < 0.0001); effect of PA ($F_{(1, 39)}$ = 3.362, P = 0.074); effect of postnatal day: ($F_{(4, 39)}$ = 59.475, P < 0.0001) and effect of interaction ($F_{(4, 39)}$ = 13.784, P < 0.0001). (**i**) *vocalisations %* ($F_{(9, 39)}$ = 32.933, P < 0.0001); effect of PA ($F_{(1, 39)}$ = 3.362, P = 0.074); effect of postnatal day: ($F_{(4, 39)}$ = 59.475, P < 0.0001) and effect of interaction ($F_{(4, 39)}$ = 13.784, P < 0.0001). Benjamini-Hochberg was used as a post hoc test for comparisons between CS and AS groups. *P < 0.05, **P < 0.01, ***P < 0.001 and ****P < 0.0001.

Table 2. Effect perinatal asphyxia on glutathione levels in neonatal rat brain. The brain was dissected at postnatal day (P) 1, 3, 7 or 14, from control (CS) and asphyxia-exposed (AS) rats. For determination of GSH and GSSG was measured by a kinetic method at 412 nm and the concentration normalized by total protein, interpolating the slope values into the corresponding calibration curves. All values are expressed as means ± S.E.M., from at least *n=6* independent experiments in duplicated (n= 6-13).

Table 2A

P1			P3			P7			P14		
GSH µmol/ mg protein	**GSSG µmol/ mg protein**	**GSSG: GSH ratio**	**GSH µmol/ mg protein**	**GSSG µmol/ mg protein**	**GSSG: GSH ratio**	**GSH µmol/ mg protein**	**GSSG µmol/ mg protein**	**GSSG: GSH ratio**	**GSH µmol/ mg protein**	**GSSG µmol/ mg protein**	**GSSG: GSH ratio**
CS Mesencephalon n=6-8											
5.59 ±1.135	0.078 ±0.014	0.0145 ±0.0017	5.05 ±0.6	0.028 ±0.003 §§§§	0.006 ±0.001 €€€€	8.07 ±0.57 π	0.09 ±0.006	0.012 ±0.001	11.52 ±1.2 π π π π	0.065 ±0.004	0.006 ±0.0005 €€€€
AS Mesencephalon n=6-8											
6.03 ±0.72	**0.15 ±0.01 (>1.5X) ******	**0.0254 ±0.002 (>1.7X) ******	3.19 ±0.17 α	0.036 ±0.002 £££££	**0.011 ±0.001 (>1.6X) **/¥¥¥¥**	6.04 ±0.39	**0.13 ±0.004 (>1.45X) *****	**0.02 ±0.002 (>1.6X) ******	**7.02 ±0.35 (>1.6X) *****	**0.12 ±0.006 (>1.8X) ****/£££**	**0.018 ±0.002 (>3X) */¥¥¥¥**

Unbalanced two-way ANOVA was significant **(a) for GSH levels** ($F_{(7, 46)}$ =12.900, P< 0.0001); effect of PA ($F_{(1, 46)}$ =17.115, P= 0.0001); effect of postnatal days ($F_{(3, 46)}$ =20.485, P< 0.0001) and interaction ($F_{(3, 46)}$ =3.908, P= 0.014). **(b) For GSSG levels** two-way ANOVA was significant ($F_{(7, 46)}$ =46.585, P< 0.0001); effect of PA ($F_{(1, 46)}$ =79.209, P< 0.0001); effect of postnatal days ($F_{(3, 46)}$ =73.278, P< 0.0001) and interaction ($F_{(3, 46)}$ =9.018, P< 0.0001).**(c) For GSSG: GSH ratio** two-way ANOVA was significantly ($F_{(7, 46)}$ =42.155, P< 0.0001); effect of PA ($F_{(1, 46)}$ =38.932, P< 0.0001); effect of postnatal days ($F_{(3, 46)}$ =69.860, P< 0.0001) and interaction ($F_{(3, 46)}$ =15.525, P< 0.0001). *Benjamini-Hochberg* was used as a *post-hoc* test. Asterisks represent the comparisons between AS group and its respective CS group. € § π represent the comparisons between CS group and CS P1. ¥ £ α represent the comparisons between AS group and AS P1. In general symbols represent the next statistical significances: *P<0.05; **P<0.01; ***P<0.001, ****P<0.0001 (* is used as example).

Table 2B

	P1			P3			P7			P14	
GSH µmol/ mg protein	**GSSG µmol/ mg protein**	**GSSG: GSH ratio**	**GSH µmol/ mg protein**	**GSSG µmol/ mg protein**	**GSSG: GSH ratio**	**GSH µmol/ mg protein**	**GSSG µmol/ mg protein**	**GSSG: GSH ratio**	**GSH µmol/ mg protein**	**GSSG µmol/ mg protein**	**GSSG: GSH ratio**
CS Telencephalon n=7-11											
6.153 ±0.941	0.0895 ±0.006	0.0173 ±0.003	8.01 ±1.4	0.075 ±0.01	0.011 ±0.002	12.02 ±0.88	0.092 ±0.004	0.008 ±0.0006 €	10.90 ±1.38 π	0.083 ±0.006	0.008 ±0.001 €
AS Telencephalon n=7-11											
5.043 ±0.54	**0.12 ±0.007 (>1.8X) *****	**0.03 ±0.007 (>1.6X) ****	8.89 ±0.98	0.06 ±0.006 £££££	0.008 ±0.001 ¥¥¥¥	**17.96 ±2.57 (>1.5X) **/ α α α α**	0.102 ±0.01	0.006 ±0.004 ¥¥¥¥	**17.05 ±1.99 (>1.56X) **/α α α α**	0.07 ±0.008 £££££	0.004 ±0.0002 ¥¥¥¥

Unbalanced two-way ANOVA was significant (**a**) **for GSH levels** ($F_{(7, 61)}$ =9.261, P< 0.0001); effect of PA ($F_{(1, 61)}$ =7.781, P=0.007); effect of postnatal days ($F_{(3, 61)}$ =16.383, P=0.007) and interaction ($F_{(3, 61)}$ =2.633, P=0.058). (**b**) **For GSSG levels** two-way ANOVA was significant ($F_{(7, 61)}$ =7.464, P< 0.0001); effect of PA ($F_{(1, 61)}$ =1.143, P=0.289); effect of postnatal days ($F_{(3, 61)}$ =12.506, P< 0.0001) and interaction ($F_{(3, 61)}$ =4.529, P=0.006). (**c**) **For GSSG: GSH ratio** two-way ANOVA was significantly ($F_{(7, 61)}$ =9.066, P< 0.0001); effect of PA ($F_{(1, 61)}$ =0.045, P=0.833); effect of postnatal days ($F_{(3, 61)}$ =17.407, P< 0.0001) and interaction ($F_{(3, 61)}$ =3.732, P=0.016). *Benjamini-Hochberg* was used as a *post-hoc* test. Asterisks represent the comparisons between AS group with its respective CS group. € π represent the comparisons between CS group and CS P1. ¥ £ α represent the comparisons between AS group and AS P1. In general symbols represent the next statistical significances: *P<0.05; **P<0.01; ***P<0.001, ****P<0.0001 (* is used as example).

Table 2C

P1			P3			P7			P14		
GSH µmol/ mg protein	**GSSG µmol/ mg protein**	**GSSG: GSH ratio**	**GSH µmol/ mg protein**	**GSSG µmol/ mg protein**	**GSSG: GSH ratio**	**GSH µmol/ mg protein**	**GSSG µmol/ mg protein**	**GSSG: GSH ratio**	**GSH µmol/ mg protein**	**GSSG µmol/ mg protein**	**GSSG: GSH ratio**
CS Hippocampus n=7-13											
4.915 ±0.413	0.08 ±0.004	0.0173 ±0.003	4.82 ±0.19	0.044 ±0.003 §§§§	0.0095 ±0.001 €	3.36 ±0.18 π	0.024 ±0.002 §§§§	0.007 ±0.0005 €	11.17 ±0.66 π π π π	0.086 ±0.005	0.008 ±0.0006 €
AS Hippocampus n=7-13											
4.279 ±0.76	**0.12 ±0.005 (>1.5X) ******	**0.036 ±0.005 (>2X) ******	4.15 ±0.305	**0.06 ±0.004 (>1.3X) **/£££££**	**0.015 ±0.001 (>1.6X) **/¥¥¥**	2.65 ±0.26 α	**0.046 ±0.002 (>1.9X) ****/£££££**	**0.02 ±0.003 (>2X) **/¥¥¥¥**	**5.83 ±0.73 (>1.9X) ***/α α α α**	**0.11 ±0.005 (>1.2X) **/£££**	**0.02 ±0.003 (>2.5X) **/¥¥¥¥**

Unbalanced two-way ANOVA was significant (**a**) **for GSH levels** ($F_{(7, 81)}$ =24.874, P< 0.0001); effect of PA ($F_{(1, 81)}$ =21.308, P< 0.0001); effect of postnatal days ($F_{(3, 81)}$ =40.756, P< 0.0001) and interaction ($F_{(3, 81)}$ =10.179, P< 0.0001). (**b**) **For GSSG levels** two-way ANOVA was significant ($F_{(7, 81)}$ =85.284, P< 0.0001); effect of PA ($F_{(1, 81)}$ =97.07, P< 0.0001); effect of postnatal days ($F_{(3, 81)}$ =161.402, P< 0.0001) and interaction ($F_{(3, 81)}$ =5.237, P= 0.002). (**c**) **For GSSG: GSH ratio** two-way ANOVA was significantly ($F_{(7, 81)}$ =15.523, P< 0.0001); effect of PA ($F_{(1, 81)}$ =53.617, P< 0.0001); effect of postnatal days ($F_{(3, 81)}$ =15.55, P< 0.0001) and interaction ($F_{(3, 81)}$ =2.798, P= 0.045). *Benjamini-Hochberg* was used as a *post-hoc* test. Asterisks represent the comparisons between AS group with its respective CS group. € § π represent the comparisons between CS group and CS P1. ¥ £ α represent the comparisons between AS group and AS P1. In general symbols represent the next statistical significances: *P<0.05; **P<0.01; ***P<0.001, ****P<0.0001 (* is used as example).

Table 3. Effect of perinatal asphyxia on tissue reducing capacity (FRAP) in neonatal rat brain. The brain was dissected at P1, 3, 7 and 14 from control (CS) and asphyxia-exposed (AS) rats. The capacity to reduce Fe (III) was determined by a Potassium Ferricyanide Reducing Power Assay in mesencephalon, telencephalon and hippocampus. Reducing capacity (Fe(II) is expressed in equivalents in µM, normalised by total protein in µg). Data are means ± SEM from at least N=6 independent experiments in triplicated.

	P1	**P3**	**P7**	**P14**
	FRAP µM/µg protein	**FRAP µM/µg protein**	**FRAP µM/µg protein**	**FRAP µM/µg protein**
CS				
Mesencephalon; N=6-8	1.577 ± 0.059	1.27 ± 0.05 π	3.749 ± 0.129 π π π π	4.124 ± 0.139 π π π π
Telencephalon; N=7-11	3.581 ± 0.105	4.327 ± 0.151 §§	3.682 ± 0.123	4.74 ± 0.181 §§§
Hippocampus; N= 7-13	2.068 ± 0.124	4.44 ± 0.258 €€€€	3.844 ± 0.038 €€€€	4.558 ± 0.229 €€€€
AS				
Mesencephalon; N= 6-8	**1.187 ± 0.036 (by 24%)****	**0.76 ± 0.08 (by 40%)***/** α α	**2.627 ± 0.102 (by 30%)****/** α α α α	**3.45 ± 0.08 (by 17%)****/**α α α α
Telencephalon; N= 7-11	3.89 ± 0.123	4.51 ± 0.34 £	**4.768 ± 0.121 (>1.2 X)***/**££	**6.338 ± 0.201 (>1.3 X)****/**££££
Hippocampus; N= 7-13	**1.239 ± 0.089 (by 40%)******	**3.176 ± 0.114 (by 30%)****/**¥/¥/¥/¥	**1.715 ± 0.266 (by 50%)******	**3.723 ± 0.132 (by 20%)***/**¥/¥/¥/¥

Unbalanced two-way ANOVA showed (**a**) *in mesencephalon* a statistical significant effect of PA and postnatal days was found: ($F_{(7, 76)} = 199.896$, $P < 0.0001$); effect of PA was ($F_{(1, 76)} = 89.347$, $P < 0.0001$); effect of postnatal days was ($F_{(3, 76)} = 431.769$, $P < 0.0001$) and interaction between PA and postnatal days was ($F_{(3, 76)} = 4.873$, $P = 0.004$). (**b**) *In telencephalon* unbalanced two-way ANOVA showed statistical significance of PA and postnatal days ($F_{(7, 85)} = 25.549$, $P < 0.0001$); effect of PA was ($F_{(1, 85)} = 32.395$, $P < 0.0001$); effect of postnatal days was ($F_{(3, 85)} = 42.853$, $P < 0.0001$) and interaction between PA and postnatal days was ($F_{(3, 85)} = 5.963$, $P = 0.001$). (**c**) *In hippocampus* unbalanced two-way ANOVA showed statistical significance of PA and postnatal days ($F_{(7, 91)} = 63.297$, $P < 0.0001$); effect of PA was ($F_{(1, 91)} = 104.903$, $P < 0.0001$); effect of

postnatal days was ($F_{(3, 91)} = 106.512$, $P < 0.0001$) and interaction between PA and postnatal days was ($F_{(3, 91)} = 6.213$, $P = 0.001$). Benjamini-Hochberg was used as a post hoc test. Asterisks represent the comparisons between AS group with its respective CS group. € § π represent the comparisons between CS group and CS P1. ¥ £ α represent the comparisons between AS group and AS P1. In general symbols represent the next statistical significances: *P<0.05; **P<0.01; ***P<0.001, ****P<0.0001 (* is used as example).

Table 4. Effect of perinatal asphyxia on protein and catalase activity in neonatal rat brain. The brain was dissected at P1, 3, 7 and 14 from control (CS) and asphyxia-exposed (AS) rats. Tissue samples from mesencephalon (M), telencephalon (T), and hippocampus (H) were analysed by Western blots (WB) and ELISA, determining protein and catalase activity, respectively. Densitometry was performed for quantification, determining catalase and total protein. The values were normalized by the sum method, and catalase values divided by total normalized protein values (loading control), obtaining the quantity of catalase, represented as catalase protein normalized levels in arbitrary units (a. u.). Enzymatic activity was determined by the constant (k) rate from the exponential decomposition of hydrogen peroxide (min), normalized by catalase relative levels and total protein in milligram (mg). Relative catalase protein levels were obtained dividing absorbance values by total protein (mg). Data are means ± S.E.M from at least N=3 independent experiments by duplicated.

Table 4A

P1			**P3**			**P7**			**P14**		
Total protein (A.U.) (WB)	**A /mg protein (ELISA)**	**Activity (k/catalase /mg protein)**	**Total protein (A.U.) (WB)**	**A /mg protein (ELISA)**	**Activity (k/catalase /mg protein)**	**Total protein (A.U.) (WB)**	**A /mg protein (ELISA)**	**Activity (k/catalase /mg protein)**	**Total protein (A.U.) (WB)**	**A /mg protein (ELISA)**	**Activity (k/catalase /mg protein)**
CS Mesencephalon n=5-8											
1.383 ± 0.15	0.181 ± 0.019	0.021 ± 0.003	0.976 ± 0.079 §	0.194 ± 0.031	0.017 ± 0.001	1.015 ± 0.07 §	0.094 ± 0.011 €€	0.004 ± 0.0001 π π π π	0.885 ± 0.057 §§	0.083 ± 0.0186 €€€€	0.0033 ± 0.0003 π π π π
AS Mesencephalon n=5											
1.109 ± 0.069	0.134 ± 0.015	**0.011 ± 0.001 (by 48%) *****	0.887 ± 0.061	**0.109 ± 0.022 (by 44%) ****	**0.01 ± 0.002 (by 47%) *****	1.024 ± 0.082	0.082 ± 0.0043 ¥	0.003 ± 0.0001 ££	0.958 ± 0.104	0.056 ± 0.006 ¥¥¥	0.002 ± 0.0002 ££

(a) For catalase protein determined by Western blot unbalanced two-way ANOVA was statistically significant ($F_{(7, 56)} = 3.283$, $P < 0.005$). The following results were found for the effect of PA ($F_{(1, 56)} = 1{,}263$, $P = 0.266$); effect of postnatal days ($F_{(3, 56)} = 5.789$, $P<0.01$); and interaction between PA and postnatal days ($F_{(3, 56)} = 1.451$, $P = 0.238$). **(b)** For catalase relative levels unbalanced two-way ANOVA revealed statistically

significant differences ($F_{(7, 22)} = 12.907$, $P < 0.0001$); effect of PA ($F_{(1, 22)} = 11.2$, $P< 0.003$); for effect of postnatal days ($F_{(3, 22)} = 23.924$, $P < 0.0001$). The interaction between PA and postnatal days did not reach the statistically significant level ($F_{(3, 22)} = 2.46$, $P = 0.09$). **(c)** For catalase activity unbalanced two-way ANOVA was significant ($F_{(7, 16)} = 28.511$, $P < 0.0001$); also for the effect of PA ($F_{(1, 16)} = 28.417$, $P < 0.0001$); and postnatal days ($F_{(3, 16)} = 50.882$, $P < 0.0001$); and interaction between PA and postnatal days ($F_{(3, 16)} = 6.172$, $P = 0.005$). Benjamini-Hochberg was used as a post hoc test. Asterisks represent the comparisons between AS group with its respective CS group. € § π represent the comparisons between CS group and CS P1. ¥ £ represent the comparisons between AS group and AS P1. In general symbols represent the next statistical significances: *P<0.05; **P<0.01; ***P<0.001, ****P<0.0001. (* is used as example).

Table 4B

P1			P3			P7			P14		
Total protein (A.U.) (WB)	**A /mg protein (ELISA)**	**Activity (k/catalase /mg protein)**	**Total protein (A.U.) (WB)**	**A /mg protein (ELISA)**	**Activity (k/catalase /mg protein)**	**Total protein (A.U.) (WB)**	**A /mg protein (ELISA)**	**Activity (k/catalase /mg protein)**	**Total protein (A.U.) (WB)**	**A /mg protein (ELISA)**	**Activity (k/catalase /mg protein)**
CS Telencephalon n=5-7											
1.05 ± 0.129	0.16 ± 0.014	0.007 ± 0.0003	1.056 ± 0.09	0.136 ± 0.011	0.006 ± 0.0005	0.98 ± 0.053	0.112 ± 0.005	0.005 ± 0.0008	0.854 ± 0.13	0.085 ± 0.004 €€€€	0.004 ± 0.001
AS Telencephalon n=5											
1.216 ± 0.119	0.16 ± 0.01	0.007 ± 0.0009	1.044 ± 0.052	0.141 ± 0.011	0.007 ± 0.0008	0.834 ± 0.056	0.115 ± 0.007	0.006 ± 0.001	0.723 ± 0.068 ¥¥¥	0.102 ± 0.02 ££	0.005 ± 0.001

(a) For catalase protein determined by Western blot unbalanced two-way ANOVA was significantly ($F_{(7, 48)} = 3.050$, $P = 0.01$). No statistically significant effect was found for PA ($F_{(1, 48)} = 0.483$, $P = 0.491$); effect of postnatal days ($F_{(3, 48)} = 6.101$, $P = 0.001$) and interaction between PA and postnatal days ($F_{(3, 48)} = 0.853$, $P = 0.472$). **(b)** For catalase relative levels unbalanced two-way ANOVA was significant ($F_{(7, 42)} = 6.388$, $P < 0.0001$); effect of PA ($F_{(1, 42)} = 0.445$, $P = 0.508$); effect of postnatal days ($F_{(3, 42)} = 14.504$, $P < 0.0001$) and interaction between PA and postnatal days ($F_{(3, 42)} = 0.252$, $P = 0.860$). **(c)** For catalase activity unbalanced two-way ANOVA was significantly ($F_{(7, 40)} = 2.523$, $P = 0.03$); effect of PA ($F_{(1, 40)} = 1.225$, $P = 0.275$); effect of postnatal days ($F_{(3, 40)} = 5.192$, $P = 0.004$) and interaction between PA and postnatal days ($F_{(3, 40)} = 0.287$, $P = 0.834$). Benjamini-Hochberg was used as a post hoc test. Asterisks represent the comparisons between AS group with its respective CS group. € represents the comparisons between CS group and CS P1. ¥ £ represent the comparisons between AS group and AS P1. In general symbols represent the next statistical significances: *P<0.05; **P<0.01; ***P<0.001, ****P<0.0001 (* is used as example).

Table 4C

P1			P3			P7			P14		
Total protein (A.U.) (WB)	**A /mg protein (ELISA)**	**Activity (k/catalase /mg protein)**	**Total protein (A.U.) (WB)**	**A /mg protein (ELISA)**	**Activity (k/catalase /mg protein)**	**Total protein (A.U.) (WB)**	**A /mg protein (ELISA)**	**Activity (k/catalase /mg protein)**	**Total protein (A.U.) (WB)**	**A /mg protein (ELISA)**	**Activity (k/catalase /mg protein)**
CS Hippocampus n=5-6											
0.864 ± 0.049	0.202 ± 0.019	0.12 ± 0.006	0.919 ± 0.056	0.119 ± 0.009	0.036 ± 0.005 π π π π	1.135 ± 0.04 §§	0.206 ± 0.003	0.067 ± 0.006 π π π π	0.871 ± 0.075	0.066 ± 0.006 €€€€	0.013 ± 0.001 π π π π
AS Hippocampus n=5											
0.845 ± 0.046	0.19 ± 0.013	**0.086 ± 0.001 (by 28%) ******	**1.187 ± 0.037 (>29%) ***/¥¥¥¥**	**0.22 ± 0.025 (by 84%) ******	**0.061 ± 0.003 (>1.6 X) ****/** α α α α	1.156 ± 0.055 ¥¥¥	0.182 ± 0.011	**0.031 ± 0.003 (by 54%) ****/** α α α α	0.98 ± 0.05 ¥¥¥	0.094 ± 0.006 £££££	**0.005 ± 0.001 (by 70%) */** α α α α

(a) For catalase protein determined by western blot unbalanced two-way ANOVA was significant ($F_{(7, 40)} = 7.569$, $P < 0.0001$); effect of PA ($F_{(1, 40)} = 6.638$, $P = 0.014$); effect of postnatal days ($F_{(3, 40)} = 12.463$, $P < 0.0001$) and interaction between PA and postnatal days ($F_{(3, 40)} = 2.985$, $P = 0.042$). **(b)** For catalase relative levels unbalanced two-way ANOVA was significant ($F_{(7, 24)} = 18.846$, $P < 0.0001$); effect of PA ($F_{(1, 24)} = 6.088$, $P = 0.021$); effect of postnatal days ($F_{(3, 24)} = 33.147$, $P < 0.0001$) and interaction between PA and postnatal days ($F_{(3, 24)} = 8.798$, $P = 0.0004$). **(c)** For catalase activity unbalanced two-way ANOVA was significant ($F_{(7, 29)} = 135.114$, $P < 0.0001$); effect of PA ($F_{(1, 29)} = 28.153$, $P < 0.0001$); effect of postnatal days ($F_{(3, 29)} = 275.427$, $P < 0.0001$) and interaction between PA and postnatal days ($F_{(3, 29)} = 30.456$, $P < 0.0001$). Benjamini-Hochberg was used as a post hoc test. Asterisks represent the comparisons between AS group with its respective CS group. § € π represent the comparisons between CS group and CS P1. ¥ £ α represent the comparisons between AS group and AS P1. In general symbols represent the next statistical significances: *P<0.05; **P<0.01; ***P<0.001, ****P<0.0001 (* is used as example).

Table 5. Effect of perinatal asphyxia on procaspase-3 and cleaved caspase-3 levels in neonatal rat brain. The brain was dissected at P1, 3, 7 and 14 from control (CS) and asphyxia-exposed (AS) rats. Tissue samples from mesencephalon, telencephalon and hippocampus were analysed by immunoblotting with caspase-3 (1:500). Densitometry was performed, quantifying procaspase -3 and total cleaved caspase-3 (p19/17/12), also total protein (*Ponceau* stained membranes). The values were normalized by the sum method and divided by total normalized protein values to determine caspase-3 normalized levels in arbitrary units (a. u.). Data are means ± S.E.M from *N=5* independent experiments.

Table 5A

P1		**P3**		**P7**		**P14**	
Procaspase-3 (A.U.)	**Cleaved caspase-3 (A.U.)**	**Procaspase-3 (A.U.)**	**Cleaved caspase-3 (A.U.)**	**Procaspase-3 (A.U.)**	**Cleaved caspase-3 (A.U.)**	**Procaspase-3 (A.U.)**	**Cleaved caspase-3 (A.U.)**
CS Mesencephalon n=5							
1.143 ± 0.173	2.256 ± 0.226	0.92 ± 0.146	1.6 ± 0.159 §	0.908 ± 0.51	1.933 ± 0.1089	0.609 ± 0.106 €€	0.927 ± 0.071 §§§§
AS Mesencephalon n=5							
1.662 ± 0.173 (>1.4X) *	**3.104 ± 0.266 (>1.3 X) ****	1.143 ± 0.144 ££	**2.522 ± 0.358 (>1.5 X) **/¥**	1.115 ± 0.016 ££	2.478 ± 0.094 (>1.2 X) ¥	0.667 ± 0.141 £££££	**1.294 ± 0.07 (>1.3X) */¥¥¥¥**

(a) For procaspase-3 unbalanced two-way ANOVA was significant ($F_{(7, 32)} = 6.466$, $P<0.0001$); effect of PA ($F_{(1, 32)} = 7.450$, $P=0.01$); effect of postnatal days ($F_{(3, 32)} = 11.506$, $P<0.0001$) and interaction between PA and postnatal days ($F_{(3, 32)} = 1.098$, $P= 0.364$). **(b)** For cleaved caspase- 3 unbalanced two-way ANOVA was significant ($F_{(7, 32)} = 13.546$, $P<0.0001$); effect of PA ($F_{(1, 32)} = 23.118$, $P<0.0001$); effect of postnatal days ($F_{(3, 32)} = 22.961$, $P<0.0001$) and interaction between PA and postnatal days ($F_{(3, 32)} = 0.942$, $P= 0.432$). *Benjamini-Hochberg* was used as a post-hoc test. Asterisks represent the comparisons between AS group with its respective CS group. § and € represent the comparisons between CS group and CS P1. ¥ and £ represent the comparisons between AS group and AS P1. In general symbols represent the next statistical significances: *P<0.05; **P<0.01; ***P<0.001, ****P<0.0001 (* is used as example).

Table 5B

P1		P3		P7		P14	
Procaspase-3 (A.U.)	**Cleaved caspase-3 (A.U.)**	**Procaspase-3 (A.U.)**	**Cleaved caspase-3 (A.U.)**	**Procaspase-3 (A.U.)**	**Cleaved caspase-3 (A.U.)**	**Procaspase-3 (A.U.)**	**Cleaved caspase-3 (A.U.)**
CS Telencephalon n=5							
1.147 ± 0131	2.103 ± 0.187	1.199 ± 0.108	2.479 ± 0.427	1.062 ± 0.098	2.066 ± 0.348	0.559 ± 0.078	0.999 ± 0.136 §
AS Telencephalon n=5							
1.01 ± 0.187	1.743 ± 0.161	1.436 ± 0.258	2.8 ± 0.188	1.001 ± 0.101	2.733 ± 0.396 ¥	0.685 ± 0.075	1.298 ± 0.147

(a) For procaspase-3 unbalanced two-way ANOVA was significant ($F_{(7, 32)} = 3.870$, P=0.004); effect of PA ($F_{(1, 32)} = 0.165$, P=0.687); effect of postnatal days ($F_{(3, 32)} = 8.251$, P=0.0003) and interaction between PA and postnatal days ($F_{(3, 32)} = 0.724$, P= 0.545). **(b)** For cleaved caspase- 3 unbalanced two-way ANOVA was significantly ($F_{(7, 32)} = 5.702$, P=0.0002); effect of PA ($F_{(1, 32)} = 1.437$, P=0.239); effect of postnatal days ($F_{(3, 32)} = 11.591$, P<0.0001) and interaction between PA and postnatal days ($F_{(3, 32)} = 1.234$, P= 0.313). *Benjamini-Hochberg* was used as a post-hoc test. § represent the comparisons between CS group and CS P1. ¥ represent the comparisons between AS group and AS P1. In general symbols represent the next statistical significances: §P<0.05; §§P<0.01; §§§ P<0.001, §§§§ P<0.0001. (§ is used as example).

Table 5C

P1		P3		P7		P14	
Procaspase-3 (A.U.)	**Cleaved caspase-3 (A.U.)**	**Procaspase-3 (A.U.)**	**Cleaved caspase-3 (A.U.)**	**Procaspase-3 (A.U.)**	**Cleaved caspase-3 (A.U.)**	**Procaspase-3 (A.U.)**	**Cleaved caspase-3 (A.U.)**
CS Hippocampus n=5							
1.555 ± 0.156	3.194 ± 0.308	1.121 ± 0.087 €	2.962 ± 0.413	0.788 ± 0.121 €€€	2.239 ± 0.25 §	0.672 ± 0.105 €€€€	1.054 ± 0.103 §§§§
AS Hippocampus n=5							
1.338 ± 0.074	2.625 ± 0.199	1.031 ± 0.095	**3.81 ± 0.342 (>1.3X) ***	0.811 ± 0.083 ££	**5.004 ± 0.313 (>2 X) ****/¥¥¥¥**	0.937 ± 0.076 £	1.304 ± 0.114 ¥¥

(a) For procaspase-3 unbalanced two-way ANOVA was significantly ($F_{(7, 32)} = 8.383$, $P<0.0001$); effect of PA ($F_{(1, 32)} = 0.004$, $P= 0.952$); effect of postnatal days ($F_{(3, 32)} = 17.579$, $P<0.0001$) and interaction between PA and postnatal days ($F_{(3, 32)} = 1.979$, $P= 0.137$). **(b)** For cleaved caspase- 3 unbalanced two-way ANOVA was significantly ($F_{(7, 32)} = 21.131$, $P<0.0001$); effect of PA ($F_{(1, 32)} = 19.991$, $P<0.0001$); effect of postnatal days ($F_{(3, 32)} = 29.895$, $P<0.0001$) and interaction between PA and postnatal days ($F_{(3, 32)} = 12.747$, $P<0.0001$). *Benjamini-Hochberg* was used as a post-hoc test. Asterisks represent the comparisons between AS group with its respective CS group. § and € represent the comparisons between CS group and CS P1. ¥ and £ represent the comparisons between AS group and AS P1. In general symbols represent the next statistical significances: *P<0.05; **P<0.01; ***P<0.001, ****P<0.0001 (* is used as example).

Table 6. Apgar and postnatal evaluation. Apgar scale evaluating the consequences of PA induced by immersing foetus-containing uterine horns (removed from ready to delivery rat dams) into a water bath at 37 °C for 21 min. The Apgar scale was applied 40 min after delivery to both asphyxia-exposed (AS) and sibling caesarean delivered neonates, used as controls (CS). The following parameters were also monitored at postnatal day 1 (P1) and P14 after delivery: (**a**) survival (yes/no, following intensive resuscitation manoeuvres for at least 5 min; in% of the corresponding litter). (**b**) Body weight (g). (**c**) Presence of gasping (yes/no; in % of the corresponding litter). (**d**) Respiratory frequency (events/min). (**e**) Skin colour (pink to blue, P, PB, BP or B). (**f**) Spontaneous movements (0–4; 0 = no movements; 4 = coordinated movements of forward and hind legs, as well as head and neck). (**g**) Vocalisation (yes/no; in % of the corresponding litter). Data is expressed as means ± SEM, whenever the parameters are monitored by continuous scales, or by % of the corresponding litter in cases of qualitative no continuous scales (n, number of pups; m, number of dams).

CS (Caesarean delivered; 0 min asphyxia) (*n*= 280; *m*=24)							
Parameters	**40 min**	**P1**			**P14**		
Treatment	**-**	**-**	**Veh**	**Nicotinamide**	**-**	**Veh**	**Nicotinamide**
Survival (%)	100	100	100	100	100	100	100
Body weight (g)	6.11 ± 0.56	7.01 ± 0.29	6.54 ± 0.18	6.63 ± 0.22	25.08 ±0.88	24.10 ±0.78	24.20 ±0.82
Gasping (%)	0.053 ± 0.03	0	0	0	0	0	0
Respiratory frequency (events/min)	75.04±0.87	78.32 ± 2.04	78.55 ± 1.99	86.36 ± 2.13	99.09 ± 2.07	103.09 ±2.31	101.73 ±2.70
Skin colour (P-B; %)	P (100)	Not Evaluated	Not Evaluated	Not Evaluated	Not Evaluated	Not Evaluated	Not Evaluated
Spontaneous Movements (4-0)	3.90 ±0.03	4	4	4	4	4	4
Vocalizations (%)	99.21± 0.39	100	100	100	100	100	100
AS (21 min asphyxia) (*n* = 44; *m* = 5)							
Parameters	**40 min**	**P1**			**P14**		
Survival (%)	**60.81 ± 2.55 (by 61%)******	100	100	100	100	100	100
Body weight (g)	5.96 ± 0.55	6.75 ± 0.22	6.32 ± 0.17	6.56 ± 0.24	24.00 ± 0.97	23.50 ± 0.60	25.28 ± 0.70

Gasping (%)	**43.72 ± 4.35 (>8X)******	0	0	0	0	0	0
Respiratory frequency (events/min)	**36.54 ± 1.43 (by 52%)******	**40.55 ± 3.53 (by 48%)******	**38.27 ± 3.73 (by 51%)******	**57.92 ± 1.59 (by 33%)******	**63.64 ± 3.57 (by 36%)******	**61.64 ± 3.35 (by 40%)******	**82.09 ± 2.54 (by 19%)******
Skin colour (P-B; %)	**PB (77.85 ± 4.37)****** **BP (29.51 ± 5.54)******	Not Evaluated	Not Evaluated	Not Evaluated	Not Evaluated	Not Evaluated	Not Evaluated
Spontaneous Movements (4-0)	**0.72 ± 0.08 (by 82%)*****	4	4	4	4	4	4
Vocalizations (%)	**50.22 ± 3.88 (by 49%)******	100	100	100	100	100	100

One-way ANOVA was used for testing the significant differences among groups at 40min on (**a**) *survival*: ($F_{(1, 227)} = 235.912$, $P < 0.0001$). (**b**) *body weight* ($F_{(1, 279)} = 0.463$, $P = 0.497$). (**c**) *gasping* ($F_{(1, 227)} = 100.744$, $P < 0.0001$). (**d**) *respiratory frequency* ($F_{(1,279)} = 527.138$, $P < 0.0001$). (**e**) *Skin colour* ($F_{(2, 101)} = 100.581$, $P < 0.0001$). (**f**) *spontaneous movements* ($F_{(1, 278)} = 1495.367$, $P < 0.0001$). (**g**) *vocalisations %* ($F_{(1, 226)} = 159.290$, $P < 0.0001$). One-way ANOVA indicated a significant difference among groups on *respiratory frequency* ($F_{(5, 131)} = 61.934$, $P < 0.0001$) at P1 and ($F_{(5, 131)} = 46.059$, $P < 0.0001$) at P14. Benjamini-Hochberg was used as a post hoc test. Asterisks represent the comparisons between CS and AS groups. Statistical significance: *P < 0.05, **P < 0.01, ***P < 0.001 and ****P < 0.0001.

Table 7. A. Effect of perinatal asphyxia (PA) and **B**. nicotinamide on glutathione levels monitored in hippocampus of rat neonates at P1 and P14**.** (comparisons: AS versus CS; CS nicotinamide versus CS vehicle; AS nicotinamide versus AS vehicle). The concentrations of GSH and GSSG were expressed as μmol/mg protein, GSSG:GSH ratio is a measured of oxidative stress. All values are means ± S.E.M., from at least N=4-6 independent experiments in duplicated.

Postnatal day		**P1**			**P14**	
	GSH μmol/mg protein	**GSSG μmol/ mg protein**	**GSSG: GSH ratio**	**GSH μmol/mg protein**	**GSSG μmol/ mg protein**	**GSSG: GSH ratio**
A. ***Effect of PA;*** N= 4 independent experiments						
CS; n=8	7.49 ±0.70	0.08 ±0.01	0.011 ±0.0005	8.91 ±0.30	0.07 ±0.01	0.008±0.001
AS; n=8-9	7.32 ±0.31	**0.15±0.01 (>1.9x)******	**0.02 ±0.002 (>1.9X)******	**5.71±0.59 (by 35.85%)******	**0.16±0.01 (>2.5x)******	**0.031±0.003 (>4.1X)******
B. Effect of Nicotinamide; N=4-5 independent experiments						
CS Vehicle; n=8-10	7.13 ±0.44	0.07 ±0.02	0.01 ± 0.0011	10.09 ±1.01	0.08 ±0.01	0.01±0.001
CS Nicotinamide; n=9-10	**12.11±0.88 (>1.7X)******	0.08 ±0.01	**0.007 ± 0.001 (by 32.81%)***	**23.06±1.30 (>2.4X)******	0.08 ±0.01	**0.004±0.001 (by 61.76%)******
AS Vehicle; n=8-10	7.53 ±0.65	0.16 ±0.01	0.02±0.001	4.83 ±0.49	0.14 ±0.005	0.03±0.002
AS Nicotinamide; n=9-12	**13.70±1.09 (>1.8X)******	**0.09±0.01 (by 42.78%)******	**0.007±0.0003 (by 68.79%)******	**11.82±1.08 (>2.8X)******	**0.07±0.003 (by 44.04%)******	**0.007±0.001 (by 75.26%)******

(a) For GSH levels unbalanced two-way ANOVA indicated (**i**) a significant effect of PA and postnatal days on GSH ($F_{(3, 29)} = 23.534$, $P < 0.0001$); effect of PA on GSH levels was ($F_{(1, 29)} = 55.915$, $P < 0.0001$); effect of postnatal days was ($F_{(1, 29)} = 12.122$, $P = 0.002$) and interaction between PA and post-natal days on GSH levels was ($F_{(1, 29)} = 2.566$, $P = 0.120$). (**ii**) The effect of nicotinamide and postnatal days was statistically significant on GSH ($F_{(7, 69)} = 44.998$, $P < 0.0001$); effect of nicotinamide on GSH levels was ($F_{(3, 69)} = 82.353$, $P < 0.0001$); effect of post-natal days was ($F_{(1, 69)} = 43.384$, $P < 0.0001$) and interaction between nicotinamide and post-natal days on GSH levels was ($F_{(3, 69)} = 8.181$, $P < 0.0001$).

(b) For GSSG levels unbalanced two-way ANOVA indicated (**i**) a significant effect of PA and postnatal days ($F_{(3, 29)} = 12.473$, $P < 0.0001$); effect of PA on GSSG levels was ($F_{(1, 29)} = 11.231$, $P = 0.002$); effect of postnatal days was ($F_{(1, 29)} = 17.022$, $P = 0.0003$) and interaction between PA and post-natal days was ($F_{(1, 29)} = 9.165$, $P = 0.005$). (**ii**) The effect of nicotinamide and postnatal days on GSSG levels was statistically significant ($F_{(7, 69)} = 60.604$, $P < 0.0001$); effect of nicotinamide on GSSG levels was ($F_{(3, 69)} = 127.0171$, $P < 0.0001$); effect of post-natal days was ($F_{(1, 69)} = 16.161$, $P = 0.0001$) and interaction between nicotinamide and post-natal days on GSSG levels was ($F_{(3, 69)} = 8.952$, $P < 0.0001$).

(c) For GSSG:GSH ratio unbalanced two-way ANOVA indicated (**i**) a significant effect of PA and postnatal days ($F_{(3, 29)} = 17.096$, $P < 0.0001$); effect of PA on GSSG:GSH ratio was ($F_{(1, 29)} = 8.040$, $P < 0.0001$); effect of post-natal days was ($F_{(1, 29)} = 27.169$, $P < 0.0001$) and interaction between PA and post-natal days was ($F_{(1, 29)} = 16.079$, $P < 0.0001$). (**ii**) The effect of nicotinamide and postnatal days was statistically significant on GSSG:GSH ratio ($F_{(7, 69)} = 61.584$, $P < 0.0001$); effect of nicotinamide was ($F_{(3, 69)} = 131.943$, $P < 0.0001$); effect of post-natal days was ($F_{(1, 69)} = 12.698$, $P = 0.001$) and interaction between nicotinamide and post-natal days was ($F_{(3, 69)} = 7.522$, $P = 0.0002$). Benjamini-Hochberg was used as a post-hoc test. Asterisks represent the comparisons between AS group with its respective CS group and between CS nicotinamide/AS nicotinamide group with its respective CS vehicle/AS vehicle group. Statistical significance: *P<0.05; **P<0.01; ***P<0.001, ****P<0.0001.

Table 8. A. Effect of perinatal asphyxia (PA) and **B**. nicotinamide on glutathione reductase (GR) activity monitored in hippocampus of rat neonates at P1 and P14**.** (Comparisons: AS versus CS; CS nicotinamide versus CS vehicle; AS nicotinamide versus AS vehicle). GR activity is expressed as mU/ml/µg protein. All values are expressed as means ± S.E.M., from at least N=4 independent experiments by duplicated.

Postnatal day	**P1**	**P14**
	GR	**GR**
	mU/mL/µg protein	**mU/mL/µg protein**
A. Effect of PA; N=4-7 independent experiments		
CS; n=9-14	8.39 ±0.60	5.12 ±0.33
AS; n=10	**5.36 ±0.71**	**3.75 ±0.28**
	(by 29.2%) **	**(by 27.9%) ****
B. Effect of Nicotinamide; N=4-8 independent experiments		
CS Vehicle; n=9	7.58 ±0.63	5.91 ±0.31
CS Nicotinamide; n=10-16	**13.28 ±1.24**	**7.89 ±0.57**
	(> 1.7X)**	**(> 1.3X)***
AS Vehicle; n=8-11	4.54 ±0.39	4.40 ±0.25
AS Nicotinamide; n=8-10	**14.73 ±2.09**	**7.78 ±0.55**
	(> 3.6X)****	**(> 1.8X)******

Unbalanced two-way ANOVA indicated (**i**) a significant effect of PA and postnatal days on GR ($F_{(3, 40)} = 43.897$, $P < 0.0001$); effect of PA on GR was ($F_{(1, 40)} = 112.408$, $P < 0.0001$); effect of post-natal days was ($F_{(1, 40)} = 2.401$, $P = 0.129$) and interaction between PA and post-natal days on GR was ($F_{(1, 40)} = 16.881$, $P = 0.0002$). (**ii**) The effect of nicotinamide and postnatal days was statistically significant ($F_{(7, 69)} = 15.810$, $P < 0.0001$); effect of nicotinamide on GR was ($F_{(3, 69)} = 24.239$, $P < 0.0001$); effect of post-natal days was ($F_{(1, 69)} = 4,706$, $P = 0.034$) and interaction between nicotinamide and post-natal days on GR was ($F_{(3, 69)} = 4.505$, $P = 0.014$). Benjamini-Hochberg was used as a post-hoc test. Asterisks represent the comparisons between AS group with its respective CS group and between CS nicotinamide/AS nicotinamide group with its respective CS vehicle/AS vehicle group. Statistical significance: *P<0.05; **P<0.01; ***P<0.001, ****P<0.0001.

Table 9. A. Effect of perinatal asphyxia (PA) and **B**. nicotinamide on glutathione peroxidase (GPx) activity monitored in hippocampus of rat neonates at P1 and P14**.** (Comparisons: AS versus CS; CS nicotinamide versus CS vehicle; AS nicotinamide versus AS vehicle). GPx activity is expressed as NADPH nmol/ml/mg protein. All values are expressed as means ± S.E.M., from at least N=3 independent experiments by duplicated.

Postnatal day	**P1**	**P14**
	GPX (NADPH nmol/mL/mg protein)	**GPX (NADPH nmol/mL/mg protein)**
A. Effect of PA; N=3-4 independent experiments		
CS; n=6-8	786.69±109.46	839.31±53.09
AS; n=6-7	**369.80±29.28 (by 51.4%)****	**385.27±49.41 (by 52.7%)******
B. Effect of Nicotinamide; N=3-5 independent experiments		
CS Vehicle; n=6	656.06±35.16	808.21±76.14
CS Nicotinamide; n=10	772.16±36.90	**1764.97±138.44 (>2.3X)******
AS Vehicle; n=6	408.88±28.85	459.90±45.38
AS Nicotinamide; n=10	**904.32±95.99 (>2.3X)******	**1315.88±140.71 (>3.1X)******

Unbalanced two-way ANOVA indicated (**i**) a significantly effect of PA and postnatal days on GPx activity ($F_{(3, 23)} = 55.633$, $P < 0.0001$); effect of PA on GPx was ($F_{(1, 23)} = 149.002$, $P < 0.0001$); effect of post-natal days was ($F_{(1, 23)} = 13.852$, $P = 0.001$) and interaction between PA and post-natal days on GPx was ($F_{(1, 23)} = 4.041$, $P = 0.056$). (**ii**) The effect of nicotinamide and postnatal days was statistically significant on GPx activity ($F_{(7, 49)} = 37.536$, $P < 0.0001$); effect of nicotinamide on GPx was ($F_{(3, 49)} = 54.039$, $P < 0.0001$); effect of post-natal days was ($F_{(1, 49)} = 74.822$, $P = 0.034$) and interaction between nicotinamide and post-natal days on GPx was ($F_{(3, 49)} = 8.605$, $P = 0.0001$). Benjamini-Hochberg was used as a

post-hoc test. Asterisks represent the comparisons between AS group with its respective CS group and between CS nicotinamide/AS nicotinamide group with its respective CS vehicle/AS vehicle group. Statistical significance: *P<0.05; **P<0.01; ***P<0.001, ****P<0.0001.

Table 10. A. Effect of perinatal asphyxia (PA) and **B**. nicotinamide on catalase protein levels and activity monitored in hippocampus of rat neonates at P1 and P14.(Comparisons: AS versus CS; CS nicotinamide versus CS vehicle; AS nicotinamide versus AS vehicle). Normalized catalase protein by western blot (N=5 independent experiments) is expressed in arbitrary units (a. u.), relative catalase levels by ELISA is expressed in absorbance values by total protein (mg) and catalase activity by ELISA is expressed as constant (k) rate from the exponential decomposition of hydrogen peroxide (min), normalized by catalase relative levels and total protein in milligram (mg). Data are means ± S.E.M from N=3 independent experiments.

Postnatal day		**P1**			**P14**	
	Catalase WB (a.u.)	**Catalase ELISA (absorbance/ mg protein)**	**CatalaseActivity (k/catalase/ mg protein)**	**Catalase WB (a.u.)**	**Catalase ELISA (absorbance/ mg protein)**	**CatalaseActivity (k/catalase/ mg protein)**
A. Effect of PA; N= 5 (WB); N= 4 (ELISA and activity) independent experiments						
CS; n=(10); (4-5)	0.94±0.10	0.368±0.099	0.150±0.022	1.074±0.052	0.176±0.018	0.017±0.003
AS; n=(10-12); (4-5)	1.04±0.08	0.206±0.034 **(by 36.31%)****	0.053±0.009 **(by 64.46%)******	0.966±0.054	0.105±0.016 **(by 41.73%)***	0.004±0.0003 **(by 71.23%)*****
B. Effect of Nicotinamide; N= 5 (WB); 4 (ELISA and activity) independent experiments						
CS Vehicle; n=(10-12); (4-5)	0.98±0.07	0.212±0.029	0.102±0.009	1.016±0.045	0.150±0.012	0.011±0.001
CS Nicotinamide; n=(12); (4-5)	1.19±0.08	0.363±0.047 **(> 1.8X)****	0.214±0.020 **(> 2.2X)*****	0.982±0.080	0.124±0.028	0.009±0.001

AS Vehicle; n=(12-18); (4-5)	1.05±0.07	0.168±0.075	0.065±0.015	0.995±0.052	0.078±0.004	0.005±0.001
AS Nicotinamide; n=(12); (4-5)	1.27±0.06 **(> 1.2X)***	0.399±0.065 **(> 3.8X)****	0.145±0.015 **(> 2.5X)*****	1.35±0.076 **(> 1.3X)****	0.145±0.021 **(> 1.8X)****	0.023±0.007 **(> 5.8X)****

(a) For catalase protein determined by Western blots two-way ANOVA indicated (**i**) a significant effect of PA and postnatal days on catalase levels ($F_{(3, 39)} = 32.261$, $P < 0.0001$); effect of PA on catalase levels was ($F_{(1, 39)} = 62.197$, $P < 0.0001$); effect of postnatal days was ($F_{(1, 39)} = 27.090$, $P < 0.0001$) and interaction between PA and postnatal days on catalase levels was ($F_{(1, 39)} = 7.496$, $P = 0.009$). (**ii**) The effect of nicotinamide and postnatal days was statistically significant on catalase levels ($F_{(7, 98)} = 56.185$, $P < 0.0001$); effect of nicotinamide on catalase levels was ($F_{(3, 98)} = 76.576$, $P < 0.0001$); effect of postnatal days on catalase was ($F_{(1, 98)} = 34.227$, $P < 0.0001$) and interaction between nicotinamide and postnatal days was ($F_{(3, 98)} = 26.383$, $P < 0.0001$).

(b) For catalase relative levels determined by ELISA unbalanced two-way ANOVA indicated (**i**) a significant effect of PA and postnatal days on catalase relative levels ($F_{(3, 15)} = 11.349$, $P = 0.0004$); effect of PA was ($F_{(1, 15)} = 26.214$, $P = 0.0001$); effect of post-natal days was ($F_{(1, 15)} = 0.232$, $P= 0.637$) and interaction between PA and post-natal days was ($F_{(1, 15)} = 7.601$, $P = 0.015$). (**ii**) The effect of nicotinamide on catalase relative levels reached the statistically significant level ($F_{(7, 29)} = 3.954$, $P = 0.004$); effect of nicotinamide was ($F_{(3, 29)} = 7.494$, $P = 0.001$); effect of postnatal days was ($F_{(1, 29)} = 0.15$, $P = 0.701$) and interaction between nicotinamide and post-natal days was ($F_{(3, 29)} = 1.681$, $P = 0.193$).

(c) For catalase activity unbalanced two-way ANOVA indicated (**i**) a significant effect of PA and postnatal days on catalase activity ($F_{(3, 13)} = 22.186$, $P < 0.0001$); effect of PA on catalase activity was ($F_{(1, 13)} = 40.626$, $P < 0.0001$); effect of postnatal days was ($F_{(1, 13)} = 7.533$, $P = 0.017$) and interaction between PA and postnatal days was ($F_{(1, 13)} = 18.399$, $P = 0.001$). (**ii**) The effect of nicotinamide and postnatal days was significantly ($F_{(7, 29)} = 7.833$, $P < 0.0001$); effect of nicotinamide was ($F_{(3, 29)} = 10.959$, $P < 0.0001$); effect of postnatal days was ($F_{(1, 29)} = 8.226$, $P = 0.008$) and interaction between nicotinamide and postnatal days was ($F_{(3, 29)} = 4.575$, $P = 0.01$). Benjamini-Hochberg was used as a post-hoc test. Asterisks represent the comparisons between AS group with its respective CS group and between CS nicotinamide/AS nicotinamide group with its respective CS vehicle/AS vehicle group. Statistical significance: *P<0.05; **P<0.01; ***P<0.001, ****P<0.0001.

Table 11. A. Effect of perinatal asphyxia (PA) and **B**. nicotinamide on TIGAR protein levels monitored in hippocampus of rat neonates at P1 and P14.(Comparisons: AS versus CS; CS nicotinamide versus CS vehicle; AS nicotinamide versus AS vehicle).TIGAR normalized levels are expressed in arbitrary units (a. u.). Data are means ± S.E.M. from N=5 independent experiments.

Postnatal day	**P1**	**P14**
	TIGAR (a.u.)	**TIGAR (a.u.)**
A. Effect of PA; N=5 independent experiments		
CS; n=5	1.38 ±0.15	0.92 ±0.04
AS; n=5	**0.80 ±0.08 (by 35.9%)****	**1.29 ±0.14 (> 1.4X)****
B. Effect of Nicotinamide; N=5 independent experiments		
	TIGAR (a.u.)	**TIGAR (a.u.)**
CS Vehicle; n=5	1.18 ±0.07	0.95 ±0.05
CS Nicotinamide; n=5	0.95 ±0.07	**0.71 ±0.07 (by 28.1%)****
AS Vehicle; n=5	0.94 ±0.09	1.44 ±0.15
AS Nicotinamide; n=5	0.88 ±0.08	**0.82 ±0.10 (by 40.7 %)****

Two-way ANOVA indicated (**i**) a significant effect of PA and postnatal days on TIGAR levels ($F_{(3, 37)} = 50.557$, $P < 0.0001$); effect of PA on TIGAR levels was ($F_{(1, 37)} = 91.25$, $P < 0.0001$); effect of post-natal days was ($F_{(1, 37)} = 25.71$, $P < 0.0001$) and interaction between PA and post-natal days was ($F_{(1, 37)} = 34.71$, $P < 0.0001$). (**ii**) The effect of nicotinamide and postnatal days was statistically significantly ($F_{(7, 73)} = 56, 911$, $P < 0.0001$); effect of nicotinamide on TIGAR levels was ($F_{(3, 73)} = 117.538$, $P < 0.0001$); effect of post-natal days was ($F_{(1, 73)} = 14.993$, $P = 0.0002$) and interaction between nicotinamide and post-natal days was ($F_{(3, 73)} = 10.256$, $P < 0.0001$). Benjamini-Hochberg was used as a post-hoc test. Asterisks represent the comparisons between AS group with its respective CS group and between CS nicotinamide/AS nicotinamide group with its respective CS vehicle/AS vehicle group. Statistical significance: *P<0.05; **P<0.01; ***P<0.001, ****P<0.0001.

Table 12. A. Effect of perinatal asphyxia (PA) and **B**. nicotinamide on XRCC1 protein levels monitored in hippocampus of rat neonates at P1 and P14. The XRCC1 protein levels are represented as protein normalized levels in arbitrary units (a. u.). Data are means ± S.E.M. from N=5 independent experiments.

Postnatal day	**P1**	**P14**
	XRCC1 (a.u.)	**XRCC1 (a.u.)**
A. Effect of PA; N=5 independent experiments		
CS n=5	0.88 ±0.06	1.10 ±0.05
AS n=5	**1.14 ±0.03 (> 1.3X)****	0.96 ±0.06
B. Effect of Nicotinamide; N=5 independent experiments		
	XRCC1 (a.u.)	**XRCC1 (a.u.)**
CS Vehicle n=5	1.01 ±0.07	1.19 ±0.11
CS Nicotinamide n=5	0.93 ±0.03	0.94 ±0.10
AS Vehicle n=5	1.16 ±0.06	0.93 ±0.06
AS Nicotinamide n=5	**0.81 ±0.06 (by 29.34 %)*****	0.93 ±0.10

Two-way ANOVA indicated (**i**) a significant effect of PA and postnatal days on XRCC1 levels ($F_{(3, 31)} = 21.033$, $P < 0.0001$); effect of PA on XRCC1 levels was ($F_{(1, 31)} = 43.834$, $P < 0.0001$); effect of post-natal days was ($F_{(1, 31)} = 17.018$, $P = 0.0003$) and interaction between PA and post-natal days was ($F_{(1, 31)} = 2.248$, $P = 0.144$). (**ii**) The effect of nicotinamide and postnatal days was statistically significant ($F_{(7, 65)} = 69.192$, $P < 0.0001$); effect of nicotinamide was ($F_{(3, 65)} = 140.079$, $P < 0.0001$); effect of post-natal days was ($F_{(1, 65)} = 26.327$, $P < 0.0001$) and interaction between nicotinamide and post-natal days was ($F_{(3, 65)} = 12.595$, $P < 0.0001$). Benjamini-Hochberg was used as a post-hoc test. Asterisks represent the comparisons between AS group with its respective CS group and between CS nicotinamide/AS nicotinamide group with its respective CS vehicle/AS vehicle group. Statistical significance: *P<0.05; **P<0.01; ***P<0.001, ****P<0.0001.

Table 13. A. Effect of perinatal asphyxia (PA) and **B.** nicotinamide on calpain activity monitored in hippocampus of rat neonates at P1 and P14. (Comparisons: AS versus CS; CS nicotinamide versus CS vehicle; AS nicotinamide versus AS vehicle). Calpain activity is expressed in units/mg protein. Data are means ± S.E.M. from N=4 independent experiments in duplicated.

Postnatal day	**P1**	**P14**
	Calpain activity (units/mg total protein)	**Calpain activity (units/mg total protein)**
A. Effect of PA; N=4 independent experiments		
CS; n=8	1346.07 ±69.07	2962.24 ±102.08
AS; n=8	1500.19 ±60.92	**6228.25 ±400.74 (>2.05X)******
B. Effect of Nicotinamide; N=4 independent experiments		
CS Vehicle; n=8	1357.35 ±45.57	2783.57 ±160.74
CS Nicotinamide; n=8	1313.15 ±51.36	2627.08 ±204.60
AS Vehicle; n=8	1478.33 ±53.41	5972.28 ±463.16
AS Nicotinamide; n=8	1597.31 ±115.82	2247.91 ±74.04 **(by 62.40%)******

Two-way ANOVA indicated (**i**) a significant effect of PA and postnatal days on calpain activity ($F_{(3, 27)} = 111.989$, $P < 0.0001$); effect of PA was ($F_{(1, 27)} = 65.660$, $P < 0.0001$); effect of postnatal days was ($F_{(1, 27)} = 219.338$, $P < 0.0001$) and interaction between PA and postnatal days on calpain activity was ($F_{(1, 27)} = 50.971$, $P < 0.0001$). (**ii**) The effect of nicotinamide and postnatal days was statistically significant on calpain activity ($F_{(7, 52)} = 56.117$, $P < 0.0001$); effect of nicotinamide was ($F_{(3, 52)} = 45.256$, $P < 0.0001$); effect of postnatal days was ($F_{(1, 52)} = 161.714$, $P < 0.0001$) and interaction between nicotinamide and postnatal days on calpain activity was ($F_{(3, 52)} = 31.779$, $P < 0.0001$). Benjamini-Hochberg was used as a post-hoc test. Asterisks represent the comparisons between AS group with its respective CS group and between CS nicotinamide/AS nicotinamide group with its respective CS vehicle/AS vehicle group. Statistical significance: *P<0.05; **P<0.01; ***P<0.001, ****P<0.0001.

8. Figures

Figure 1. Main Patterns of injury in term birth asphyxia. Image obtained from thesis titled¨ The Clinical Value of Intensive Monitoring in Term Asphyxiated Newborns¨. Page 51. Renate M. c. Swarte, 2010.

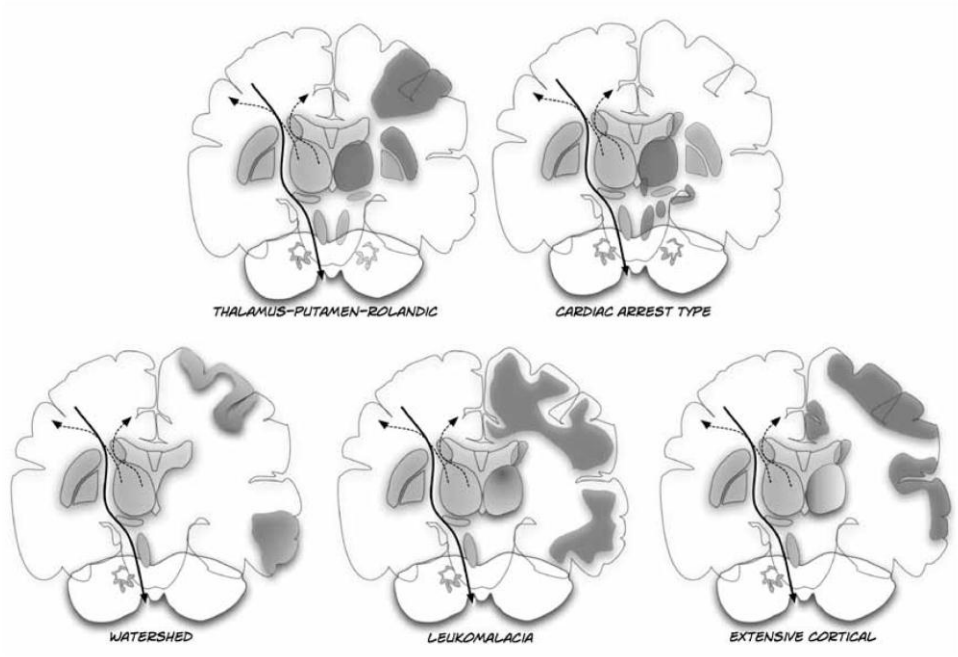

Figure 2. Main enzymatic and non-enzymes antioxidants. (Kellner M. *et al*. 2017)

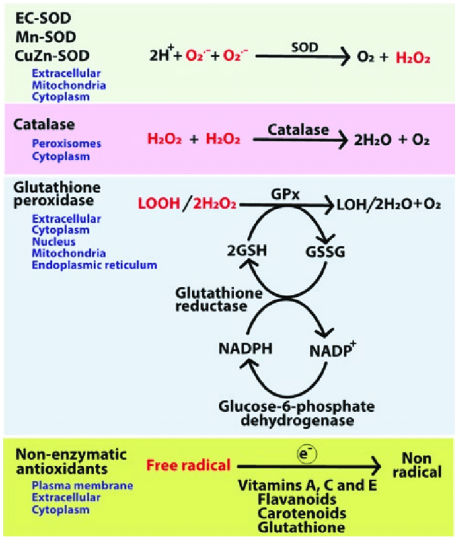

Figure 3. The pentose phosphate pathway (PPP). The enzymes involved in the oxidative phase of the PPP (highlighted by blue) are indicated by numbers. (1) G6P dehydrogenase (G6PDH); (2) 6-phosphogluconolactone (6PGL); (3) 6PGDH; (5) isomerization by Ru5P isomerase (RPI); (6) Ru5P epimerase (RPE). In the non oxidative PPP (highlighted by yellow background), (7) transketolase (TKT); (8) Transaldolase (TALDO); transketolase (TKT) (9). (Figure extracted from article the pentose phosphate pathway and cancer by Patra *et al* 2014).

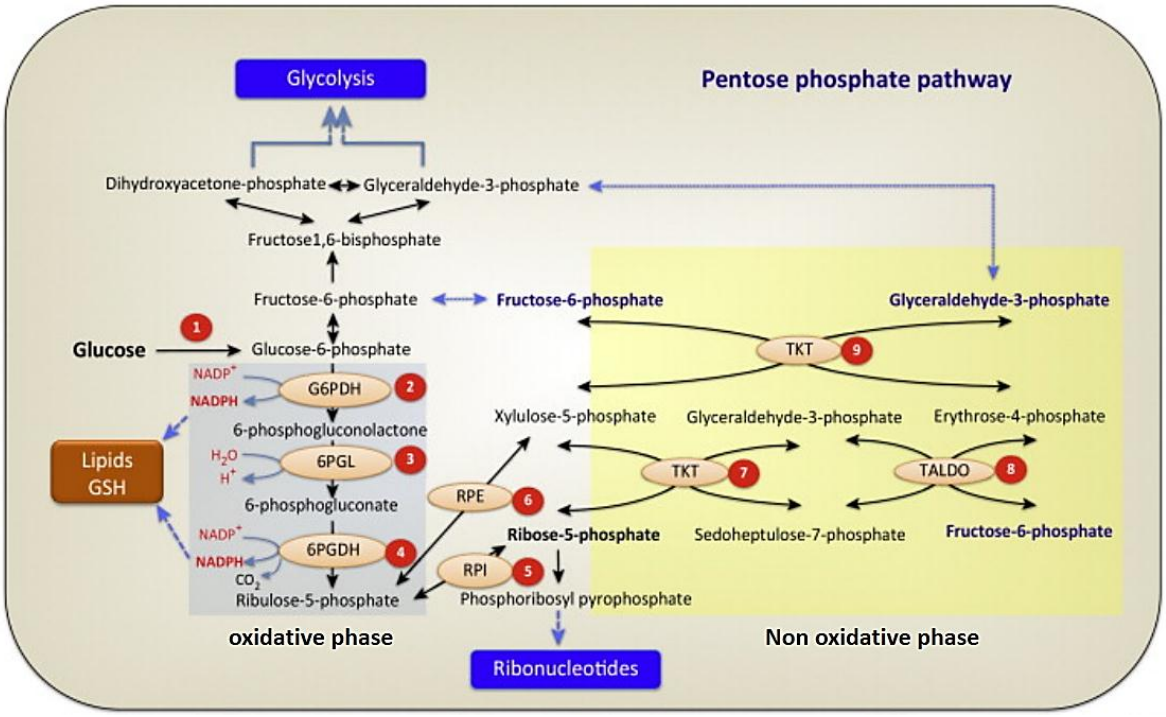

Figure 4. **The NAD$^+$ synthesis**. The *de novo* pathway represents the catabolism of the amino acid L-tryptophan to quinolinic acid through the kynurenine pathway (KP). Quinolinic acid is then converted to nicotinic acid mononucleotide (NaMN) which connects to the salvage pathway. The three different salvage pathways start either from nicotinamide (Nam), nicotinic acid (Na), or nicotinamide riboside (NR). Nicotinamide is a by-product of NAD metabolism, which is converted into nicotinamide mononucleotide (NMN) by nicotinamide phosphoribosyl transferase (NamPRT)) and then into NAD$^+$ by the action of nicotinamide mononucleotide adenylyl transferases (Na/NMNAT1, 2, and 3). NAD$^+$ is converted to NADP$^+$ by phosphate transference catalysed by NAD Kinase (NADK) (Figure extracted from review Massudi *et al*. 2012).

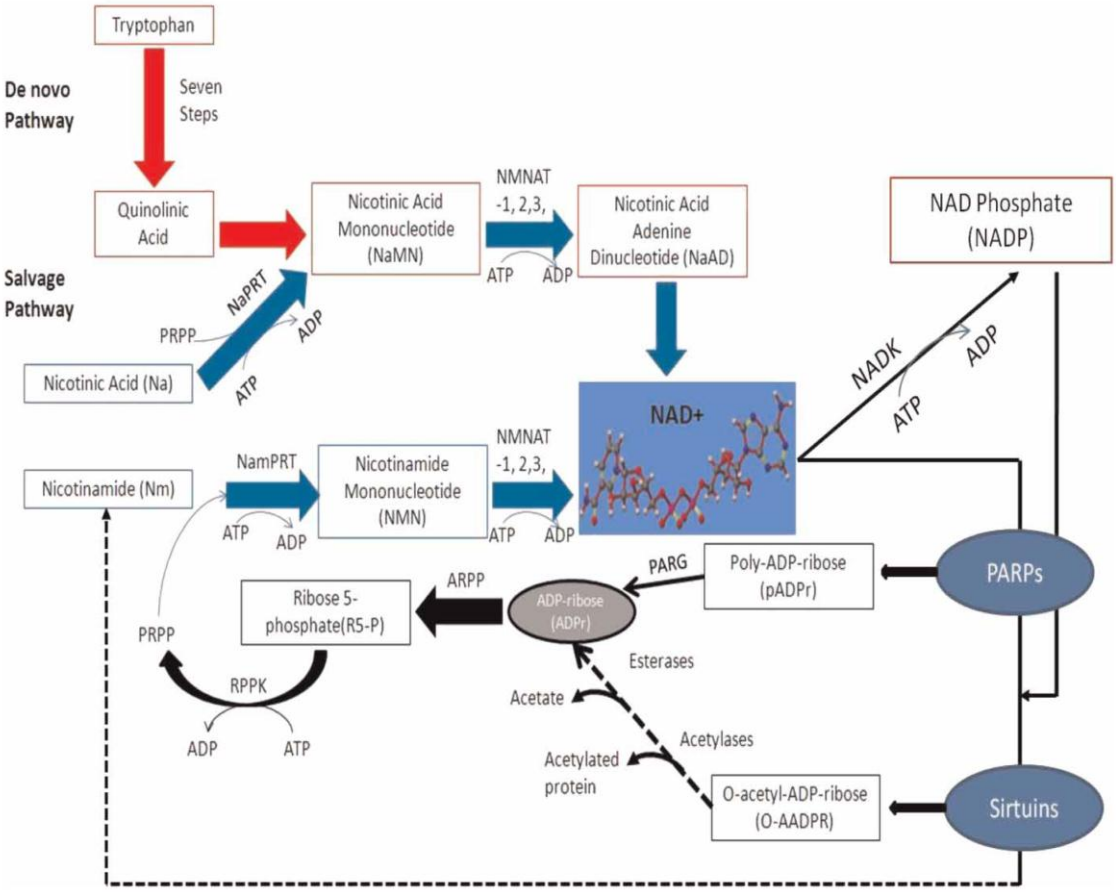

Figure 5. GSH (A), GSSG (B) levels and (C) GSSG: GSH ratio in mesencephalon of perinatal asphyxia-exposed and control rats. The effect of PA on GSH, GSSG levels (µmol/mg protein), and GSSG:GSH ratio, used as a oxidative stress index monitored at postnatal day (P) 1, 3, 7 or 14 in mesencephalon from control (CS) and asphyxia-exposed (AS) rats. All values are expressed as means ± S.E.M., from at least N=4 independent experiments in duplicated. Unbalanced two-way ANOVA indicated a significant effect of PA on GSH ($F_{(1, 46)} = 17.115$, $P = 0.0001$); GSSG ($F_{(1, 46)} = 79.209$, $P < 0.0001$) and on GSSG: GSH ratio ($F_{(1, 46)} = 38.932$, $P < 0.0001$). Benjamini-Hochberg was used as a post hoc test. The statistical differences between CS and AS groups are indicated by asterisk. (*P < 0.05, **P < 0.01, ***P < 0.001, ****P < 0.0001).

(A)

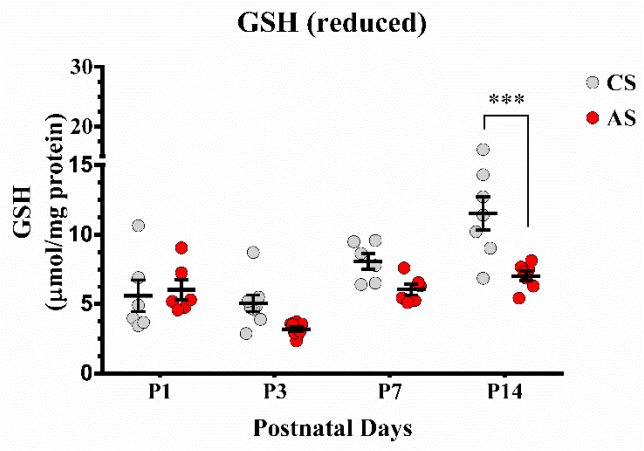

(B)

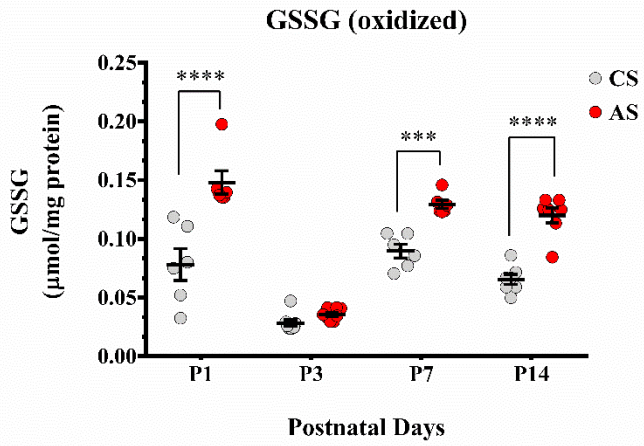

(C)

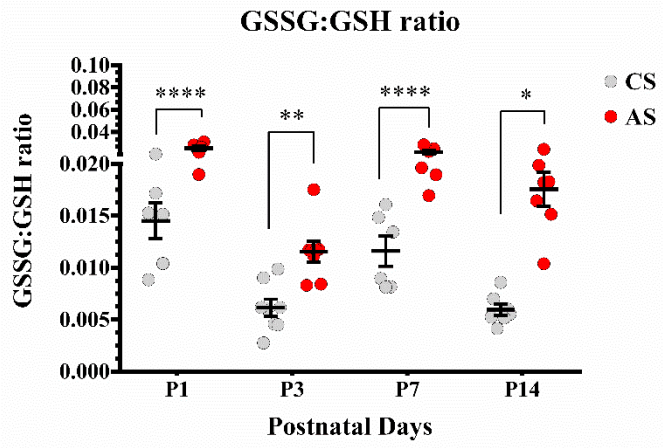
GSSG:GSH ratio
GSSG:GSH ratio
0.10
0.08
0.06
0.04
0.020
0.015
0.010
0.005
0.000
****
**
****
*
CS
AS
P1
P3
P7
P14
Postnatal Days

Figure 6. **GSH (A), GSSG (B) levels and (C) GSSG:GSH ratio in telencephalon of perinatal asphyxia-exposed rats.** The effect of PA on GSH, GSSG levels (µmol/mg protein), and GSSG:GSH ratio, used as a oxidative stress index monitored at postnatal day (P) 1, 3, 7 or 14 in mesencephalon from control (CS) and asphyxia-exposed (AS) rats. All values are expressed as means ± S.E.M., from at least N=4 independent experiments in duplicated. Unbalanced two-way ANOVA indicated a significant effect of PA on GSH ($F_{(1, 61)}$ = 7.781; P= 0.007); GSSG ($F_{(1, 61)}$ =1,143; P = 0.289) but not on GSSG: GSH ratio ($F_{(1, 61)}$ = 0.045, P= 0.833). Benjamini-Hochberg was used as a post hoc test for comparison between CS and AS groups. The statistical differences are indicated by asterisk. (*P < 0.05, **P < 0.01, ***P < 0.001, ****P < 0.0001).

(A)

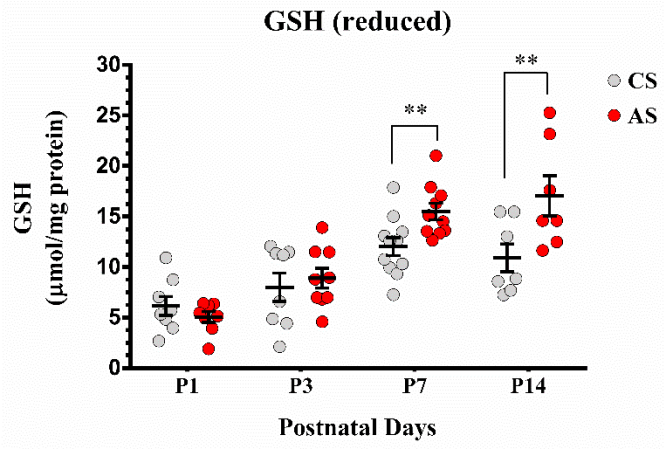

(B)

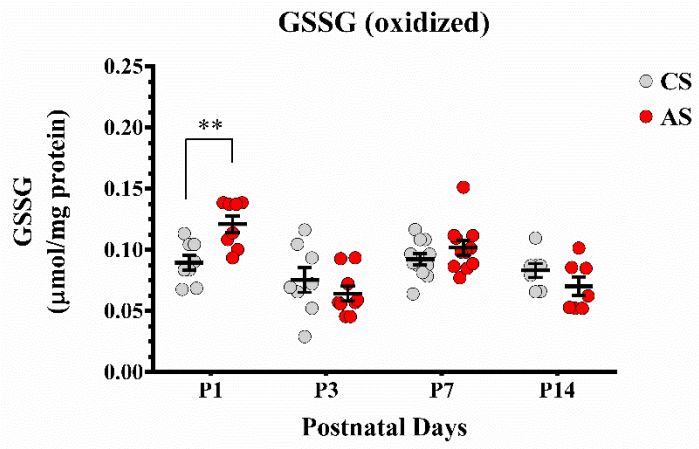

(C)

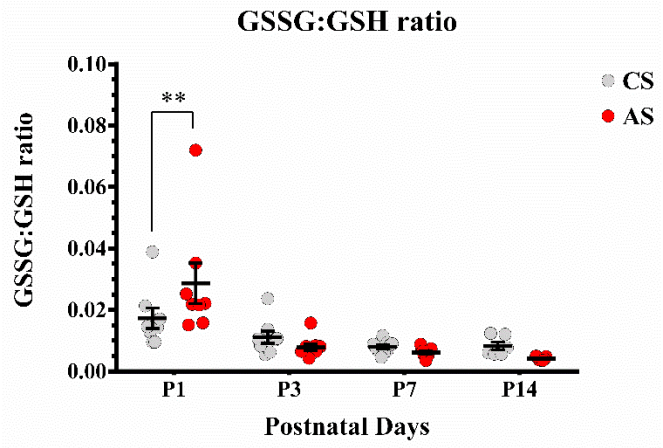
GSSG:GSH ratio
GSSG:GSH ratio
0.10
0.08
0.06
0.04
0.02
0.00
**
CS
AS
P1
P3
P7
P14
Postnatal Days

Figure 7. GSH (A), GSSG (B) levels and (C) GSSG:GSH ratio in hippocampus of perinatal asphyxia-exposed rats. The effect of PA on GSH and GSSG levels (µmol/mg protein), and GSSG:GSH ratio, used as a oxidative stress index monitored at postnatal day (P) 1, 3, 7 or 14 in mesencephalon from control (CS) and asphyxia-exposed (AS) rats. All values are expressed as means ± S.E.M., from at least N=4 independent experiments in duplicated. Unbalanced two-way ANOVA indicated a significant effect of PA on GSH ($F_{(1, 81)}$ = 21.308; P< 0.0001); GSSG ($F_{(1, 81)}$ =97.070; P< 0.0001) and GSSG: GSH ratio ($F_{(1, 84)}$ = 53.617, P < 0.0001). Benjamini-Hochberg was used as a post hoc test for comparison between CS and AS groups. The statistical differences are indicated by asterisk. (*P < 0.05, **P < 0.01, ***P < 0.001, ****P < 0.0001).

(A)

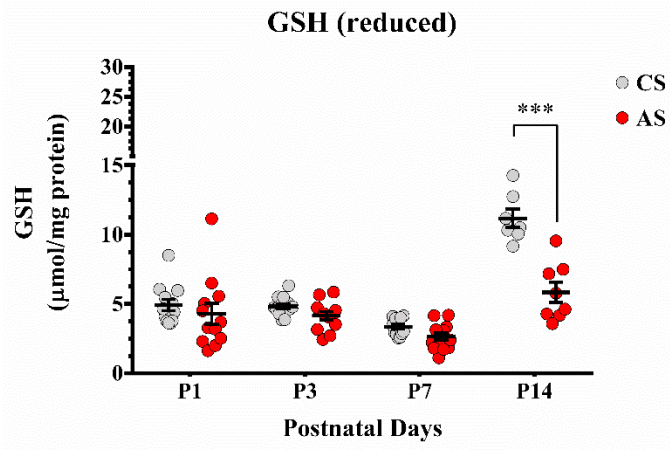

(B)

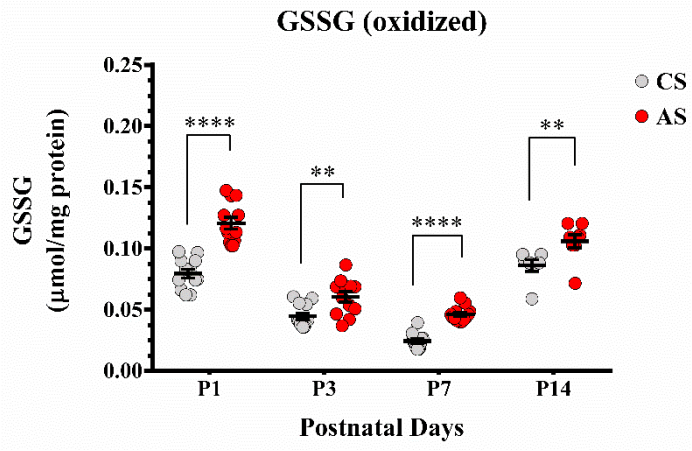

(C)

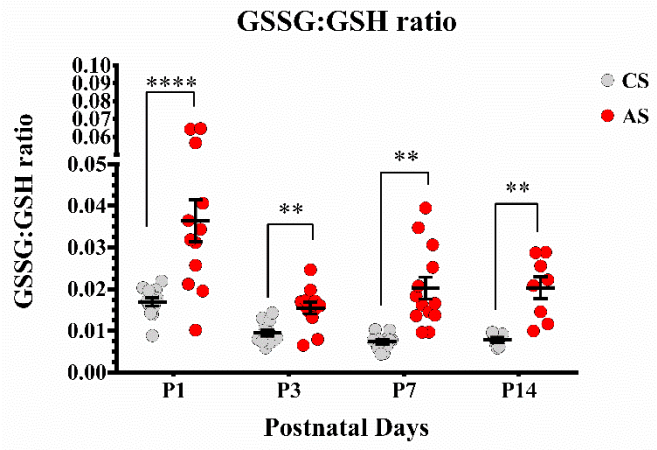
GSSG:GSH ratio
GSSG:GSH ratio
0.10
0.09
0.08
0.07
0.06
0.05
0.04
0.03
0.02
0.01
0.00
****
**
**
**
CS
AS
P1
P3
P7
P14
Postnatal Days

Figure 8. Reducing capacity (FRAP) in brain of perinatal asphyxia exposed rats. Effect of PA on FRAP (Fe(II) equivalents in µM, normalised by total protein in µg), as an index of antioxidant capacity along postnatal day (P) 1, 3, 7 or 14 in mesencephalon (A), telencephalon (B) and hippocampus (C) from control (CS) and asphyxia-exposed (AS) rats. Data are means ± SEM from at least N=6 independent experiments in triplicated. Unbalanced two-way ANOVA indicated a significant effect of PA on FRAP levels in mesencephalon ($F_{(1, 76)} = 89.347$, $P < 0.0001$), telencephalon ($F_{(1, 85)} = 32.395$, $P < 0.0001$) and hippocampus ($F_{(1, 91)} = 104.903$, $P < 0.0001$). Benjamini-Hochberg was used as a post hoc test. The statistical differences between CS and AS groups are indicated by asterisk (*P < 0.05, **P < 0.01, ***P < 0.001, ****P < 0.0001).

(A)

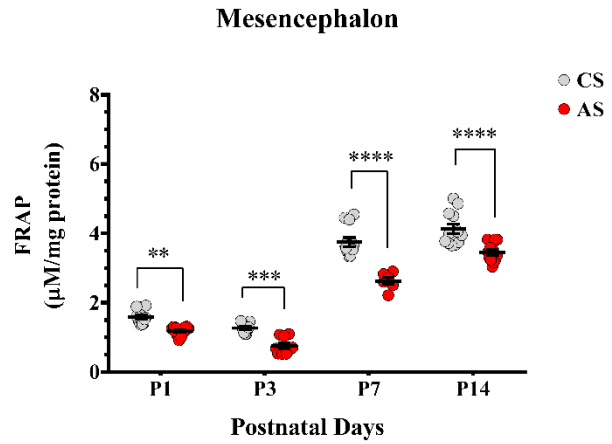

(B)

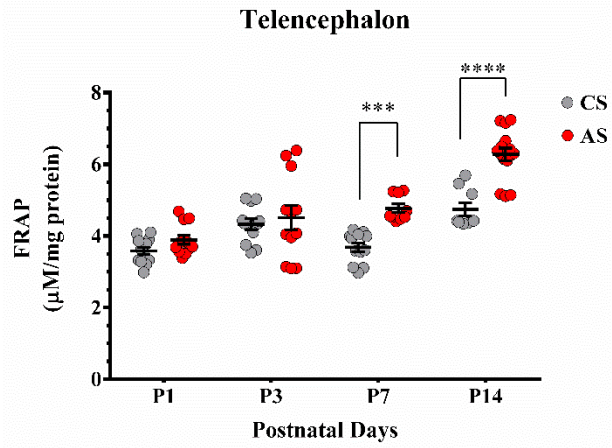

(C)

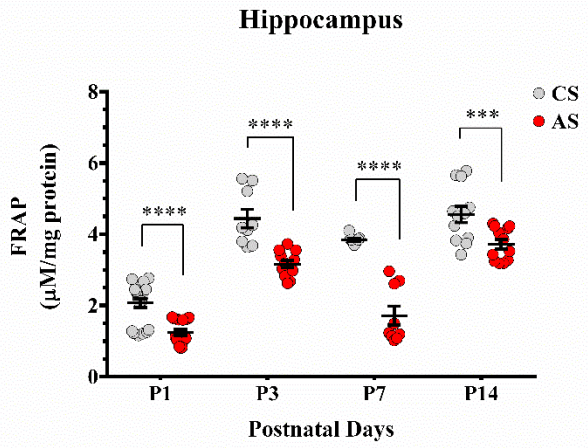
Hippocampus
FRAP
(µM/mg protein)
8
6
4
2
0
****
****
****
***
CS
AS
P1
P3
P7
P14
Postnatal Days

Figure 9. Representative Immunoblots of the effect of perinatal asphyxia (PA) on catalase protein in mesencephalon (A, B), telencephalon (C, D) and hippocampus (E, F) of neonatal rats. The effect of PA was analysed in protein extracts from tissue sampled at P1, 3, 7 and 14. Control (CS) and asphyxia-exposed (AS) samples were taken from sibling neonatal rats. Representative immunoblots for catalase and Ponceau Red staining, as loading control, are shown in (**A)** mesencephalon, (**C)** telencephalon and (**E)** hippocampus, respectively. Catalase was identified as a unique band at 60 kDa, also for extracted protein from a liver sample taken at P1. Purified catalase protein was used as a positive control. Lane C is an internal control from cerebellum, used to control variations in transference. Lane L corresponds to a ladder protein marker. Quantification of catalase was performed by densitometry. The area of catalase and total protein was determined and normalized by the sum method. Catalase values were divided by total protein values, normalized (by loading control) for obtaining the quantity of catalase. Catalase protein normalized levels are in arbitrary units (a. u.) for (**B**) mesencephalon, (**D**) telencephalon and (**F**) hippocampus. Data are means ± SEM from at least N=6 independent experiments. Unbalanced two-way ANOVA indicated a non-significant effect of PA on catalase protein evaluated *in mesencephalon* ($F_{(1, 56)}$ = 1,263, P = 0.266); and *telencephalon* ($F_{(1, 48)}$ = 0.483, P = 0.491). In *hippocampus* the effect of PA reached the statistically significant level ($F_{(1, 40)}$ = 6.638, P < 0.05). Benjamini-Hochberg was used as a post hoc test. The statistical differences between CS and AS groups are indicated by asterisks. (*P < 0.05, **P < 0.01, ***P < 0.001, ****P < 0.0001).

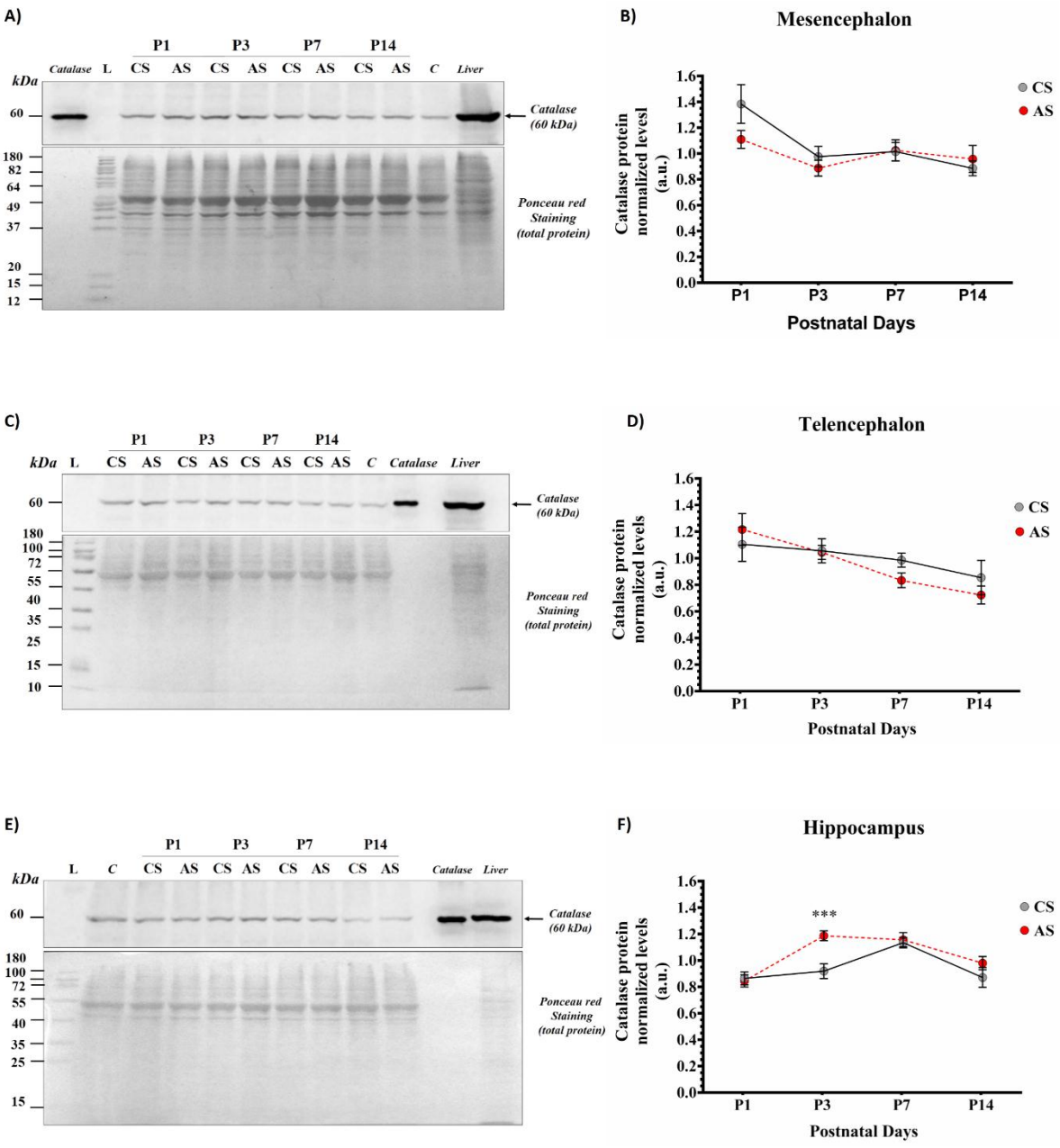
A)
P1
P3
P7
P14
kDa
Catalase
L
CS
AS
C
Liver
60
180
82
64
49
37
20
15
12
Catalase (60 kDa)
Ponceau red Staining (total protein)
B)
Mesencephalon
Catalase protein normalized levesl (a.u.)
CS
AS
Postnatal Days
C)
100
72
55
40
35
25
10
D)
Telencephalon
E)
F)
Hippocampus
***

Figure 10. Effect of perinatal asphyxia on protein and catalase activity in neonatal rat brain. The brain was dissected at P1, 3, 7 and 14 from control (CS) and asphyxia-exposed (AS) rats. Tissue samples from mesencephalon (M), telencephalon (T), and hippocampus (H) were analysed by Western blots (WB) and ELISA, determining protein and catalase activity, respectively. Densitometry was performed for quantification, determining catalase and total protein. The values were normalized by the sum method, and catalase values divided by total normalized protein values (loading control), obtaining the quantity of catalase, represented as catalase protein normalized levels in arbitrary units (a. u.). Enzymatic activity was determined by the constant (k) rate from the exponential decomposition of hydrogen peroxide (min), normalized by catalase relative levels and total protein in milligram (mg). Relative catalase protein levels were obtained dividing absorbance values by total protein (mg). Data are means ± S.E.M. Unbalanced two-way ANOVA indicated a significant effect of PA on catalase relative levels, in mesencephalon ($F_{(1, 22)} = 11.2$, P=0.003), hippocampus ($F_{(1, 24)} = 6.088$, P=0.021) but not in telencephalon ($F_{(1, 42)} = 0.445$, P=0.508). Unbalanced two-way ANOVA indicated a significant effect of PA on catalase activity in mesencephalon ($F_{(1, 16)} = 28.417$, P<0.0001), telencephalon ($F_{(1, 40)} = 1.225$, P=0.275) and hippocampus ($F_{(1, 29)} = 28.153$, P<0.0001). Benjamini-Hochberg used as a post-hoc test. The statistical differences between CS and AS groups are indicated by asterisks. *P<0.05; **P<0.01; ***P<0.001, ****P<0.0001 bold.

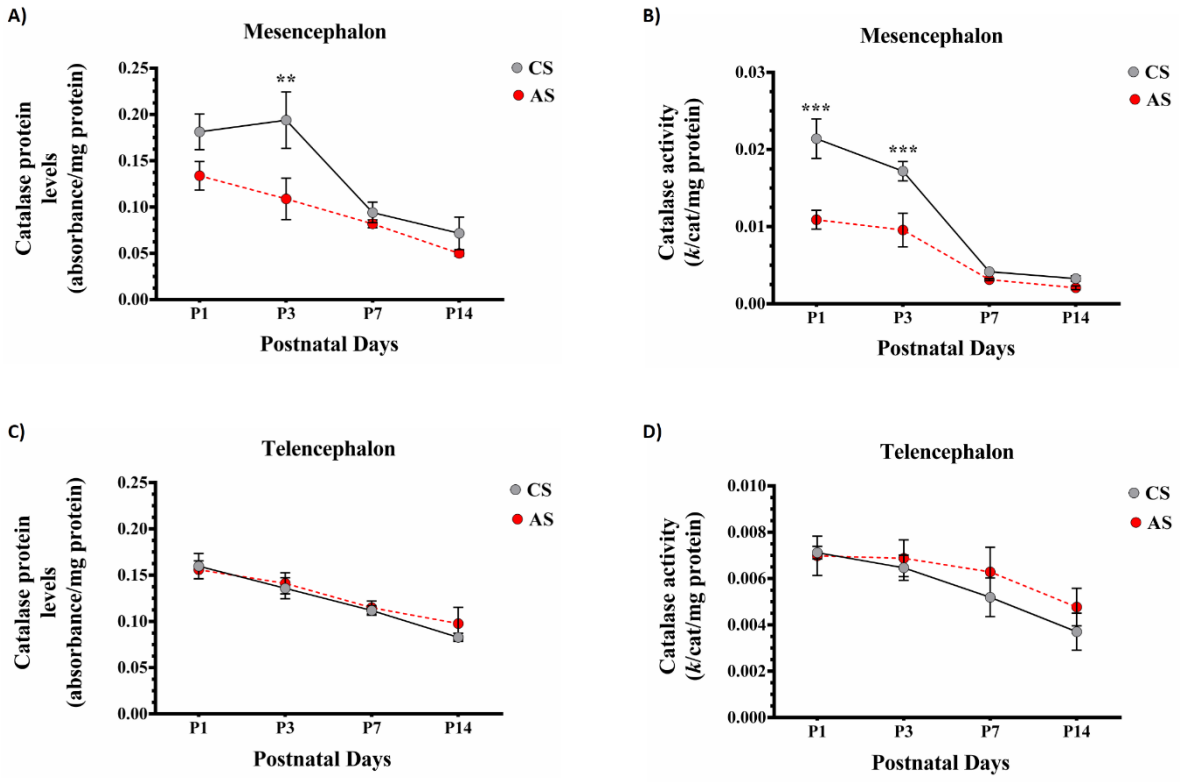

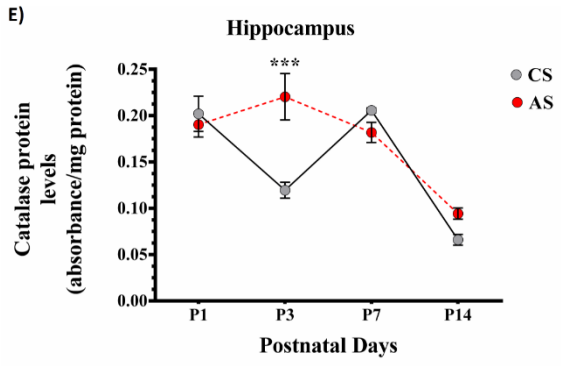
E)
Hippocampus
Catalase protein levels (absorbance/mg protein)
0.25
0.20
0.15
0.10
0.05
0.00
***
P1
P3
P7
P14
Postnatal Days
CS
AS

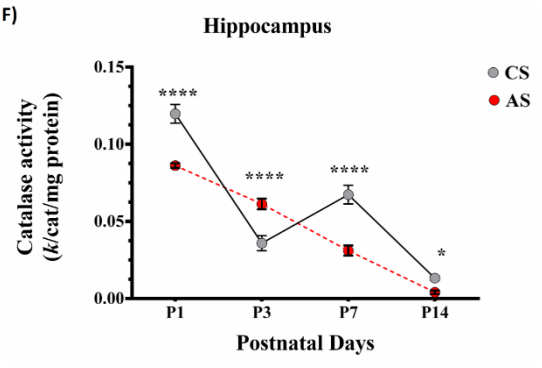
F)
Hippocampus
Catalase activity (k/cat/mg protein)
0.15
0.10
0.05
0.00
****
****
****
*
P1
P3
P7
P14
Postnatal Days
CS
AS

Figure 11. Representative Immunoblots and quantification of the effect of perinatal asphyxia on procaspase-3 and cleaved caspase-3 expression in mesencephalon (A, B), telencephalon (C, D) and hippocampus (E, F) of neonatal rat brain. The effect of perinatal asphyxia was analysed in neonatal brain samples, taken at P1, 3, 7 and 14 from control (CS) and asphyxia-exposed (AS) sibling neonatal rats. Protein extracts were used for separation by SDS-PAGE (12%) and immunoblotting for caspase-3 (1:500). Ponceau Red staining was used as loading control. Protein extract from liver (P1) was used as positive control (Lane Liver). Total protein measured in cerebellum (Lane C) was used as an internal control for transference variation. Ladder protein marker is in Lane L. Procaspase-3 was identified as bands at 36 and 35 k*D*a, cleaved fragments for active caspase-3 were identified at 19, 17 and 12 k*D*a, indicated by the arrows in mesencephalon **(A)**, telencephalon **(C)**, and (**E)** hippocampus. At P7, but only in hippocampus (**E**), a procaspase-3 *m*-calpaìn-cleaved fragment was identified at 30k*D*a, both in CS and AS samples, the signal being stronger in samples from AS than that from CS animals. The area of caspase-3 in the blots and total Ponceau stained proteins was quantified and normalized by the Sum method. The values normalized, and divided by total protein to obtain the quantity of caspase-3, in arbitrary units (a. u.) represented by graphs in **B**, **D**, and **F** for mesencephalon, telencephalon and hippocampus, respectively. Data are means ± S.E.M from *N=5* independent experiments. Two-way ANOVA indicated a significant effect of PA on cleaved caspase-3 levels in mesencephalon ($F_{(1, 32)} = 23.118$, $P<0.0001$) and hippocampus ($F_{(1, 32)} = 19.991$, $P<0.0001$), but not telencephalon ($F_{(1, 32)} = 1.234$, $P=0.313$). *Benjamini-Hochberg* was used as a post-hoc test. The statistical differences between CS and AS groups are indicated by asterisks.*P<0.05; **P<0.01; ***P<0.001, ****P<0.0001 bold.

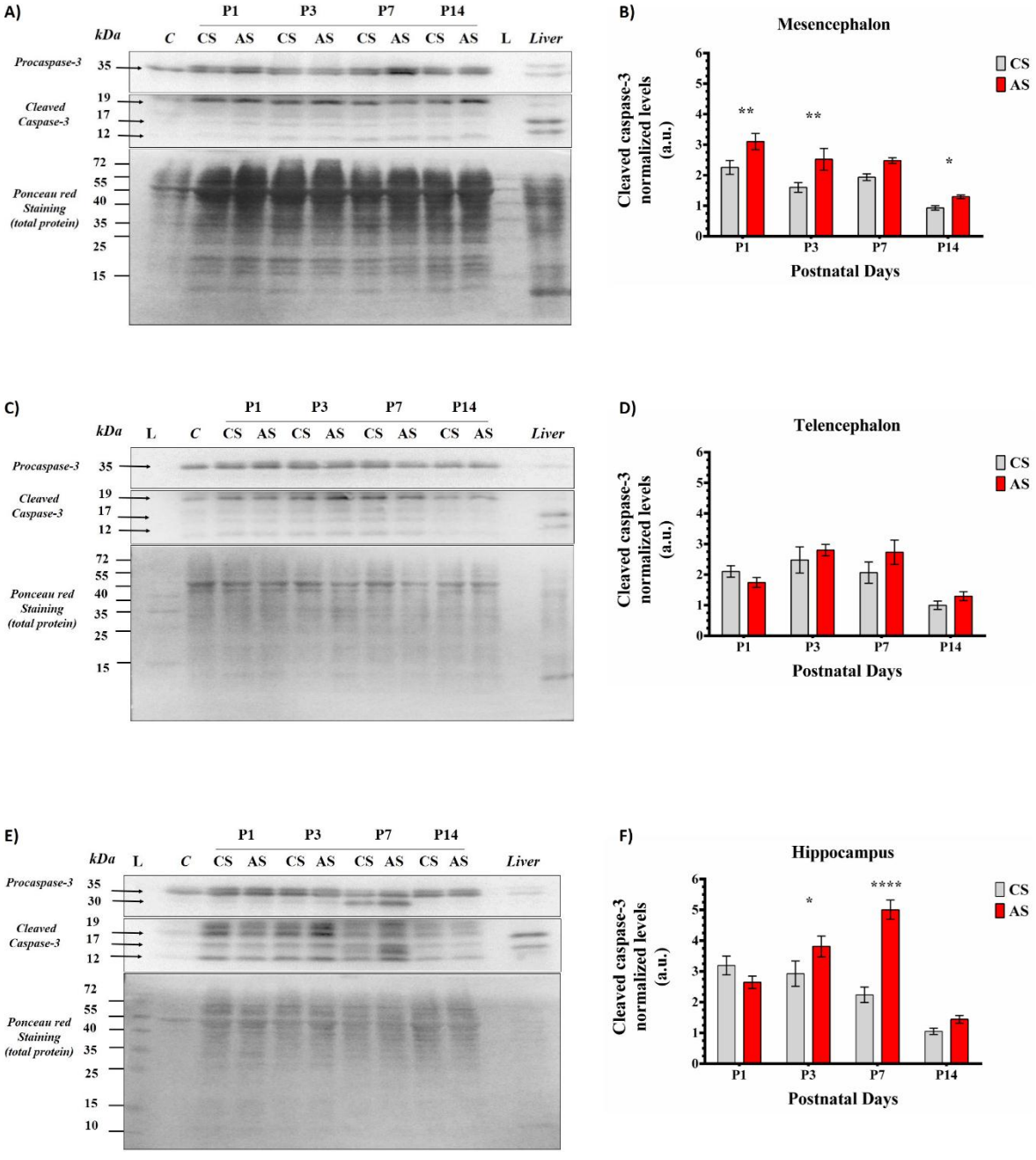
A)
P1
P3
P7
P14
kDa
C
CS
AS
CS
AS
CS
AS
CS
AS
L
Liver
Procaspase-3
35
Cleaved Caspase-3
19
17
12
Ponceau red Staining (total protein)
72
55
40
35
25
15
B)
Mesencephalon
Cleaved caspase-3 normalized levels (a.u.)
CS
AS
**
**
*
P1
P3
P7
P14
Postnatal Days
C)
kDa
L
C
Liver
Procaspase-3
Cleaved Caspase-3
Ponceau red Staining (total protein)
D)
Telencephalon
Cleaved caspase-3 normalized levels (a.u.)
Postnatal Days
E)
kDa
Procaspase-3
30
Cleaved Caspase-3
Ponceau red Staining (total protein)
10
F)
Hippocampus
Cleaved caspase-3 normalized levels (a.u.)
*
****
Postnatal Days

Figure 12. Multivariate analysis in mesencephalon. The differences along postnatal days in CS and AS groups were determined by principal factor analysis, the variables with major contribution are combined in a single variable called principal first factor F1 (axis *x*) and principal second factor F2 (axis *y*). Then, the observations at different postnatal days was correlated with F1 and F2 for determining the variables with major contribution to variations among postnatal days. The values of axis corresponding to values of correlation (*r*) for each variable that contribute to F1 and F2. In red are shown the vectors for each variable analysed, the longest vector and closest to axis indicate the variable with most contribution to F1 or F2. The red point of vector indicates the correlation value for variable with F1 or F2. (**A**) In CS groups the principal factor analysis indicated that main variations among postnatal days are explained by the principal first factor F1 in a 49,12% and by the principal second factor F2 in a 20,70%. *Cleaved caspase-3* (*r*: 0,898); *FRAP* (*r*: -0,723); *catalase activity* (*r*: 0,712) and *GSSG:GSH* ratio (*r*: 0,711) were the variables highly correlated with F1. F2 was correlated with *catalase activity* (*r*: -0,689). In the figure are shown the differences among postnatal days correlated with F1 and F2 in CS groups. P1 was positively correlated with F1 while that P14 displayed a negative correlation with F1, P3 displayed a negative correlation with F2 and P7 a positive correlation with F2. (**B**) In AS groups the principal factor analysis indicated that main variations among postnatal days are explained by the principal first factor F1 in a 50,22% and by the principal second factor F2 in a 16,57%. *Catalase activity* (*r*: 0,964); *FRAP* (*r*:-0,811) and *cleaved caspase-3* (*r*: 0,784) were the variables highly correlated with F1. F2 was correlated with GSSG: GSH ratio (*r*: -0,764). In the figure are shown the differences among postnatal days correlated with F1 and F2 observed in AS groups. P1 was positively correlated with F1 while that P14 displayed a negative correlation with F1, P3 displayed a positive correlation with F2 and P7 a negative correlation with F2.

(A)

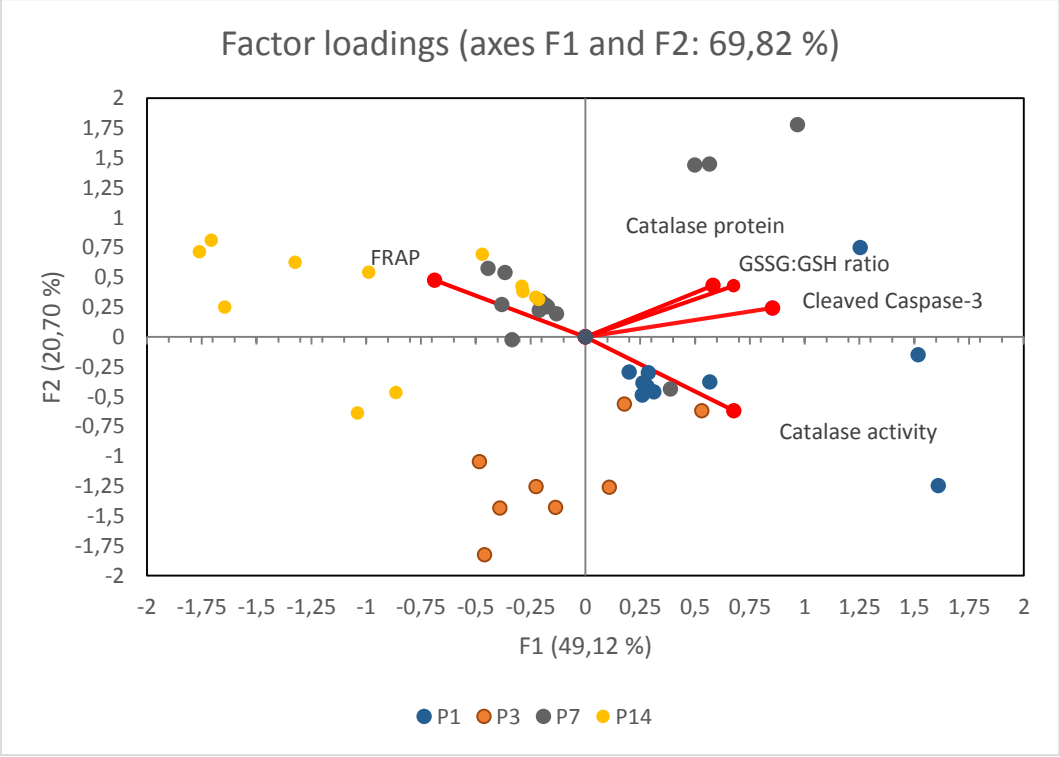

(B)

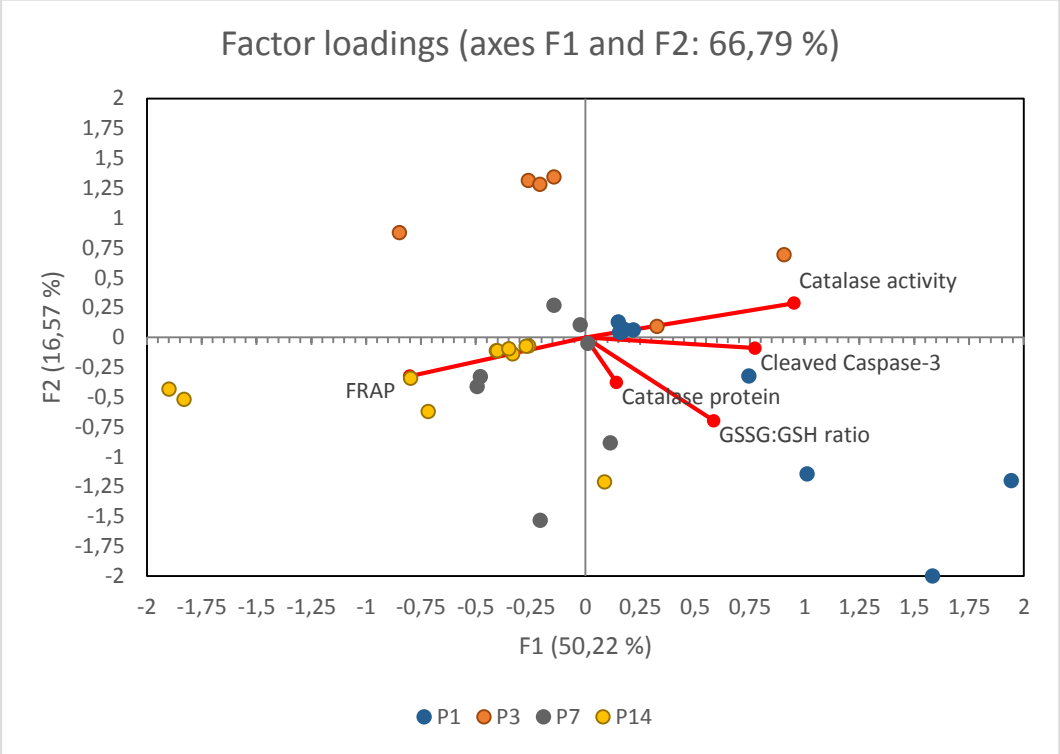
Factor loadings (axes F1 and F2: 66,79 %)
F2 (16,57 %)
F1 (50,22 %)
Catalase activity
Cleaved Caspase-3
Catalase protein
GSSG:GSH ratio
FRAP
P1
P3
P7
P14

Figure 13. Multivariate analysis in telencephalon. The differences along postnatal days in CS and AS groups were determined by principal factor analysis, the variables with major contribution are combined in a single variable called principal first factor F1 (axis *x*) and principal second factor F2 (axis *y*). Then, the observations at different postnatal days are correlated with F1 and F2 for determining the variables with major contribution to variations among postnatal days. The values of axis corresponding to values of correlation for each variable that contribute to F1 and F2. In red are shown the vectors for each variable analysed, the longest vector and closest to axis indicate the variable with most contribution to F1 or F2. The red point of vector indicates the correlation value for variable with F1 or F2. (**A**) In CS groups the principal factor analysis indicated that main variations among postnatal days are explained by the first principal component F1 in a 41,34% and by the second principal component F2 in an 8,47%. F1 was correlated with *catalase activity* (*r*: 0,983). F2 was correlated with *GSSG:GSH ratio* (*r*: 0,555). In the figure are shown the differences among postnatal days correlated with F1 and F2 in CS groups. P1 was positively correlated with F1 while that P14 displayed a negative correlation with F1, P3 displayed a positive correlation with F1 and P7 a positive correlation with F2. (**B**) In AS groups the principal factor analysis indicated that main variations among postnatal days are explained by the first principal component F1 in a 39,53% and by the second principal component F2 in a 12,41%. F1 was correlated with *FRAP* (*r*: 0,923) and *GSSG:GSH ratio* (*r*:-0,884). F2 was correlated with *cleaved caspase-3* (*r*: -0,717). In the figure are shown the differences among postnatal days correlated with F1 and F2 in AS groups. P1 was positively correlated with F1 while that P14 displayed a positive correlation with F2, P3 displayed a positive correlation with F2 and P7 a negative correlation with F2.

(A)

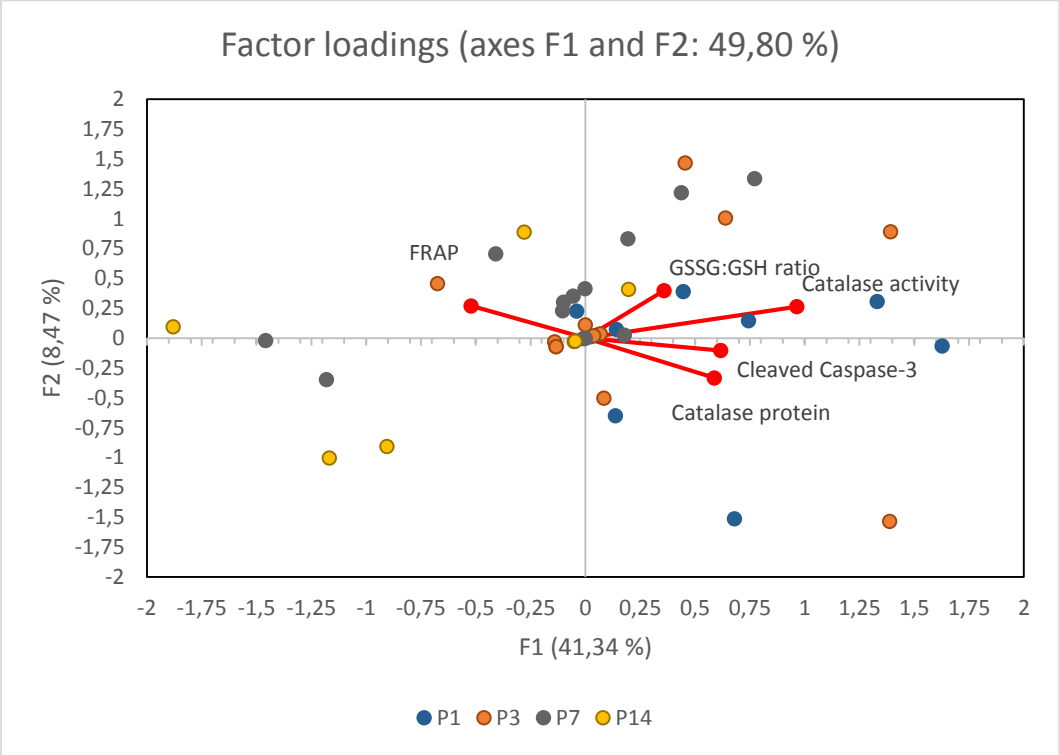

(B)

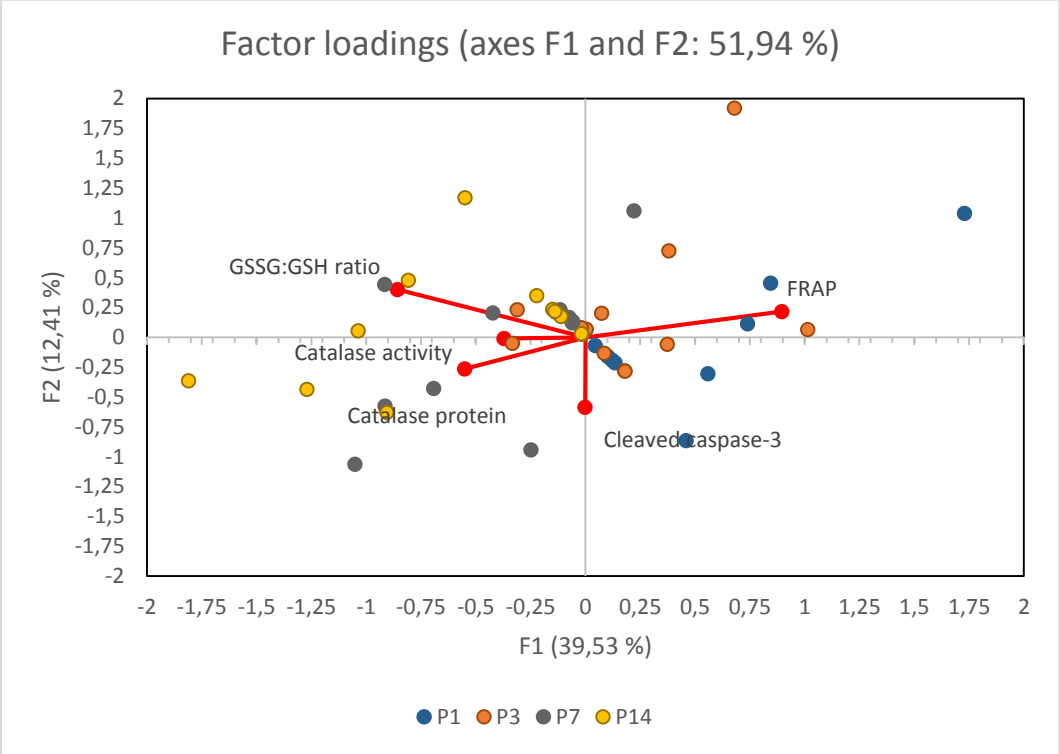
Factor loadings (axes F1 and F2: 51,94 %)
F2 (12,41 %)
F1 (39,53 %)
GSSG:GSH ratio
FRAP
Catalase activity
Catalase protein
Cleaved caspase-3
P1
P3
P7
P14

Figure 14. Multivariate analysis in hippocampus. The differences along postnatal days in CS and AS groups were determined by principal factor analysis, the variables with major contribution are combined in a single variable called principal first factor F1 (axis *x*) and principal second factor F2 (axis *y*). Then, the observations at different postnatal days are correlated with F1 and F2 for determining the variables with major contribution to variations among postnatal days. The values of axis corresponding to values of correlation (*r*) for each variable that contribute to F1 and F2. In red are shown the vectors for each variable analysed, the longest vector and closest to axis indicate the variable with most contribution to F1 or F2. The red point of vector indicates the correlation value for variable with F1 or F2. (**A**) In CS groups the principal factor analysis indicated that main variations among postnatal days are explained by the first principal component F1 in a 56,36% and by the second principal component F2 in a 22,34%. F1 was correlated with *FRAP (r:* 0,990*); catalase activity (r:-0,907); cleaved caspase-3 (r: -0,712) and GSSG:GSH ratio (r: -0,671).* F2 was correlated with *catalase protein (r: -0,991).* In the figure are shown the differences among postnatal days correlated with F1 and F2 in CS groups. P1 was positively correlated with F1 and F2 while that P14 displayed a negative correlation with F1, P3 displayed a negative correlation with F1 and P7 a negative correlation with F2. (**B**) In AS groups the principal factor analysis indicated that main variations among postnatal days are explained by the first principal component F1 in a 33,50% and by the second principal component F2 in a 28,85%. F1 was correlated with *GSSG:GSH ratio (r: 0,898).* F2 was correlated with *cleaved caspase-3 (r: 0,899).* In the figure are shown the differences among postnatal days correlated with F1 and F2 in AS groups. P1 is negatively correlated with F1 while that P14 displayed a positive correlation with F1, P3 displayed a positive correlation with F1 and P7 a negative correlation with F1.

(A)

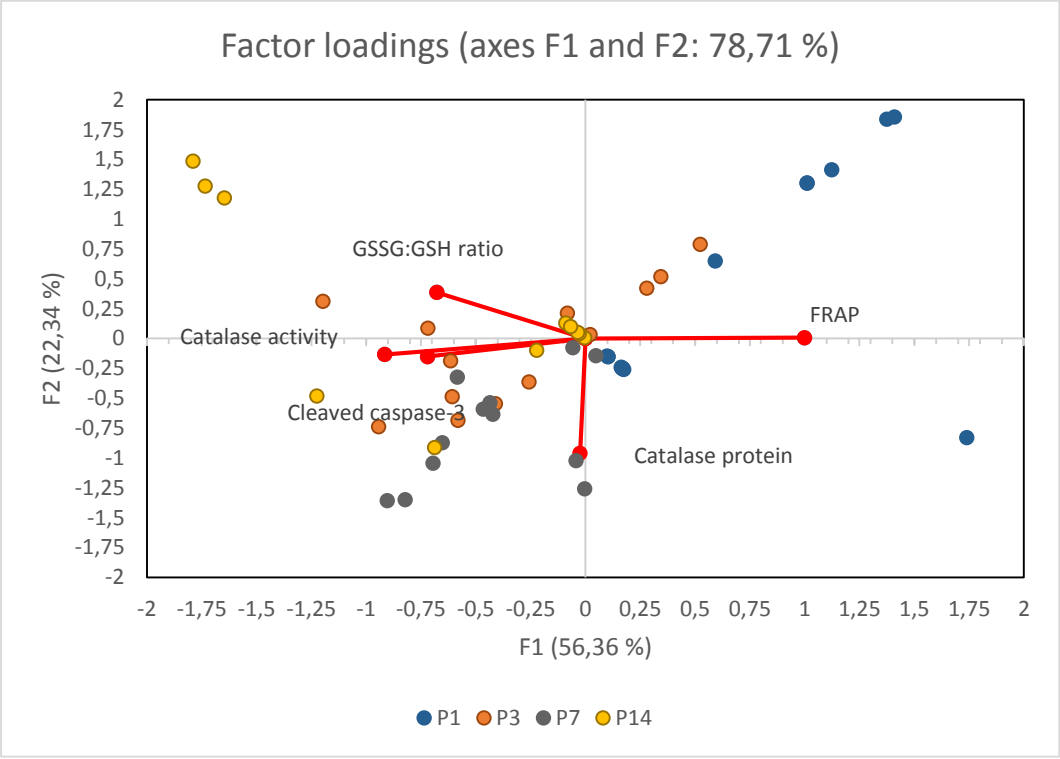

(B)

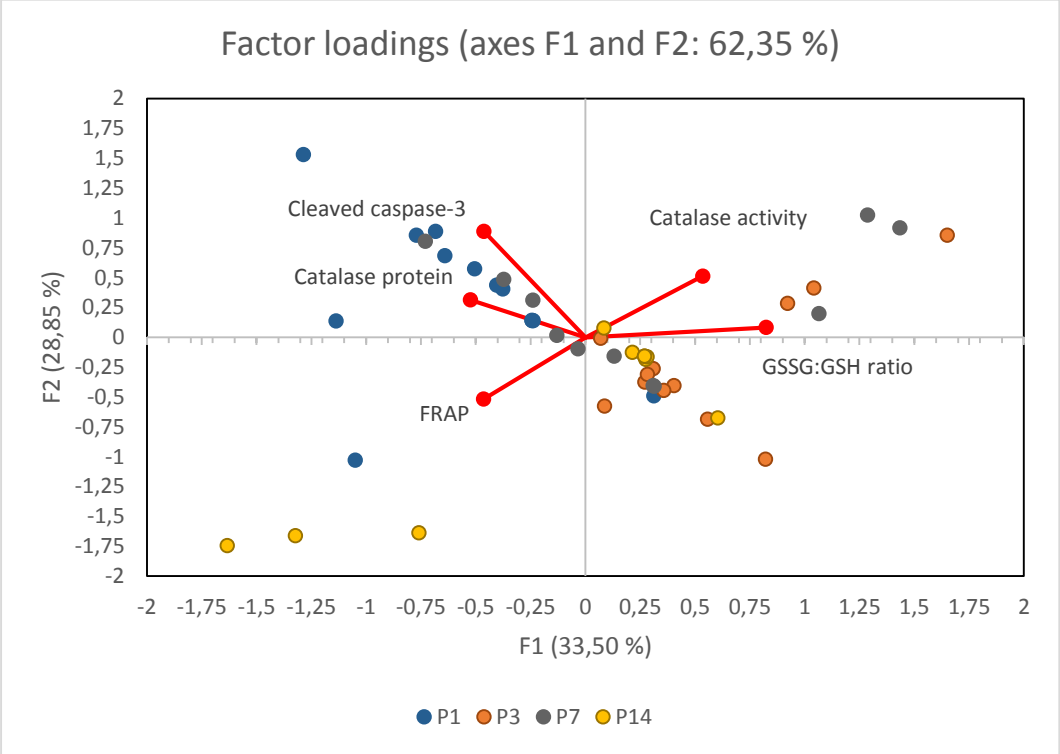
Factor loadings (axes F1 and F2: 62,35 %)
F2 (28,85 %)
F1 (33,50 %)
Cleaved caspase-3
Catalase activity
Catalase protein
GSSG:GSH ratio
FRAP
P1
P3
P7
P14

Figure 15. **Effect of asphyxia and nicotinamide on glutathione in the hippocampus from neonatal rats**. The hippocampus was dissected at P1 and P14 from control (CS), asphyxia-exposed (AS) animals and (CS), (AS) pups treated one hour after birth with an intraperitoneal injection of nicotinamide (CS/AS Nicotinamide; 0.8 mmol/kg, i.p.) or 100 µl of NaCl 0.9% (CS/AS Vehicle; 0.1 ml, i.p.). The percentage of change from baseline corresponding to CS group at P1 and P14 respectively, was computed for representing the effect asphyxia and nicotinamide on (**A**) GSH, (**B**) GSSG and (**C**) GSSG: GSH ratio at P1 and P14. Data were expressed as means ± S.E.M., from at least N=4 independent experiments in duplicated. ANOVA indicated a significant effect of PA, postnatal days and nicotinamide. Benjamini-Hochberg was used as a post hoc test, comparisons were between CS (baseline) and experimental groups at P1 and P14, respectively. Significant differences are shown by asterisks. (*P < 0.05, **P < 0.01, ***P < 0.001, ****P < 0.0001).

(A)

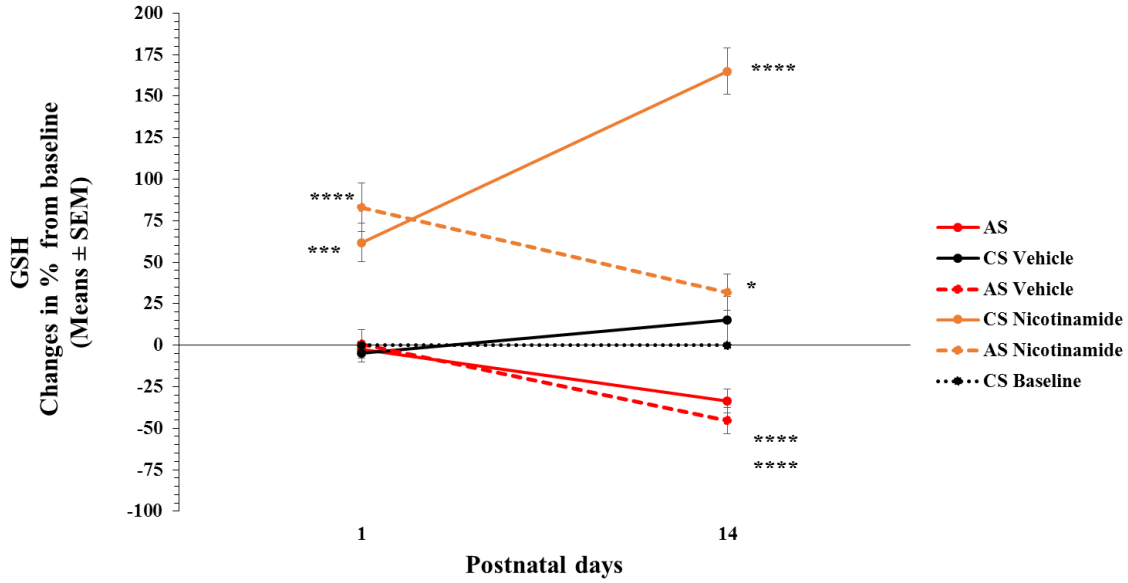

B)

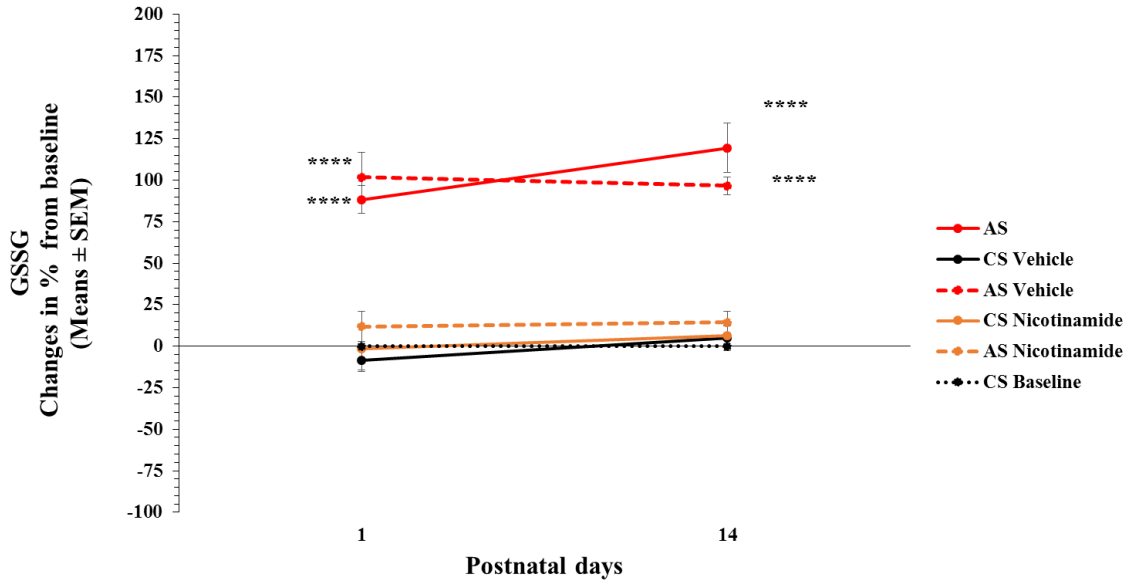
GSSG
Changes in % from baseline
(Means ± SEM)
200
175
150
125
100
75
50
25
0
-25
-50
-75
-100
1
14
Postnatal days
****
****
****
****
AS
CS Vehicle
AS Vehicle
CS Nicotinamide
AS Nicotinamide
CS Baseline

C)

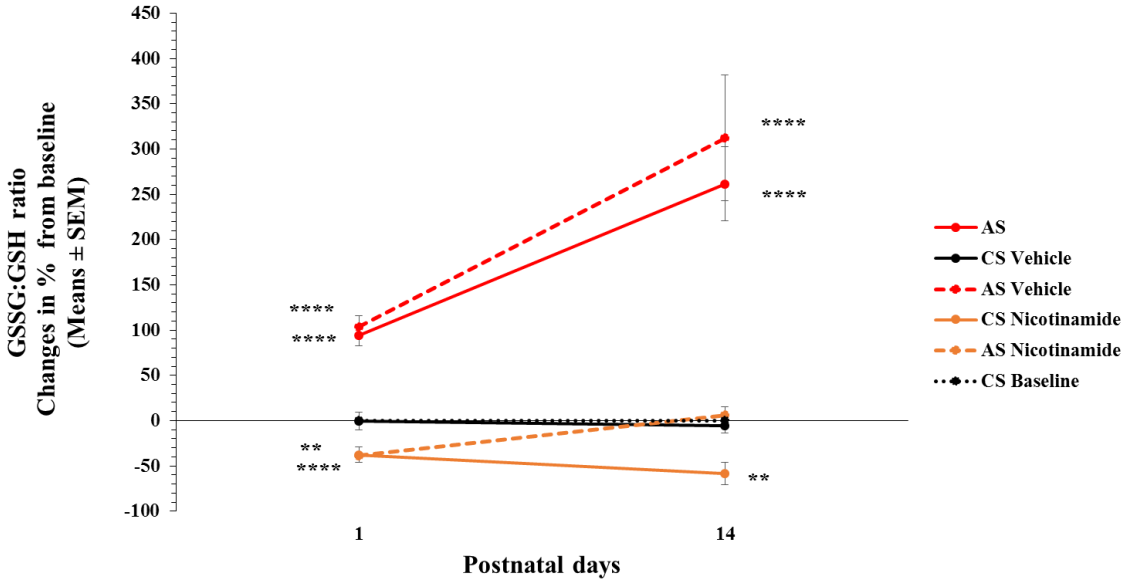
GSSG:GSH ratio
Changes in % from baseline
(Means ± SEM)
450
400
350
300
250
200
150
100
50
0
-50
-100
1
14
Postnatal days
****
****
****
****
**
****
**
AS
CS Vehicle
AS Vehicle
CS Nicotinamide
AS Nicotinamide
CS Baseline

Figure 16. **Effect of asphyxia and nicotinamide on glutathione reductase activity in the hippocampus from neonatal rats**. The hippocampus was dissected at P1 and P14 from control (CS) and asphyxia-exposed (AS) animals, (CS) and (AS) pups treated one hour after birth with an intraperitoneal injection of nicotinamide (CS/AS Nicotinamide; 0.8 mmol/kg, i.p.) or 100 µl of NaCl 0.9% (CS/AS Vehicle; 0.1 ml, i.p.). The percentage of change from baseline corresponding to CS group at P1 and P14 respectively, was computed for representing the effect asphyxia and nicotinamide on glutathione reductase activity at P1 and P14. Data were expressed as means ± S.E.M., from at least N=4 independent experiments in duplicated. ANOVA indicated a significant effect of PA, postnatal days and nicotinamide. Benjamini-Hochberg was used as a post hoc test, comparisons were between CS (baseline) and experimental groups at P1 and P14, respectively. Significant differences are shown by asterisks. (*P < 0.05, **P < 0.01, ***P < 0.001, ****P < 0.0001).

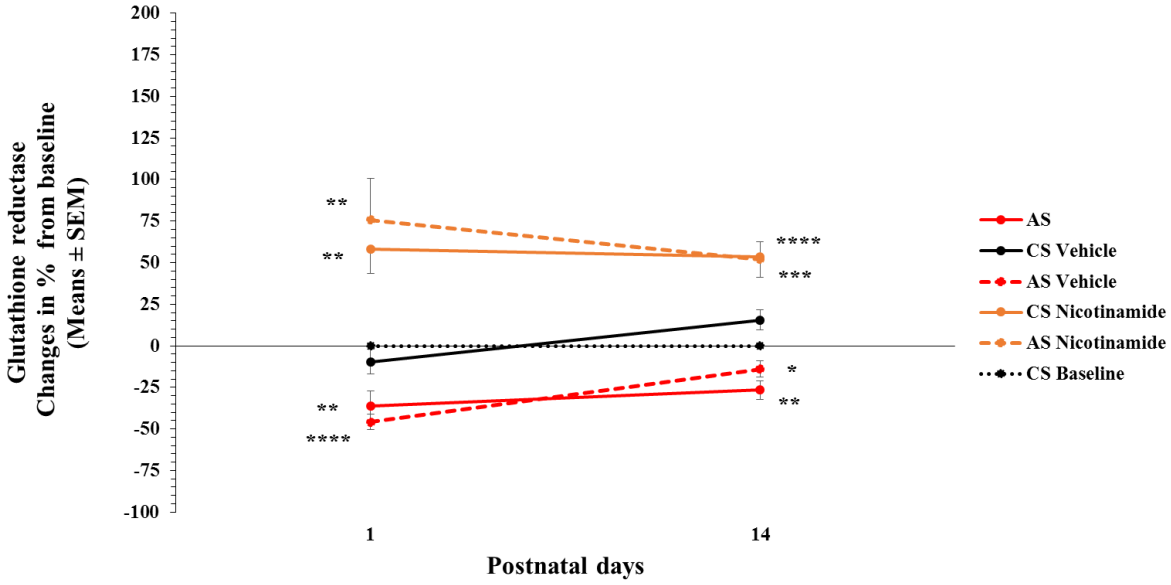

Figure 17. **Effect of asphyxia and nicotinamide on glutathione peroxidase in the hippocampus from neonatal rats**. The hippocampus was dissected at P1 and P14 from control (CS) and asphyxia-exposed (AS) animals, (CS) and (AS) pups treated one hour after birth with an intraperitoneal injection of nicotinamide (CS/AS Nicotinamide; 0.8 mmol/kg, i.p.) or 100 µl of NaCl 0.9% (CS/AS Vehicle; 0.1 ml, i.p.). The percentage of change from baseline corresponding to CS group at P1 and P14 respectively, was computed for representing the effect asphyxia and nicotinamide on glutathione peroxidase activity at P1 and P14. Data were expressed as means ± S.E.M., from at least N=3 independent experiments in duplicated. ANOVA indicated a significant effect of PA, postnatal days and nicotinamide. Benjamini-Hochberg was used as a post hoc test, comparisons were between CS (baseline) and experimental groups at P1 and P14, respectively. Significant differences are shown by asterisks. (*P < 0.05, **P < 0.01, ***P < 0.001, ****P < 0.0001).

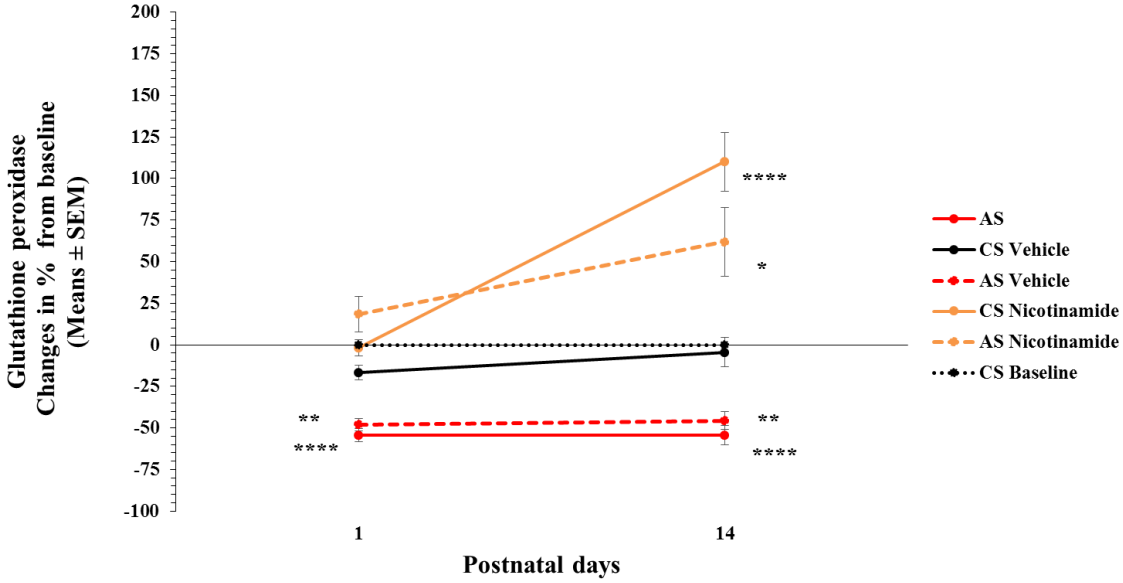

Figure 18. Representative immunoblots of the effect of perinatal asphyxia (PA) and nicotinamide on catalase protein in hippocampus of rats at P1 (A) and P14 (B). The effect of PA on catalase was evaluated in hippocampus dissected at P1 and P14 from control (CS) and asphyxia-exposed (AS) animals. The effect of nicotinamide was evaluated from (CS) and (AS) pups treated one hour after birth with an intraperitoneal injection of nicotinamide (CS/AS Nico; 0.8 mmol/kg, i.p.) or 100 µl of NaCl 0.9% (CS/AS Veh; 0.1 ml, i.p.). Representative Immunoblots for catalase and loading controls, corresponding to β-actin and Ponceau red staining are shown. Catalase was identified as a unique band at 60 kDa. Extracted protein from a liver sample taken at P1 and purified catalase protein were used as positive controls. Lane Cer is an internal control from cerebellum, used to control variations in transference. Lane L corresponds to a ladder protein marker. Quantification of catalase was performed by densitometry. The area of catalase, β-actin and total protein was determined and normalized by the sum method. Catalase values were divided by β-actin and total protein values (used as loading controls), for obtaining the quantity of catalase (**B**, **D**), represented as catalase protein normalized levels in arbitrary units (a. u.). Data are means ± S.E.M from N=5 independent experiments. Two-way ANOVA indicated a significant effect of PA ($F(1, 39) = 62.197$, $P < 0.0001$) and nicotinamide treatment ($F(3, 98) = 76.576$, $P < 0.0001$) on hippocampus catalase levels. Benjamini-Hochberg was used as a post-hoc test for differences among experimental groups. Asterisks in figure B (*P<0.05; **P<0.01; ***P<0.001, ****P<0.0001) [AS Veh *vs* AS Nico, p= 0.048; CS Veh *vs* CS Nico, p = 0.054].

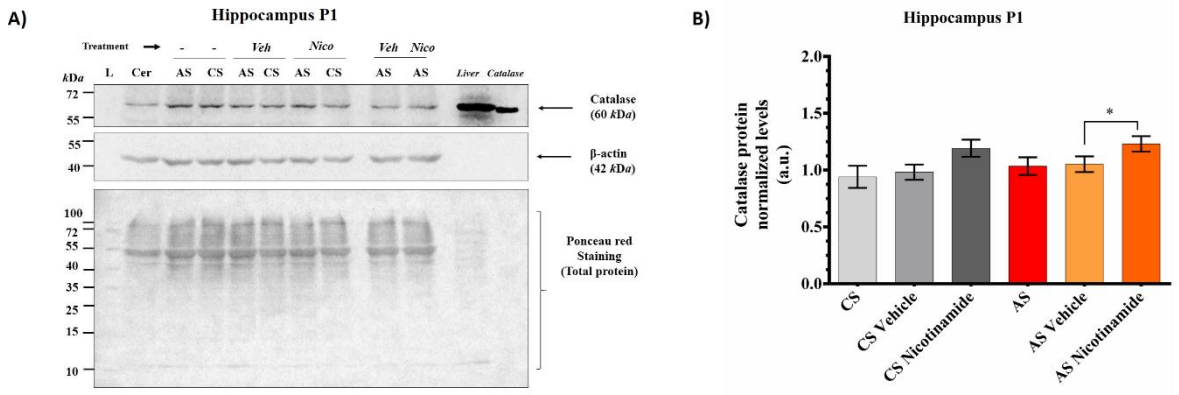

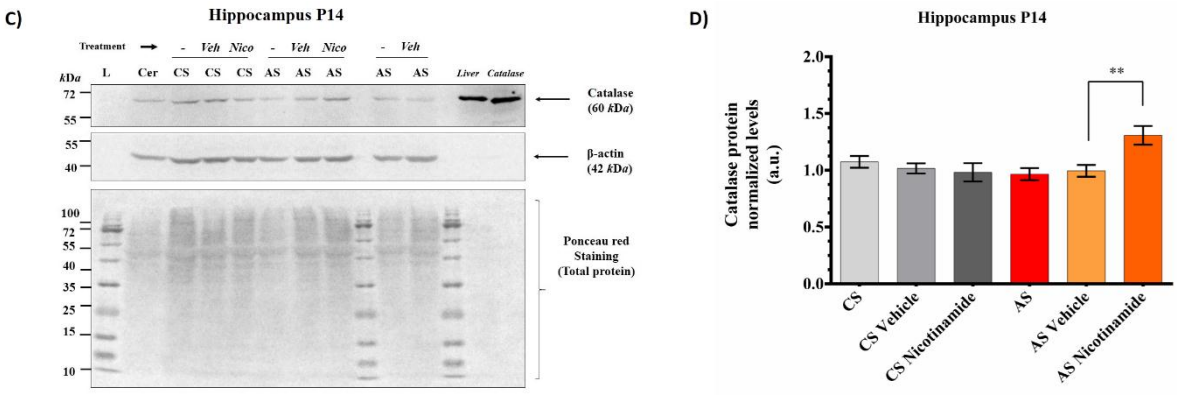
C)
Hippocampus P14
Treatment
-
Veh
Nico
-
Veh
Nico
-
Veh
kDa
L
Cer
CS
CS
CS
AS
AS
AS
AS
AS
Liver
Catalase
72
55
Catalase
(60 kDa)
55
40
β-actin
(42 kDa)
100
72
55
40
35
25
15
10
Ponceau red
Staining
(Total protein)
D)
Hippocampus P14
Catalase protein
normalized levels
(a.u.)
2.0
1.5
1.0
0.5
0.0
**
CS
CS Vehicle
CS Nicotinamide
AS
AS Vehicle
AS Nicotinamide

Figure 19. **Effect of asphyxia and nicotinamide on catalase in the hippocampus from neonatal rats**. The hippocampus was dissected at P1 and P14 from control (CS) and asphyxia-exposed (AS) animals, (CS) and (AS) pups treated one hour after birth with an intraperitoneal injection of nicotinamide (CS/AS Nicotinamide; 0.8 mmol/kg, i.p.) or 100 µl of NaCl 0.9% (CS/AS Vehicle; 0.1 ml, i.p.). The percentage of change from baseline corresponding to CS group at P1 and P14 respectively, was computed for representing the effect asphyxia and nicotinamide on catalase (**A**) protein levels by western blot, (**B**) activity and (**C**) relative protein levels by ELISA at P1 and P14. Data were expressed as means ± S.E.M., from at least N=3 independent experiments in duplicated. ANOVA indicated a significant effect of PA, postnatal days and nicotinamide. Benjamini-Hochberg was used as a post hoc test, comparisons were between CS (baseline) and experimental groups at P1 and P14, respectively. Significant differences are shown by asterisks. (*P < 0.05, **P < 0.01, ***P < 0.001, ****P < 0.0001).

(**A**)

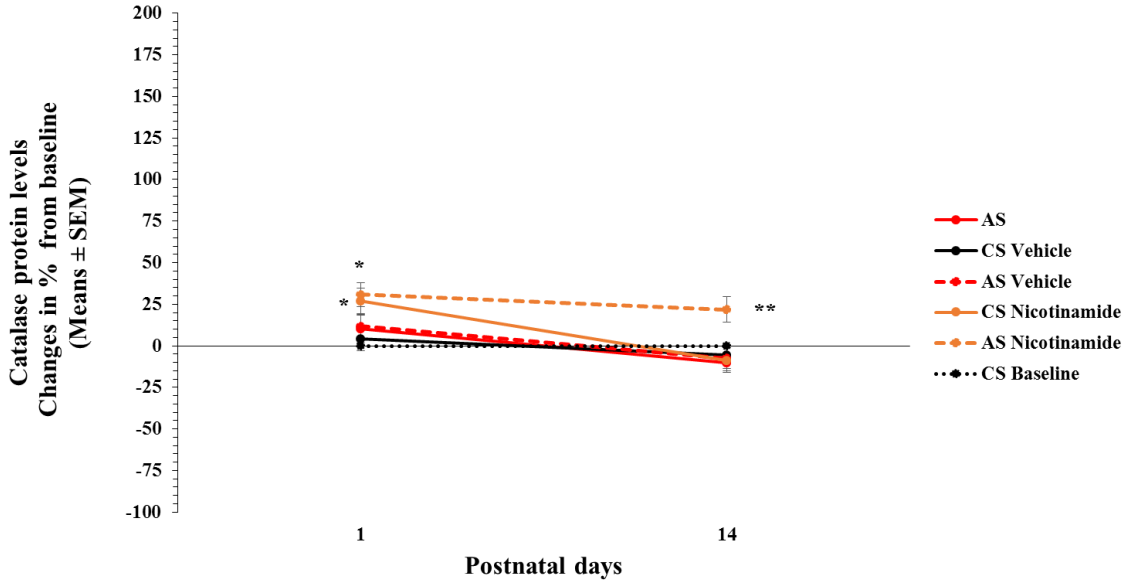

(B)

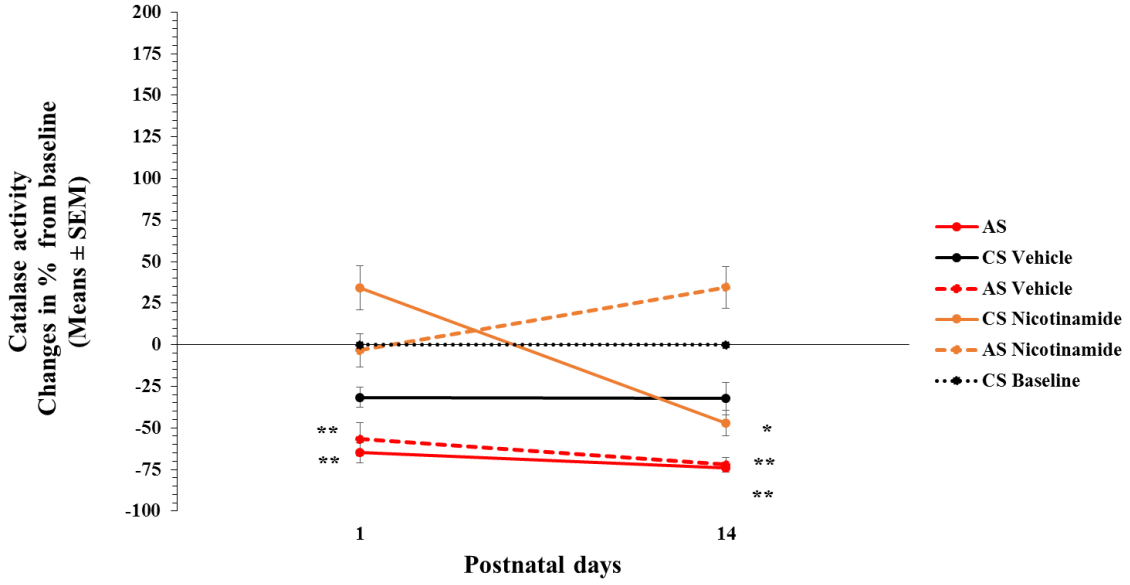
Catalase activity
Changes in % from baseline
(Means ± SEM)
200
175
150
125
100
75
50
25
0
-25
-50
-75
-100
1
14
Postnatal days
**
**
*
**
**
AS
CS Vehicle
AS Vehicle
CS Nicotinamide
AS Nicotinamide
CS Baseline

(C)

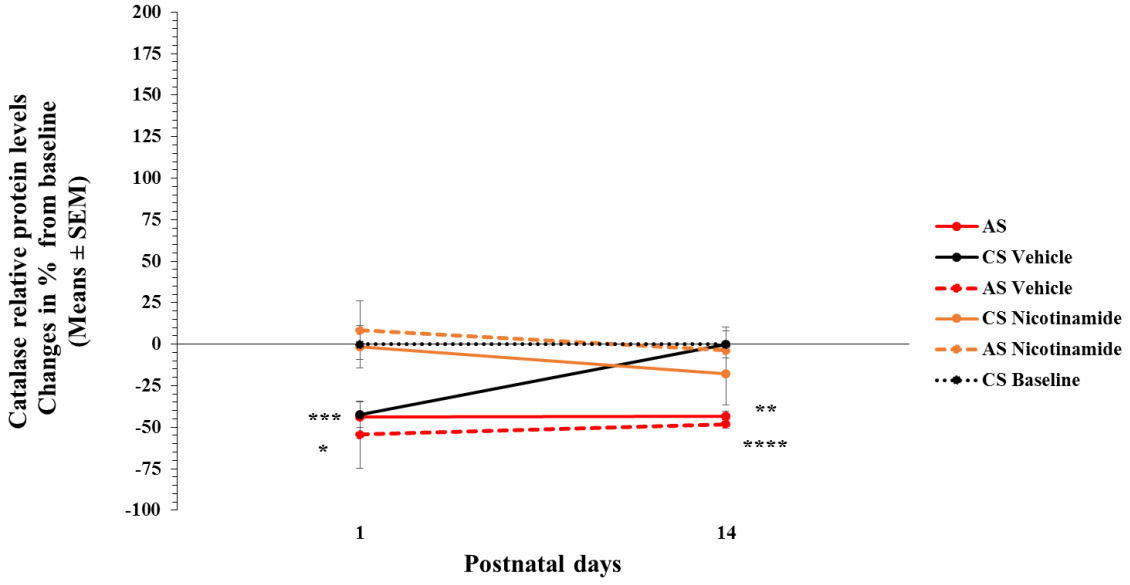
Catalase relative protein levels
Changes in % from baseline
(Means ± SEM)
200
175
150
125
100
75
50
25
0
-25
-50
-75
-100
1
14
Postnatal days
***
*
**
****
AS
CS Vehicle
AS Vehicle
CS Nicotinamide
AS Nicotinamide
CS Baseline

Figure 20. Representative immunoblots of the effect of perinatal asphyxia and nicotinamide on TIGAR protein levels in hippocampus of rats at P1 (A) and P14 (B). The effect of PA was evaluated in hippocampus dissected at P1 from control (CS) and asphyxia-exposed (AS) animals. The effect of nicotinamide was evaluated from (CS) and (AS) pups treated one hour after birth with an intraperitoneal injection of nicotinamide (CS/AS Nico; 0.8 mmol/kg, i.p.) or 100 µl of NaCl 0.9% (CS/AS Veh; 0.1 ml, i.p.). Representative immunoblots for TIGAR and loading controls, corresponding to β-actin and Ponceau red staining are shown. TIGAR was identified as a unique band at 30 kDa. Lane Cer is an internal control from cerebellum, used to control variations in transference. Lane L corresponds to a ladder protein marker. Quantification of TIGAR was performed by densitometry. The area of TIGAR, β-actin and total protein was determined and normalized by the sum method. TIGAR values were divided by β-actin values and total protein values (used as loading controls), for obtaining the quantity of TIGAR, expressed as TIGAR protein normalized levels in arbitrary units (a. u.). The quantity of TIGAR is in graphs **B**, **D,** as TIGAR protein normalized levels in arbitrary units (a. u.). Data are means ± S.E.M from N=5 independent experiments. Two-way ANOVA indicated a significant effect of PA on TIGAR protein ($F_{(1, 37)}$ = 91.25, P < 0.0001) and a significant effect of nicotinamide on TIGAR protein ($F_{(3, 73)}$ = 117.538, P < 0.0001). The comparison between experimental groups was analysed by Benjamini-Hochberg post-hoc test, the statistically significant differences are indicated by asterisks (*P<0.05; **P<0.01; ***P<0.001, ****P<0.0001).

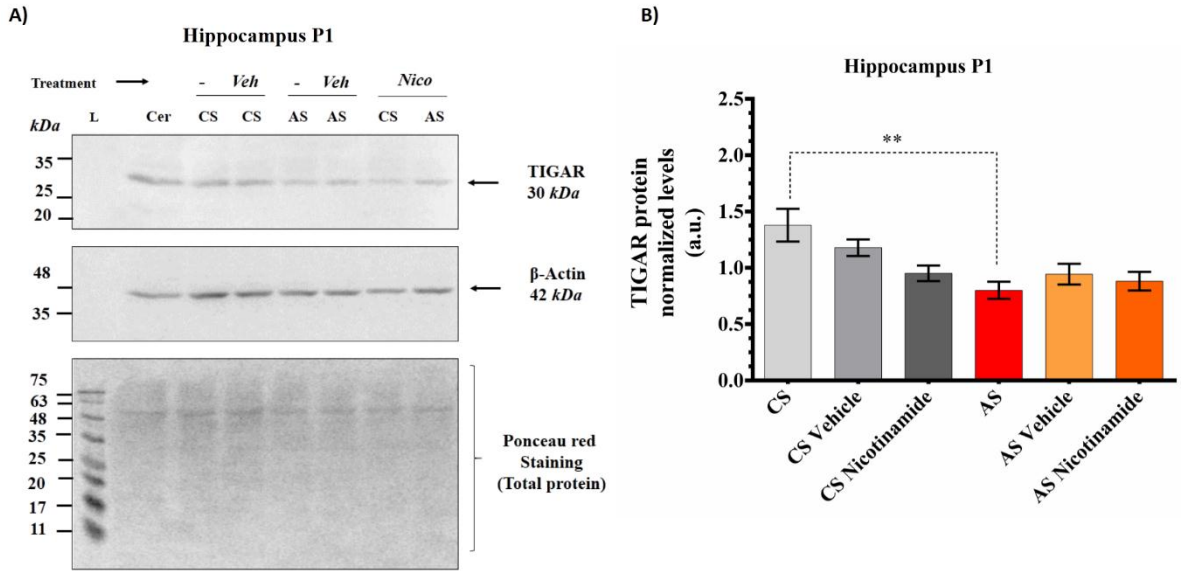

C)

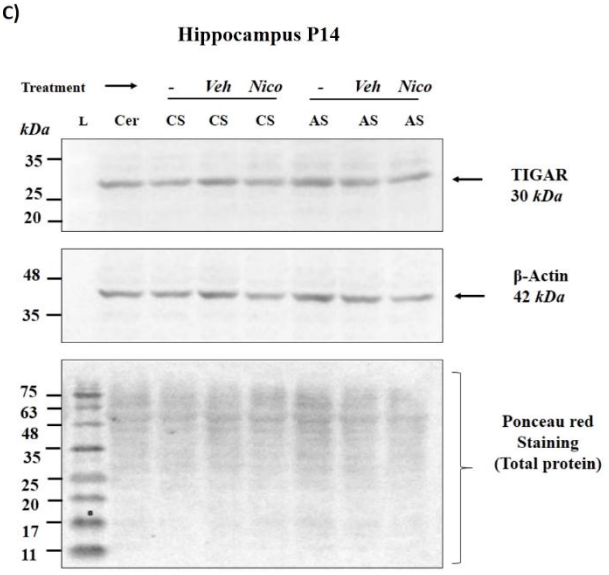
Hippocampus P14
Treatment
-
Veh
Nico
-
Veh
Nico
kDa
L
Cer
CS
CS
CS
AS
AS
AS
35
25
20
TIGAR
30 kDa
48
35
β-Actin
42 kDa
75
63
48
35
25
20
17
11
Ponceau red
Staining
(Total protein)

D)

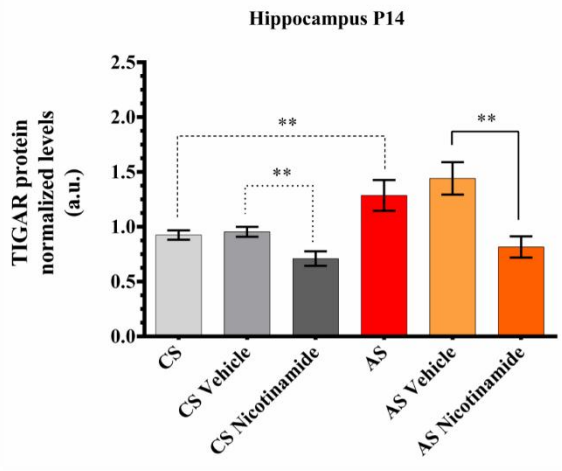
Hippocampus P14
TIGAR protein
normalized levels
(a.u.)
2.5
2.0
1.5
1.0
0.5
0.0
**
**
**
CS
CS Vehicle
CS Nicotinamide
AS
AS Vehicle
AS Nicotinamide

Figure 21. **Effect of asphyxia and nicotinamide on TIGAR in the hippocampus from neonatal rats**. The hippocampus was dissected at P1 and P14 from control (CS) and asphyxia-exposed (AS) animals, (CS) and (AS) pups treated one hour after birth with an intraperitoneal injection of nicotinamide (CS/AS Nicotinamide; 0.8 mmol/kg, i.p.) or 100 µl of NaCl 0.9% (CS/AS Vehicle; 0.1 ml, i.p.). The percentage of change from baseline corresponding to CS group at P1 and P14 respectively, was computed for representing the effect asphyxia and nicotinamide on TIGAR protein levels at P1 and P14. Data were expressed as means ± S.E.M., from at least N=5 independent experiments. ANOVA indicated a significant effect of PA, postnatal days and nicotinamide. Benjamini-Hochberg was used as a post hoc test, comparisons were between CS (baseline) and experimental groups at P1 and P14, respectively. Significant differences are shown by asterisks. In figure * is for comparisons between CS and AS vehicle, CS nicotinamide, AS nicotinamide at P1 (*P < 0.05, **P < 0.01, ***P < 0.001, ****P < 0.0001).

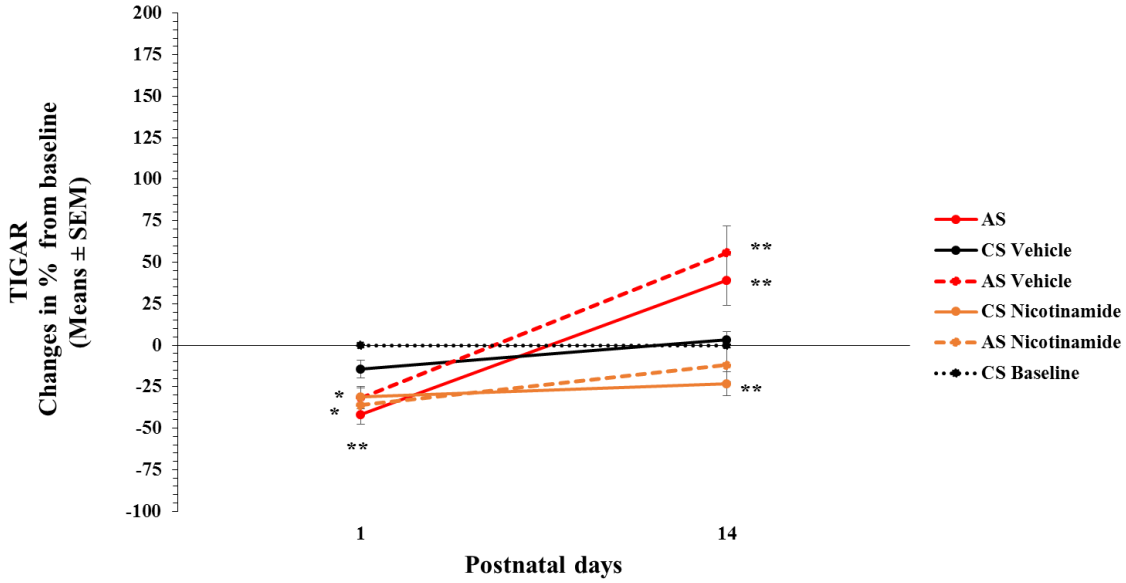

Figure 22. Representative immunoblots of the effect of perinatal asphyxia and nicotinamide on XRCC1 protein in hippocampus of rats at P1 (A) and P14 (B). The effect of PA was evaluated in hippocampus dissected at P1 and P14 from control (CS) and asphyxia-exposed (AS) animals. The effect of nicotinamide was evaluated from (CS) and (AS) pups treated one hour after birth with an intraperitoneal injection of nicotinamide (CS/AS Nico; 0.8 mmol/kg, i.p.) or 100 µl of NaCl 0.9% (CS/AS Veh; 0.1 ml,i.p.).Representative immunoblots of XRCC1 and loading controls, corresponding to α-tubulin and Ponceau red staining, are shown. XRCC1 was identified as a unique band at 96 kDa. Lane Cer is an internal control from cerebellum, used to control variations in transference. Lane L corresponds to a ladder protein marker. Quantification of XRCC1 was performed by densitometry. The area for XRCC1, α-tubulin and total protein was determined and normalized by the sum method. XRCC1 values were divided by α-tubulin values and total protein values (used as loading controls), for obtaining the quantity of XRCC1, represented as XRCC1 protein normalized levels in arbitrary units (a. u.) in graphs **B**, **D**. Data are means ± S.E.M from N=5 independent experiments. Two-way ANOVA indicated a significant effect of PA on XRCC1 levels in hippocampus ($F_{(1, 31)} = 43.834$, $P < 0.0001$). The effect of nicotinamide on XRCC1 levels was also significant ($F_{(3, 65)} = 140.079$, $P < 0.0001$). Benjamini-Hochberg was used as a post-hoc test. *P<0.05; **P<0.01; ***P<0.001, ****P<0.0001.

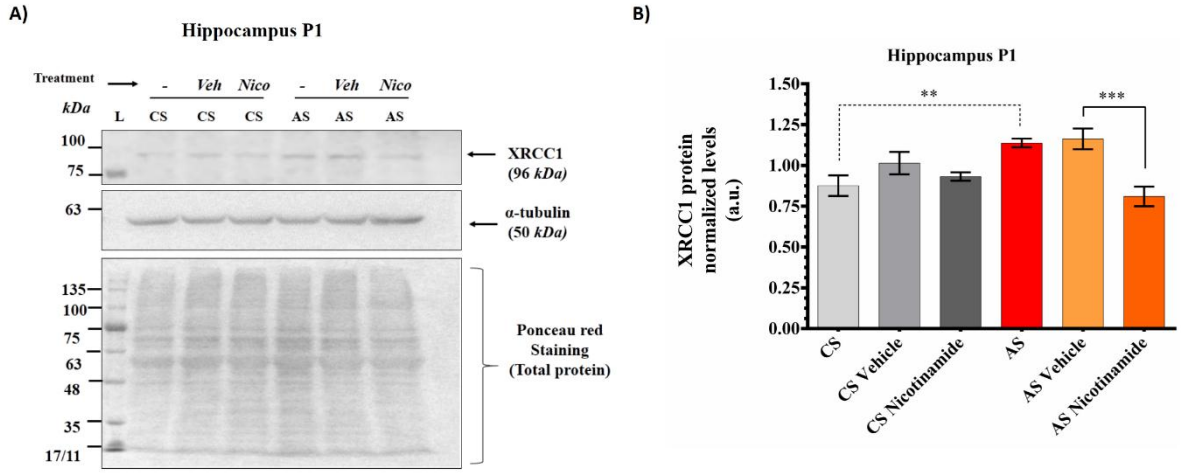

C)

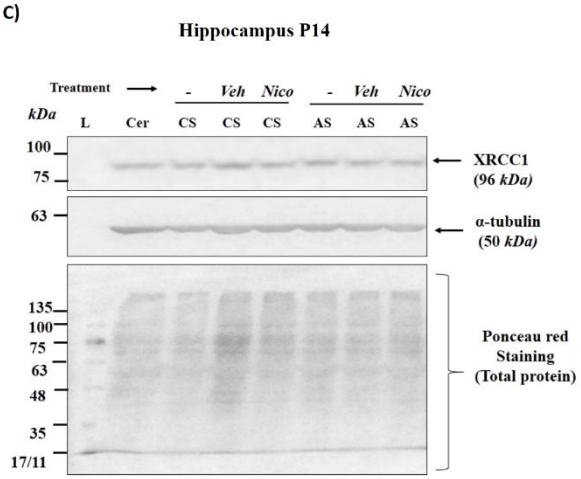
Hippocampus P14
Treatment
-
Veh
Nico
-
Veh
Nico
kDa
L
Cer
CS
CS
CS
AS
AS
AS
100
75
63
135
100
75
63
48
35
17/11
XRCC1
(96 kDa)
α-tubulin
(50 kDa)
Ponceau red
Staining
(Total protein)

D)

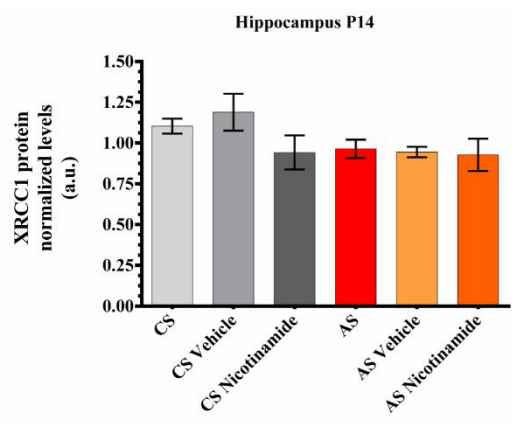
Hippocampus P14
XRCC1 protein
normalized levels
(a.u.)
1.50
1.25
1.00
0.75
0.50
0.25
0.00
CS
CS Vehicle
CS Nicotinamide
AS
AS Vehicle
AS Nicotinamide

Figure 23. **Effect of asphyxia and nicotinamide on XRCC1 in the hippocampus from neonatal rats**. The hippocampus was dissected at P1 and P14 from control (CS) and asphyxia-exposed (AS) animals, (CS) and (AS) pups treated one hour after birth with an intraperitoneal injection of nicotinamide (CS/AS Nicotinamide; 0.8 mmol/kg, i.p.) or 100 µl of NaCl 0.9% (CS/AS Vehicle; 0.1 ml, i.p.). The percentage of change from baseline corresponding to CS group at P1 and P14 respectively, was computed for representing the effect asphyxia and nicotinamide on XRCC1 protein levels at P1 and P14. Data were expressed as means ± S.E.M., from at least N=5 independent experiments. ANOVA indicated a significant effect of PA, postnatal days and nicotinamide. Benjamini-Hochberg was used as a post hoc test, comparisons were between CS (baseline) and experimental groups at P1 and P14, respectively. Significant differences are shown by asterisks. (*P < 0.05, **P < 0.01, ***P < 0.001, ****P < 0.0001).

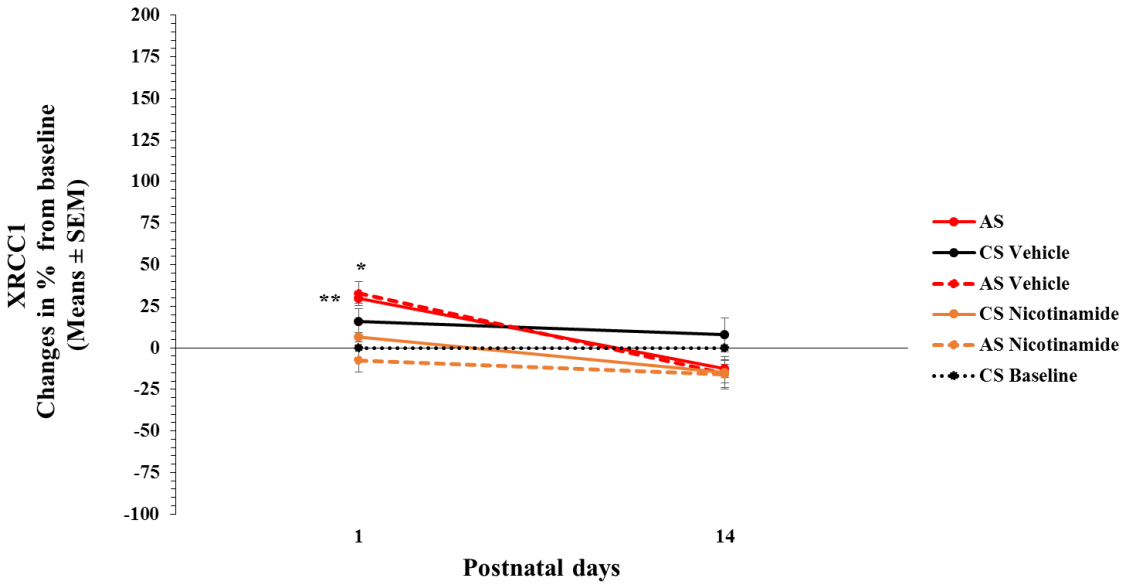

Figure 24. **Effect of asphyxia and nicotinamide on Calpain in the hippocampus from neonatal rats**. The hippocampus was dissected at P1 and P14 from control (CS) and asphyxia-exposed (AS) animals, (CS) and (AS) pups treated one hour after birth with an intraperitoneal injection of nicotinamide (CS/AS Nicotinamide; 0.8 mmol/kg, i.p.) or 100 µl of NaCl 0.9% (CS/AS Vehicle; 0.1 ml, i.p.). The percentage of change from baseline corresponding to CS group at P1 and P14 respectively, was computed for representing the effect asphyxia and nicotinamide on calpain activity at P1 and P14. Data were expressed as means ± S.E.M., from at least N=4 independent experiments in duplicated. ANOVA indicated a significant effect of PA, postnatal days and nicotinamide. Benjamini-Hochberg was used as a post hoc test, comparisons were between CS (baseline) and experimental groups at P1 and P14, respectively. Significant differences are shown by asterisks. (*P < 0.05, **P < 0.01, ***P < 0.001, ****P < 0.0001).